

# **Base Catalyzed Glycerolysis of Fatty Acid Methyl Esters: Investigations towards the Development of a Continuous Process**

vorgelegt von  
M.Tech.  
Devender Singh Negi  
aus Almora, Indien

von der Fakultät II-Mathematik und Naturwissenschaften  
der Technischen Universität Berlin  
Institut für Chemie  
Fachgebiet Technische Chemie  
zur Erlangung des akademischen Grades

Doktor der Ingenieurwissenschaften  
-Dr.-Ing.-  
genehmigte Dissertation

Promotionsausschuss:

Vorsitzender: Prof. Dr. M. Lerch  
Berichter: Prof. Dr. R. Schomäcker  
Berichter: Prof. Dr. G. Wozny

Tag der wissenschaftlichen Aussprache: 07 Juni 2006

Berlin 2006  
D 83

## Abstract

The base catalyzed glycerolysis of fatty acid methyl esters (FAME) has been investigated in this work with the aim to develop a continuous process for this reaction. Mono- and diglycerides are the main products of this reaction, which find major use as emulsifiers in food and pharmaceutical products. Monoglycerides are commercially manufactured by the base catalyzed glycerolysis of fats and oils, mostly using batch reactors. However, the glycerolysis of fatty acid methyl esters can be used to produce monoglycerides with desirable emulsification properties for specific end uses. The glycerolysis reaction represents an equilibrium limited liquid-liquid reaction where the reaction kinetics and phase behavior were not properly understood at the beginning of this project. For selecting favorable process alternatives for this reaction, a prerequisite was the identification and characterization of the factors that affect the reaction kinetics.

Following previous investigations on FAME glycerolysis, the effect of mass transfer limitations and liquid-liquid solubility on the reaction rate was studied in this work. The drop size distribution was investigated parallel to the ester conversion during batch reactions. It was found that under well stirred conditions the reaction is not limited by mass transfer. Rather, the changing glycerol solubility was found to be responsible for the observed reaction rate behavior. The glycerol solubility in the ester phase as predicted by the activity coefficient models UNIFAC and UNIFAC-Dortmund was found to deviate largely from the experimentally observed values in the presence of monoglyceride. A kinetic model based on Kimmel's work [1] was used in this study. In this model an empirical relation was used for the glycerol concentration in the ester phase. To determine the model parameters, experiments were carried out in a batch reactor.

As a continuous reactor, a bubble cap tray column was considered potentially advantageous as faster reaction rates and higher conversions were expected by efficiently removing the by-product methanol from the liquid reaction mixture. Experiments with a single bubble cap tray supported this fact but the simulations carried out for a cascade of trays showed low overall conversions. Simulations for a continuous flow stirred tank reactor (CSTR) with methanol removal showed higher overall conversions as compared to a cascade of trays with the same total liquid holdup as the volume of a single CSTR. Experiments were carried out in a CSTR for the verification of the simulations. The experimentally obtained ester conversion and monoglyceride selectivity was found to be in good agreement with simulation results.

# Zusammenfassung

Die basekatalysierte Glycerolyse von Fettsäuremethylester (FAME) wurde in dieser Arbeit mit dem Ziel untersucht, einen kontinuierlichen Prozess für diese Reaktion zu entwickeln. Die Hauptprodukte der Umsetzung sind Mono- und Diglyceride, welche überwiegend als Emulgatoren in Lebensmitteln und pharmazeutischen Produkten verwendet werden. Monoglyceride werden kommerziell über die basekatalysierte Glycerolyse von Fetten und Ölen hergestellt, meist in Batch-Reaktoren. Durch die Glycerolyse von Fettsäuremethylester können Monoglyceride mit der gewünschten Eigenschaften für spezifische Anwendungen bereitgestellt werden, da dafür Ester einzelner Fettsäuren eingesetzt werden können. Die Glycerolyse stellt eine gleichgewichtlimitierte flüssig-flüssig-Reaktion dar, wobei die Reaktionskinetik und das Phasenverhalten des Reaktionsgemisches zu Beginn dieses Projektes noch nicht vollständig verstanden war. Voraussetzungen für die Auswahl einer günstigen Verfahrensalternative für diese Reaktion waren die Identifizierung und Charakterisierung der Faktoren, die die Reaktionskinetik beeinflussen.

Auf Basis von vorherigen Untersuchungen über FAME-Glycerolyse wurde der Effekt von Stofftransportphänomenen und der Löslichkeit von flüssig-flüssig Systemen auf die Reaktionsgeschwindigkeit untersucht. Die Tropfengrößenverteilung wurde in Abhängigkeit vom Esterumsatz in Batchreaktionen bestimmt. Es wurde herausgefunden, dass die Reaktionsgeschwindigkeit bei höherer Rührerdrehzahl unabhängig von Stofftransportlimitierungen ist. Die Glycerinlöslichkeit hat dagegen einen deutlichen Einfluss auf die Reaktionsgeschwindigkeit. Die experimentell bestimmte Löslichkeit von Glycerol in der Esterphase wich in Gegenwart von Monoglycerid stark von den mit UNIFAC und UNIFAC-Dortmund berechneten Werten ab. In dieser Arbeit wurde ein kinetisches Modell verwendet, dass auf den Untersuchungen von T. Kimmel [1] basiert. In diesem Modell wurde eine empirische Beziehung für die Glycerolkonzentration in der Esterphase benutzt. Um die Modell-Parameter zu bestimmen, wurden Experimente im Batch-Reaktor durchgeführt.

Als kontinuierlicher Reaktor wurde eine Glockenboden-Kolonne als potenziell vorteilhaft angesehen, da bei einer effizienten Entfernung des Nebenproduktes Methanol aus der flüssigen Reaktionsmischung höhere Reaktionsgeschwindigkeiten und Umsätze zu erwarten sind. Experimente mit einem einzelnen Glockenboden unterstützten zunächst diese Annahme, aber Simulation für eine Bodenkolonne zeigten eher niedrige Gesamtumsätze. Simulationen für einen kontinuierlichen Rührkessel (CSTR) mit Methanol Entfernung zeigten höhere Gesamtumsätze als eine Bodenkolonne mit gleichem Flüssigkeitsvolumen. Auf Grundlage dieser Simulationsergebnisse wurden Verifikationsexperimente ausgeführt. Die experimentell bestimmten Werte für Ester-Umsatz und Monoglycerid-Selektivität waren in guter Übereinstimmung mit der Simulationsergebnissen.

## Acknowledgements

I am glad to take this opportunity to express my gratitude to all those people who contributed towards the successful completion of this work directly or indirectly. Foremost, I wish to thank my supervisor Professor R. Schomäcker, for his trust in giving me this responsibility and for his motivation and support in numerous ways during my stay in the institute. I would like to thank Professor G. Wozny for help and discussions on technical problems and also for allowing me to join the German language course that he organized for some of his students. I also thank the members in the examination-committee: Professor M. Lerch and Professor G. Wozny for their time.

Thanks to Tobias Kimmel, who I could always ask for help, also after he left the institute. Thanks to Alexander, Yasemin and Felix for help in experimental work. Special thanks to Gabi, who was always ready to help during my work in the laboratory. Thanks to the people in glass and metal workshops and in the material section for providing me the fabricated equipments and materials. Being a part of the work-group was a nice memorable experience. I learned a lot during this time and I am grateful to all the past and present group members who I worked with. I shared some light moments with the 'Kicker group' (Arne, Benjamin, Daniel, Hartmut, Michael, Oliver and others) during the breaks between work. I feel grateful to them for those times and also for helping me frequently in language translations. Also, thanks to members in the research group at DBTA for various technical discussions.

I am grateful to the PhD students in the GRK 827 group (Andreas, Ansor, Benny, Ilja, Kasia, Miriam, Miroslav, Robert and Sonja) for discussions, for help in experiments and for encouraging me to learn German language. I enjoyed the time with them in GRK meets both official (GRK seminars and lectures) and unofficial (in the *Kneipe*). Thanks also to the staff members of GRK 827, specially to Professor M. Kraume and Mr. P. Schindler for their help in different matters.

I wish to thank my friends in Germany and in India for their constant support, especially during the time when I was not at work. Special thanks to Pranav and Shabi, who constantly inspired me to work better. I am grateful to all my friends who I met in Berlin and with whom I often had conversations on various topics, mostly non technical...thanks for giving me your time.

...and last but not the least, I wish to thank my parents and sisters in India for their love, encouragement and patience. They must have felt my absence during these years, not really knowing what I do...but are happy, hoping that I am 'studying well' far away from home.

# Contents

<b>Abstract</b>	<b>i</b>
<b>List of Symbols</b>	<b>1</b>
<b>1 Introduction</b>	<b>4</b>
1.1 Layout of the thesis . . . . .	5
1.2 Materials, equipments and softwares . . . . .	6
1.2.1 Materials . . . . .	6
1.2.2 Equipments . . . . .	7
1.2.3 Software tools . . . . .	8
<b>2 Monoglycerides: Uses and Production Technology</b>	<b>9</b>
<b>3 Liquid-Liquid Reactions and Phase Equilibrium</b>	<b>14</b>
3.1 Liquid-liquid reactions . . . . .	14
3.1.1 Reaction regimes . . . . .	15
3.1.2 FAME glycerolysis: Where does the reaction take place? . . . . .	16
3.2 Phase equilibrium . . . . .	18
3.2.1 Activity coefficient models . . . . .	19
3.2.2 UNIFAC model . . . . .	20
3.2.3 Phase equilibrium computation . . . . .	23
3.3 Experimental . . . . .	24

3.3.1	Materials and analytical equipment . . . . .	25
3.3.2	Experimental setup and procedure . . . . .	25
3.3.3	Analysis . . . . .	26
3.4	Results and discussion . . . . .	26
3.4.1	Glycerol-methyl oleate (binary): Effect of temperature . . . . .	26
3.4.2	Ternary LLE: Comparison of experimental and predicted data . .	26
3.4.3	Reliability of experimental data . . . . .	28
3.5	Summary . . . . .	30
<b>4</b>	<b>Investigations in Reactor with Single Bubble Cap Tray</b>	<b>31</b>
4.1	Liquid mixing and drop size analysis on a bubble cap tray . . . . .	32
4.1.1	Materials . . . . .	32
4.1.2	Experimental setup . . . . .	32
4.1.3	Results and discussion . . . . .	33
4.2	Reaction on the bubble cap tray . . . . .	41
4.2.1	Experimental setup and procedure . . . . .	42
4.2.2	Results and discussion . . . . .	44
4.3	Modeling and simulation . . . . .	46
4.3.1	Reaction modeling . . . . .	47
4.3.2	Results and discussion . . . . .	49
4.4	Summary . . . . .	51
<b>5</b>	<b>Investigations on FAME Glycerolysis in Stirred Tank Reactor</b>	<b>52</b>
5.1	Experimental . . . . .	53
5.1.1	Materials . . . . .	53
5.1.2	Experimental set-up and procedure . . . . .	53
5.1.3	Data analysis . . . . .	56
5.2	Modeling and simulation . . . . .	57

5.3	Results and discussion . . . . .	59
5.3.1	Batch reactor without methanol stripping . . . . .	61
5.3.2	Batch reactor with methanol stripping by inert gas . . . . .	62
5.4	Summary . . . . .	64
<b>6</b>	<b>Investigations in Continuous Flow Reactors</b>	<b>65</b>
6.1	Simulation of some continuous processes . . . . .	65
6.2	Experimental . . . . .	69
6.2.1	Materials . . . . .	69
6.2.2	Experimental setup and procedure . . . . .	69
6.3	Results and discussion . . . . .	71
6.4	Summary . . . . .	73
	<b>Appendix</b>	<b>75</b>
<b>A</b>		<b>75</b>
A.1	Component data calculations . . . . .	75
A.2	Group distribution and parameters for UNIFAC and UNIFAC-Dortmund	76
A.3	GC calibration . . . . .	79
A.4	Stirred tank design . . . . .	82
	<b>Curriculum Vitae</b>	<b>88</b>

# List of Symbols

## Latin symbols<sup>1</sup>

$d_{32}$	Sauter mean diameter, [m]
$We$	Weber number, [-]
$f$	fugacity coefficient, [-]
$f$	calibration factor, [-]
$D_{AB}$	diffusivity coefficient, [ $m^2/s$ ]
$k_l$	liquid side mass transfer coefficient, [ $m/s$ ]
$x$	mole fraction in liquid phase, [-]
$y$	mole fraction in vapor phase, [-]
$P$	total pressure, [ $N/m^2$ ]
$T$	temperature, [ $^{\circ}C$ ]
$p^o$	vapor pressure of component $i$ , [ $N/m^2$ ]
$V$	gas slot velocity (in bubble cap tray), [ $m/s$ ]
$W$	work done on the reactor content by agitation, [J]
$P$	power delivered to reactor content, [J/s]
$g$	acceleration due to gravity, [ $m/s^2$ ]
$k$	second order reaction rate constant, [ $kg/(mol \cdot min)$ ]
$C$	concentration in liquid phase, [ $mol/kg$ ]
$r$	rate of reaction, [ $mol/(kg \cdot min)$ ]
$t$	reaction time, [minutes]
$E_A$	activation energy, [ $kJ/mol$ ]
$w$	weight fraction, [-]
$M$	molecular weight, [g/mol]
$X$	conversion of limiting reactant, [-]
$S$	selectivity of desired product, [-]
$Y$	yield of desired product, [-]
$V$	liquid volume in the reactor, [ $m^3$ ]
$V_o$	volumetric flow rate, [ $m^3/s$ ]

---

<sup>1</sup>The units in text may differ according to use



### Greek symbols

$\rho$	fluid density, $[kg/m^3]$
$\phi$	dispersed phase fraction, [-]
$\phi$	fugacity coefficient, [-]
$\delta_l$	liquid film thickness, $[m]$
$\sigma$	interfacial tension, $[mN/m]$
$\eta$	liquid viscosity, $[cP]$
$\gamma$	activity coefficient, [-]
$\tau$	nominal residence time, $[minutes]$

### Superscripts

$o$	pure component or standard state
$v$	vapor phase
$L, l$	liquid phase
$'$	phase at equilibrium
$''$	phase at equilibrium
$feed$	reactor feed conditions
$exit$	reactor exit conditions

### Subscripts

$i$	component $i$
$1f$	reaction 1 forward ( $ME + G \rightarrow MG + MeOH$ )
$1r$	reaction 1 reverse ( $MG + MeOH \rightarrow ME + G$ )
$2f$	reaction 2 forward ( $MG + MG \rightarrow DG + G$ )
$2r$	reaction 2 reverse ( $DG + G \rightarrow MG + MG$ )
$3f$	reaction 3 forward ( $ME + DG \rightarrow TG + MeOH$ )
$3r$	reaction 3 reverse ( $TG + MeOH \rightarrow ME + DG$ )
$t$	time

## Abbreviations

<i>CSTR</i>	continuous flow stirred tank reactor
<i>FAME</i>	fatty acid methyl esters
<i>ME</i>	methyl ester (methyl oleate)
<i>G</i>	glycerol
<i>MG</i>	monoglycerides
<i>MeOH</i>	methanol
<i>DG</i>	diglycerides
<i>TG</i>	triglycerides
<i>UNIFAC</i>	UNIQUAC functional group activity coefficients
<i>UNIQUAC</i>	universal quasi chemical
<i>NRTL</i>	non random two liquid
<i>LLE</i>	liquid-liquid equilibrium
<i>VLE</i>	vapor-liquid equilibrium
<i>VLLE</i>	vapor-liquid-liquid equilibrium
<i>GC</i>	gas chromatography, gas chromatogram
<i>rpm</i>	rotations per minute
<i>PFR</i>	plug flow reactor

# Chapter 1

## Introduction

Mono- and diglycerides represent the most important class of food emulsifiers. They are generally produced by base catalyzed glycerolysis of fats, mostly using batch reactors. Better quality of monoglycerides for specific end use can be produced by the glycerolysis of fatty acid methyl esters (FAME). Base catalyzed glycerolysis of FAME has been investigated in this work with the aim of developing a continuous process for this reaction. FAME glycerolysis reaction mixture represents a vapor-liquid-liquid system where the reaction takes place in the liquid phase. The two reactants ester and glycerol are nearly immiscible and two liquid phases coexist throughout the reaction. The kinetics of this reaction was investigated by Kimmel [1], partly in parallel with the present work. A part of this work also included investigating the reaction kinetics. The time profile of the FAME conversion in a batch reaction run shows an 'S' shape, which is typical in autocatalytic reactions and in reactions with changing reaction regimes. In the beginning, based on previous observations, it was hypothesized that the reaction rate is dependent on the interfacial size between the two liquid reactants [2]. So initially, characterization of the interfacial size in the concerned reactor geometry was one of the objectives. Later it was discovered that interfacial reaction is not the case under well agitated conditions and the equilibrium composition in the ester phase plays an important role in deciding the reaction kinetics. Experiments and theoretical calculations were performed to quantify the model parameters. Simulations of some continuous processes and experimental verification for a continuous flow stirred tank reactor consist the final part of this work.

## 1.1 Layout of the thesis

In this section, the work done during the project is presented in an approximate chronological order. Later in the thesis, the chapters are arranged in a manner to make the motive and organization of this work easier to understand. The major route for biodiesel production is a similar process in that it utilizes the reverse reaction of FAME glycerolysis. At some instances, where it was felt relevant, references to biodiesel production processes have been made.

Chapter 2 discusses briefly why and how mono- and diglycerides are produced. A short history and an overview of some of the processes used for monoglyceride production are given in this chapter. The advantages and disadvantages of some of the processes used commercially and under research have also been discussed.

Most of the monoglycerides are produced using batch processes. The aim of this work was to develop a continuous process to produce monoglycerides through FAME glycerolysis. For this purpose, a tray (distillation) column was considered to be potentially advantageous. Lab scale experiments followed by simulations were performed to investigate the feasibility of carrying out the FAME glycerolysis reaction in a tray column. This included studies on the liquid-liquid mixing and reaction rate on a single bubble cap tray followed by the simulation of the reaction in a tray column. These studies are covered in Chapter 4.

While the investigations on the tray column were being carried out, it was discovered that during the reaction, the glycerol concentration in the ester phase was not constant. Contrary to what is generally assumed, a significant increase in glycerol solubility in the ester phase was observed. Kimmel [1] suggested a kinetic model according to which the reaction takes place in the ester phase only. He also suggested that the increasing glycerol concentration in the ester phase was responsible for the autocatalytic reaction behavior. The formation of triglyceride, which is a byproduct of the reaction, was not taken into account in this model as it was produced only in small amounts [1].

The factors affecting the glycerol solubility were not known. In the reaction kinetics model, glycerol concentration in the ester phase was correlated linearly to the ester conversion. This correlation was an approximation and experimental data were needed to determine the parameters of the correlation under specific reaction conditions. For better predictions, the factors affecting the glycerol solubility had to be identified and a theoretical model was required to quantify the equilibrium phase composition. Chapter 3 deals with the attempts made in this direction. The predictive activity coefficient models used in this work were not found adequate for the description of phase equilib-

rium for the present multicomponent system. Consequently, the empirical correlation for glycerolysis solubility was used further for simulations in this work.

The final conversion obtained during the reaction on the bubble cap tray was much higher than obtained at atmospheric pressure without methanol stripping. It was observed that at higher conversions, significant amounts of triglycerides were formed that could not be neglected. Therefore, in this work, the formation of triglycerides was also included in the kinetic model. Moreover, data on glycerol solubility under conditions of methanol stripping was required. Experiments were carried out in a stirred tank reactor in liquid-batch mode to collect the required kinetic data. The simulations and experiments performed in batch mode are discussed in Chapter 5. During this part of the work, sampling and analytical techniques were improved to get more reliable data. These aspects are also covered briefly in Chapter 5.

Finally, the required parameters for the kinetic model were quantified. Simulations were performed to compare the expected conversion and monoglyceride selectivity among some simple continuous reactors. Based on the simulation results, a single CSTR was selected for experimental verification. Chapter 6 covers these investigations done on flow reactors.

## 1.2 Materials, equipments and softwares

The investigations in this work involved experiments, chemical analysis, kinetic modeling and simulations. This required the application of different materials, equipments and computer software. This section provides an overview of these equipments, materials and software for a quick reference. The details of experimental procedures are provided in the respective chapters.

### 1.2.1 Materials

The chemicals used as reactants, catalyst, solvent etc. were the same in all the experiments. The details are given below:

**Reactants:** Glycerol (>99%, Sigma) and methyl oleate (>75%, Lancaster) were used as received.

**Catalyst:** Sodium methylate (30% in methanol, Fluka).

#### Chemicals used for GC analysis

**Calibration:** Glycerol (>99%, Sigma), methyl oleate (99%, Aldrich), monoolein (99%, Sigma), diolein (99%, Sigma), triolein (>99%, Fluka) and methanol (>99.9%, Roth) were used to obtain calibration plots for GC.

**Preparation of samples:** For sample preparation, 1,4-dioxane (>99.8%, Roth) was used as a solvent. Acetic acid (>99.8%, Fluka) was used to neutralize the catalyst. N,O-bis-(trimethylsilyl)-trifluoroacetamide (BSTFA) (98%, ABCR) was used as a silylating agent. Hexadecane (>98%, Fluka) was used as an internal standard. Details of sample preparation and analysis are given in Section 5.1.

## 1.2.2 Equipments

### Photography:

Direct photography was implemented to determine drop sizes in the liquid-liquid mixture with and without reaction. The photographic technique is explained in Section 4.1. A CCD camera (CV-M10 BX, JAI) fitted with an endoscope and synchronized with a flash (Drelloskop 250, Drello) through a computer was used to photograph the drops. The light from the flash was directed to the endoscope through an optical fiber cable.

### Liquid-liquid equilibrium (LLE) experiments

Two jacketed glass vessels were used to carry out experiments to collect LLE data. One vessel had a volume of 60 ml in which stirring was provided by a magnetic stirrer. The second had a volume of 5 ml and stirring was provided by a specially designed teflon impeller. The temperature was measured using a PT-100 probe. Heating was provided by a thermostatically controlled oil bath (HAAKE F6/B5) for both the vessels. The experiments are described in Section 3.3.

### Reactors

The glycerolysis reaction was carried out in different reactors mentioned below. In all cases, the temperature was measured by a PT-100 probe. Heating was provided by an oil bath (Haake F6/B5 or F3/S).

**Single bubble cap tray reactor:** Liquid-liquid mixing and reaction kinetics were investigated in a jacketed cylindrical glass vessel with a single a bubble cap tray. Details of the equipment and the experimental procedures are presented in Sections 4.1 and 4.2.

**Batch reactors:** A 0.5 liter glass reactor (Wertheim LF-100) was used for standard experiments. The vessel was fitted with removable four baffles and stirring was done with a standard six flat-blade turbine impeller. Dimensions of the standard reactor are given in Appendix A.4. A smaller 250 ml, four necked glass vessel with stirring provided by magnetic stirrer was used for some test reaction runs. A silicone tube with

perforations was used as gas distributor for methanol stripping. Further details can be found in Section 5.1.

**Continuous flow reactor:** The standard reactor (Wertheim LF-100) was used to carry out reactions in continuous mode. In this case the feed and exit product flow was provided by diaphragm pumps (CGM prominent, A2001).

### **Equipments for chemical and physical analysis**

**Gas chromatograph:** The chemical composition of the samples was determined by gas chromatography. The equipment was HP 5890, Series-II GC with flame ionization detector. The injection volume was 5.0  $\mu\text{m}$  (splitless). A deactivated fused silica tubing (3 m x 0.53 mm) coated with cyanophenylmethyl (VARIAN) was used as precolumn. The GC column (DB5-HT, J & W) had a length of 30 m, an inner diameter of 0.32 mm and a film thickness of 0.1  $\mu\text{m}$ . Nitrogen gas was used as carrier.

**Rotational viscometer:** The viscosity of the reactant and product liquid phases was measured in some of the experiments. A rotational viscometer (Contraves Rheomat 115) was used for this purpose (Section 4.1).

**Contact angle meter:** The surface- and interfacial tension of some liquid samples were measured using a contact angle meter (Dataphysics OCA 15) (Section 4.1).

### **1.2.3 Software tools**

All calculations regarding prediction of liquid-liquid equilibrium data were performed using MATLAB (version 6.0) programs (Chapter 3). ASPEN plus and ASPEN split (version 11.1) were used for some test simulations. Equations for kinetic modeling were solved using ASPEN custom modeler (ACM) (version 11.1). Parameter estimation were also done using ACM (Chapter 5). All process simulations, namely, tray column (Chapter 4), batch reactor (Chapter 5), and continuous reactors (Chapter 6) were carried out using ACM. The drop size analysis explained in Section 4.1 was performed using the software "Bubble count", which was developed at the Process Engineering Institute, T.U. Berlin. Origin (Version 7) was used for curve fitting to drop size distributions. A MATLAB program was also used for the analysis of the GC data.

## Chapter 2

# Monoglycerides: Uses and Production Technology

Monoglycerides are fatty acid monoesters of glycerol. They are generally available as a mixture containing large amounts of diglycerides and small amounts of fats and glycerol. Mono- and diglycerides comprise nearly 70% of the emulsifier usage in food industry [3]. These emulsifiers are allowed worldwide as food additives. In the European Union, mono- and diglycerides are classified as the food additives class E471 and in the US, they hold a GRAS (generally recognized as safe) status. In foods, they are used in baked products, chocolates, ice creams, margarine, noodles etc. Nearly 60% of all monoglycerides are used in bakery [4]. Mono- and diglycerides were the first fatty emulsifiers to be added to foods. Although these chemicals were first synthesized more than 150 years back, it took many decades until their commercial applications were discovered around 1930. The first production of monoglycerides in the USA was done in 1929 [5] and the first US patent for the use of mono- and diglycerides in food was granted in 1933 for use in emulsions and margarine [6,7]. Functions of emulsifiers in food systems are explained in literature [8,9]. Mono- and diglycerides are also used in cosmetics and pharmaceutical industry to make creams etc. They are also used as a starting material for the production of other surface active chemicals [3,10–12]. Other important uses of monoglycerides are discussed in literature [13].

Mono- and diglycerides are produced in three concentration levels: 40 to 46% monoglycerides; 52% minimum mono-glycerides; and distilled, with >90% monoglycerides content. In industry, the mixture containing high amounts of diglyceride is often referred to as mono-diglycerides to differentiate it from the distilled monoglycerides. Typical composition of mono-diglycerides and distilled monoglycerides is shown in Table 2.1. Higher fraction of monoglycerides is desired in the product mixture, since



they are better emulsifiers than diglycerides. Mono-diglycerides were first manufactured in 1853 by Berthelot through the glycerolysis of fatty acids [9]. He synthesized monoglycerides by heating stearic acid with an excess of glycerol for 20 hours at 200°C. Apparently, the first patent on fat glycerolysis was issued in 1924 to Grün [14,15]. Grün patented a process to produce mixed triglycerides in a two step process. The conversion of fats to mono- and diglycerides by glycerolysis was the first step of this process. Many processes on fat glycerolysis have been patented thereafter. Sonntag [14] provided a short list of patents on fat glycerolysis.

**Table 2.1:** Composition of mono-diglycerides and distilled monoglycerides (in wt%). Source: [5]

	Mono-diglycerides	Distilled monoglycerides
Monoglycerides	35-60	90-96
Diglycerides	35-50	1-5
Triglycerides	1-20	<1
Glycerol	1-10	<1
Free fatty acids	1-10	<1

Most of the mono- and diglycerides are manufactured by the glycerolysis of fats and oils [3, 14]. This reaction is carried out at high temperatures ( 250 – 280°C), generally in the presence of basic catalysts. After the reaction reaches equilibrium, the catalyst is deactivated by adding an acid, normally phosphoric acid and the reaction mixture is cooled down to stop the reaction. The excess glycerol is separated and the product obtained is a mixture of mono-, di-, triglycerides and dissolved glycerol. The mono- and diglyceride content in this product mixture is typically 40-60% and 30-45% respectively [3]. Acidic catalysts can also be used but acid catalyzed reactions are much slower. Acidic catalysts are preferred with feed containing high amounts of free fatty acids. Higher fractions (>90%) of monoglycerides are obtained by molecular distillation of the mixture containing mono- and diglycerides [11,13]. Monoglycerides can be manufactured either batchwise or continuously, however a large portion of the monoglyceride demand is still produced with batch process [3].

Although mono-diglycerides have been produced since many decades, the processes involved are slow and give low monoglyceride yields. There have been constant attempts to develop better processes for the production of monoglycerides. Fat glycerolysis is an equilibrium limited reaction where two liquid phases coexist throughout the reaction. The solubility of glycerol in triglycerides is limited even at high temperatures, therefore the law of mass action cannot be simply applied based on total concentrations and an excess of glycerol does not guarantee higher equilibrium conversions. To overcome these limitations, some investigators used solvents to carry out

this reaction in a homogeneous phase. Mostly, the solvents used for this purpose were pyridine, 1,4-dioxane and phenols [14]. These solvents are not suitable for producing food grade monoglycerides as they are toxic. A recent US patent [16] claims to use a food grade polar solvent (methyl lactate and lactic acid) to obtain high yields of monoglycerides. Some researchers have also used supercritical carbon dioxide as reaction media [14,17]. A US patent [18] describes a solvent free homogeneous process for monoglyceride production. In this process, very high molar ratio of glycerol to fat (3200:1) was used with and without catalyst. Another solvent and catalyst free process is mentioned in the US patent [19]. According to this process, glycerol and fats to be reacted are added at a controlled rate into a reaction mixture containing specific amounts of mono- and diglycerides under controlled condition of temperature. Both the patented processes require high temperatures ( $\sim 280^{\circ}\text{C}$ ) and claim very high content of monoglycerides ( $>80\text{ wt}\%$ ) in the processed product. Information on commercialization of these processes was not found. The use of lipase enzymes to catalyze fat glycerolysis has also been widely investigated [20–22]. Although they have not yet been commercialized for the bulk production of monoglycerides because of slower reaction rates, they provide a promising alternative that is more energy efficient and gives higher yields of monoglycerides than acid or base catalyzed fat glycerolysis. Recently some authors [23] have reported faster reactions giving high yields ( $\sim 70\text{ wt}\%$ ) of monoglyceride using enzymatic glycerolysis in tert-butyl alcohol.

The base catalyzed fat glycerolysis process itself is not well understood and is still an area of active research [14,24–26]. The kinetics of this reaction is not well known, probably owing to its multiphase nature and problems involved in sampling and analyzing the reaction mixture. A simplified chemical equation representing fat glycerolysis is shown in Figure 2.1. It is believed that the fatty acid residues of the fats are randomly distributed among the hydroxyl group of the glycerol, thus fixing the relative proportions of the components statistically [4]. Another process for monoglyceride production, the base catalyzed glycerolysis of fatty acid methyl esters is similar to fat glycerolysis but it has certain advantages over fat glycerolysis [14,27]. Compared to fat glycerolysis, this reaction is energy saving and faster reaction rates and higher final conversions can be achieved by removing the product methanol from the reaction mixture by means of vacuum or inert gas stripping. An important advantage, however, is that monoglycerides for specific end use can be prepared by selecting an ester of a desired fatty acid. A simplified chemical equation for FAME glycerolysis is shown in Figure 2.2. The relative amount of 1-monoglyceride and 2-monoglyceride in the product mixture is a result of an equilibrium which is temperature dependent. At  $200^{\circ}\text{C}$ , the equilibrium content of 1-monoglyceride is 85%, whereas at  $20^{\circ}\text{C}$  it is

95% [11]. Processes involving FAME glycerolysis have not been as much investigated as fat glycerolysis. A process based exclusively on FAME glycerolysis was patented in the recent years [27].

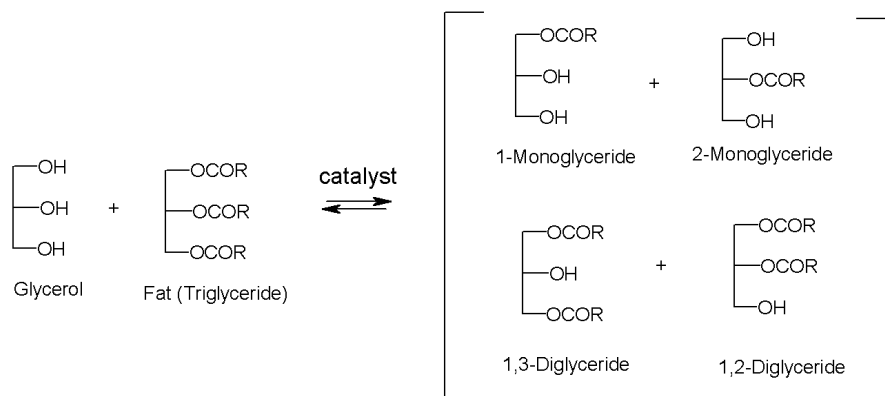


**Figure 2.1:** Simplified chemical equation for fat glycerolysis (R=alkyl chain of fatty acid, which may be same or different in the fat molecule).

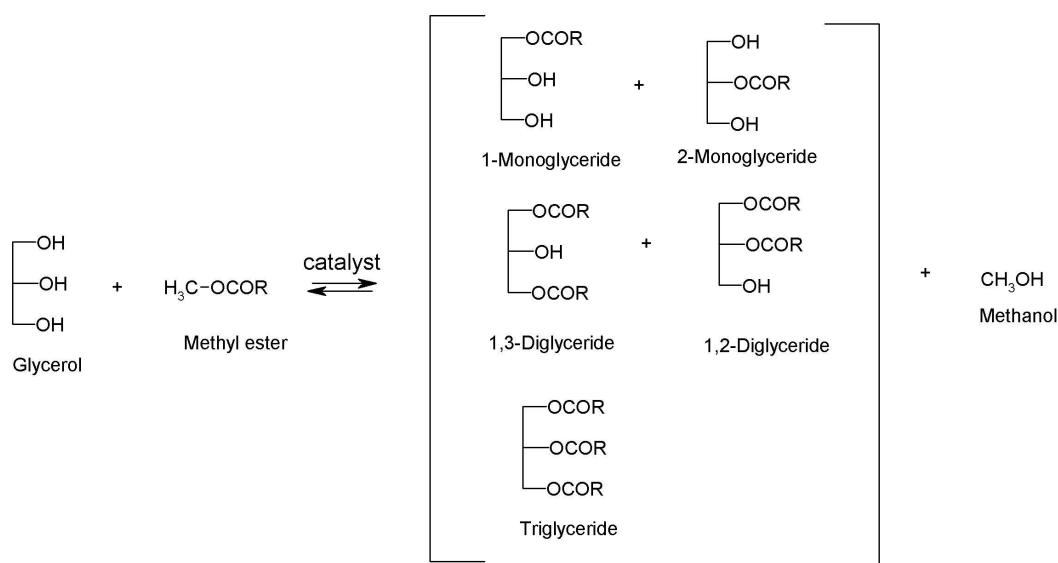


**Figure 2.2:** Simplified chemical equation for FAME glycerolysis (R=alkyl chain of fatty acid).

The reverse reaction of FAME glycerolysis, i.e., the methanolysis of fats is the major route for biodiesel production [28]. Due to depleting petroleum resources and environmental concerns, research on biodiesel production has assumed importance in the last few decades especially in Europe and USA. A large portion of biodiesel is also manufactured by batch processes and new continuous processes are being researched [29–32]. The kinetics of base catalyzed fat methanolysis has also been an active area of investigation [24,33–36].

The glycerolysis of fats/FAME and the methanolysis of fats share some common aspects and knowledge gained from one system can be useful for others as well. All of them represent liquid-liquid reaction with an alcohol and a fatty phase. Another common aspect is that in a batch reaction, the conversion-time curve of the limiting reactant, which is almost always in the fatty phase, shows an 'S' form. This means that the reaction begins with a slow rate, gets accelerated at intermediate conversions and finally slows down again as the equilibrium conversion is approached. Different authors have given different explanations for this behavior [1,24,33,37]. As it was discovered for the presently investigated glycerolysis reaction, the changing phase composition also affects the reaction rate. The aspects of phase equilibria have generally not been considered in kinetic studies in these multiphase transesterification reactions. Only recently, a group published its experimental results on phase equilibrium in a biodiesel production process [38].

An intensive study on FAME glycerolysis was carried out by Kimmel at the Institute for Chemistry, Technical University Berlin [1]. In his work, Kimmel provided answers to some of the previously unknown facts about this reaction, especially those concerning drop size distributions and reaction rate, glycerol solubility, and sampling and analysis of the reaction mixtures. Based on his studies in batch reactor, Kimmel presented a kinetic model for the reaction. The present work is in continuation to Kimmel's investigations on FAME glycerolysis. This work is focused more on the continuous production of monoglycerides.

## Chapter 3

# Liquid-Liquid Reactions and Phase Equilibrium

### 3.1 Liquid-liquid reactions

In some liquid phase reactions, the reactants may not be completely miscible under the operating conditions and two liquid phases exist partly or throughout the reaction. Such processes involving reaction between two liquid phases are not uncommon in industry [39]. Generally, agitated contactors are used for liquid-liquid reactions. In a reaction involving two liquid phases  $A$  and  $B$ , there can be many possibilities for the reaction to take place. For example; ( $a$ ): in the bulk of liquid  $A$  and/or  $B$  (slow reactions), ( $b$ ): in the film of  $A$  and/or  $B$  (usually fast reactions), ( $c$ ): all combinations of cases  $a$  and  $b$ , and ( $d$ ): at the interface (usually instantaneous reactions). Generally, the reaction regime is dependent on the operating conditions, but it is also possible that the reaction regime changes with time under the same operating conditions. Thus, in some cases the modeling of a liquid-liquid reaction can be complicated and therefore some simplifying assumptions are generally made.

FAME glycerolysis reaction involves glycerol and ester as two reactant liquid phases. It was found experimentally<sup>1</sup> that almost no ester is soluble in the glycerol phase and glycerol has a small solubility in the ester phase at the reaction temperature. The catalyst is present in both phases, although a higher fraction is dissolved in glycerol phase [1]. So the reaction in the glycerol phase can be neglected and the reaction can be considered to be taking place in the ester phase only. If glycerol and ester phases are represented by  $A$  and  $B$  respectively then the possible reaction regimes that could

---

<sup>1</sup>See Section 3.4

exist for such a system are discussed in the following section.

### 3.1.1 Reaction regimes

Depending on the relative rates of diffusion and reaction, a fluid-fluid reaction system may be classified into many regimes. In the following discussion, the reaction regimes are broadly divided into slow and fast regimes. A detailed description of different reaction regimes is given by Doraiswami and Sharma [39]. The two reactants are represented by  $A$  and  $B$ , where  $A$  is slightly soluble in  $B$ , and  $B$  is not soluble in  $A$ . Hence the reaction occurs in the  $B$  phase only and the mass transfer resistance is also confined to the  $B$  phase. The following reaction regimes are possible in such a system.

#### *Slow reaction regimes*

**Regime 1a:** This regime represents the case when the reaction between the dissolved  $A$  and  $B$  is much slower than the rate of transfer of  $A$  into  $B$ . The phase  $B$  will be saturated with solute  $A$  at any moment and the rate of product formation will be determined purely by the reaction kinetics. The mass transfer resistance and hence the size of the interface is unimportant in this regime. Here, the solubility of  $A$  in phase  $B$  is the limiting factor.

**Regime 1b:** In this regime, the rate of reaction is faster than the rate at which  $A$  is transferred into the  $B$  phase. The concentration of  $A$  in phase  $B$  is zero and the consumption of  $A$  in bulk is much higher as compared to that in film. Here, the mass transfer is the rate controlling factor and therefore the interface size comes into picture in the reaction model.

**Regime 1c:** This could be considered as a regime between the above two, i.e. the reaction is taking place in the bulk but there is a finite concentration of  $A$  in phase  $B$  which is less than the respective saturation concentration. Here also, the interface size affects the overall reaction rate.

#### *Fast reaction regimes*

**Regime 2:** This includes the cases where the reaction takes place entirely in the film or partially in the bulk and the reaction rate is determined both by mass transfer and reaction rate. Interfacial size is required for kinetics modeling.

**Regime 3 (Instantaneous reaction):** In this case, the reaction can be considered to be taking place at a plane at some distance inside the film, and the reactant consumption rate is determined by mass transfer limitations alone.

### 3.1.2 FAME glycerolysis: Where does the reaction take place?

Two liquid phases in FAME glycerolysis reaction are generally stirred at high speeds to maximize the contact between the reactants. This leads to one phase being dispersed into the another as long as the agitation is continued. Depending on the fluid properties and agitating conditions, the dispersion could be methyl ester in glycerol (ME/G) or glycerol in methyl ester (G/ME) type. The dispersion type was G/ME in most of the experiments in this study. In such cases, the reaction takes place in the continuous phase. Here the term reaction is meant to include all reaction steps. Earlier studies [1] showed that under complete dispersed conditions, higher stirring rates did not accelerate the reaction. Furthermore, a reaction carried out with an inversion (ME/G dispersion) at a stirrer speed of 600 rpm showed no different conversion rate compared to reaction in G/ME dispersion at 550 rpm and at the same temperature (Section 5.3.1). For agitated liquid-liquid systems the Sauter mean diameter  $d_{32}$  can be correlated to Weber number as:

$$d_{32} \propto We^n \quad (3.1)$$

For a stirred tank:

$$We = \frac{N^2 D^3 \rho}{\sigma} \quad (3.2)$$

here  $N$ ,  $D$  and  $\sigma$  are stirring speed, impeller diameter, and fluid-fluid interfacial tension respectively. The exponent  $n$  in Equation 3.1 is generally taken to be -0.6. For the stirred tank used in our studies, the Sauter mean diameter was better correlated to the stirrer speed by

$$d_{32} \propto N^{-1.95} \quad (3.3)$$

[1], giving a value of -0.98 for the exponent  $n$  in Equation 3.1. Hence, the Sauter mean diameter can be correlated to the continuous phase density by:

$$d_{32} \propto \rho^{-0.98} \quad (3.4)$$

The specific interfacial area can be estimated as:

$$a = \frac{6\phi}{d_{32}} \quad (3.5)$$

where  $\phi$  is the dispersed phase fraction. The continuous phase density and dispersed phase fraction were higher in ME/G dispersion ( $\phi = 0.6$ ,  $\rho = 1.26$ , initial) than in G/ME dispersion ( $\phi = 0.3$ ,  $\rho = 0.87$ , initial). Therefore, a higher interfacial area ( $\sim 2.9$

times, initially) is expected for ME/G dispersion. So the reaction rate would be higher if mass transfer were the controlling factor. The absence of mass transfer limitation would indicate that the ester phase is nearly saturated with glycerol at all times during the reaction and the reaction is taking place only in the bulk phase (Regime 1a). Earlier experiments carried out at lower stirrer speeds [2] showed dependency of reaction rate on stirrer speed, which implied that mass transfer limitation was present and the reaction was also taking place in the film near the interface (Regime 1c). These facts were apparently somewhat contradictory. In what follows, it is tried to find the reason for this behavior following film theory.

Drop size measurements during the reaction showed Sauter mean drop sizes of 80-120  $\mu m$  in a stirred tank [40]. For a glycerol:ester molar ratio of 2:1, the dispersed phase fraction is 0.30 in a G/ME dispersion. An estimate of film thickness can be made as:

$$\delta_l = \frac{D_{AB}}{k_l} \quad (3.6)$$

where  $D_{AB}$  and  $k_l$  are the diffusion coefficient and the mass transfer coefficient in the continuous phase respectively. Based on the initial reaction conditions,  $D_{AB}$  and  $k_l$  are calculated to be  $D_{AB}=5 \times 10^{-9} m^2 s^{-1}$  and  $k_l=1 \times 10^{-4} m s^{-1}$  respectively. The values of  $D_{AB}$  and  $k_l$  were calculated by Wilke-Chang and Calderbank-and-Moo-Young correlations<sup>2</sup>. With this data, Equation 3.6 gives a film thickness of 50  $\mu m$ . With this film thickness, the total film volume around the glycerol droplets was calculated to be more than the volume of the continuous phase. Hence, the continuous ester phase where the reaction is taking place can be expected to be present as a thin film and not as a bulk phase. Therefore, under well dispersed conditions, mass transfer limitation cannot be expected. The maximum average droplet size required to keep the continuous phase as a thin film can be calculated to be 400  $\mu m$  in a dispersed phase fraction of 0.30 or more. The stirrer speed needed to produce this drop size can be estimated from Equation 3.1 as:

$$N_2 = \left\{ \frac{d_{32(2)}}{d_{32(1)}} \right\}^{1/2n} \cdot N_1 \quad (3.7)$$

From a known value of  $d_{32(1)}$  ( $=200 \mu m$ ) at a stirrer speed of 550 rpm [1], the speed required to produce average drop diameter of 400  $\mu m$  is calculated to be 385 rpm. The minimum stirrer speed to disperse glycerol completely into methyl ester was around 400 rpm in experiments. Hence, mass transfer limitations can appear at lower stirrer speeds. Also, speeds much above the just fully dispersed state are not expected to

---

<sup>2</sup>See Appendix A.1



bring any significant improvement in the reaction rate. The initial drop sizes in the reactant mixture are bigger than during the reaction [40], especially on a bubble cap tray<sup>3</sup>. Therefore, the presence of an initial mass transfer limited regime (Regime 1c) can be expected in some cases, depending on the agitation conditions.

In the absence of mass transfer limitations, the reaction rate is limited by the glycerol solubility in the ester phase. The solubility of glycerol increases as the reaction proceeds and the ester phase can be assumed to be nearly saturated with glycerol at all times during the reaction. Methanol, which is one of the reaction products, favors the reverse reaction strongly. At the reaction temperature, methanol is highly volatile and its amount in the liquid phase is determined by the operating pressure, and to a lesser extent by the liquid composition. Hence, for a better understanding of the kinetics, it was a prerequisite to describe the phase equilibrium in this system. So the vapor-liquid-liquid equilibrium (VLLE) of the system was studied theoretically and experimentally. In preliminary experiments on VLLE, it was found that only methanol was present in the vapor phase. Therefore, only the liquid-liquid equilibrium was investigated in detail.

## 3.2 Phase equilibrium

In systems involving more than one phase, the equilibrium concentrations are often a limiting factor. In the present reaction system, liquid-liquid-vapor phases coexist during the reaction. Generally, the equilibrium between different phases is represented by the equality of fugacity of a component in all the phases. For example, for a liquid-liquid-vapor system at equilibrium:

$$f_i^{L1} = f_i^{L2} = f_i^v \quad (3.8)$$

Two approaches of calculating the fugacities are available, the equation of state method and the activity coefficient method.

In the *equation of state (EOS)* method:

$$f_i^v = \phi_i^v y_i P \quad (3.9)$$

$$f_i^l = \phi_i^l x_i P \quad (3.10)$$

Where  $\phi_i^v$  and  $\phi_i^l$  are the fugacity coefficients of component  $i$  in the vapor and liquid respectively and they are calculated using an equation of state.

---

<sup>3</sup>See Section 4.1

Although equation of state models have proven to be reliable in predicting properties of most hydrocarbon based fluids over a large range of operating conditions, their application has been limited to primarily non-polar or slightly polar components. At low pressures, polar or non-ideal chemical systems have traditionally been handled using dual model approach (Activity coefficient method) [41]. In this approach, an equation of state is used for predicting the vapor fugacity coefficients (normally ideal gas assumption or the Redlich Kwong, Peng-Robinson equations of state etc.) and an activity coefficient model is used for the liquid phase.

In the *activity coefficient* method:

$$f_i^v = \phi_i^v y_i P \quad (3.11)$$

$$f_i^l = x_i \gamma_i f_i^o \quad (3.12)$$

Where  $\gamma_i$  is the liquid phase activity coefficient of component  $i$  and  $f_i^o$  is the liquid fugacity of pure component  $i$  at mixture temperature. Here, the vapor phase fugacity is calculated in the same way as in the EOS method. But the second equation incorporates an activity coefficient model.

### 3.2.1 Activity coefficient models

For an ideal liquid phase, the activity coefficient of a component is equal to unity. For non-ideal liquids, the liquid phase activity coefficient can be calculated by an activity coefficient model. Commonly used models include Wilson (VLE for miscible liquids), NRTL (*Non Random Two Liquid*, for multicomponent VLE, LLE, VLLE), UNIQUAC (*Universal Quasi Chemical*, for multicomponent VLE, LLE, VLLE) and UNIFAC (*Uniquac Functional Group Activity Coefficients*, for multicomponent VLE, LLE, VLLE) [42].

UNIFAC is based on group contribution methods [43]. In such group contribution methods the multicomponent liquid mixture is considered as a mixture of so called functional groups. In this approach, each molecule is broken down into smaller functional groups. The basic idea is that the molecular interactions are not really molecule-molecule interactions, rather are interactions between specific functional groups in each molecule. All group contribution methods are approximate, because the effect of one certain group in one molecule is not necessarily exactly the same as the effect of the same group in another molecule. Since a small number of functional groups can be combined to give a large number of molecules, the advantage of this method is that data collected from a small number of experiments can be used to predict the behav-

ior of a relatively big number of mixtures. For highly non-ideal systems UNIFAC has therefore gained much popularity in the last decades.

### 3.2.2 UNIFAC model

In UNIFAC model, the activity coefficient is divided into two parts<sup>4</sup>

$$\ln \gamma_i = \ln \gamma_i^C + \ln \gamma_i^R \quad (3.13)$$

where the superscripts  $C$  and  $R$  represent the combinatorial and the residual parts respectively. The development of UNIFAC is based on the UNIQUAC model, which itself is derived based on statistical thermodynamics [45]. In UNIQUAC the combinatorial part of the activity coefficient describes the phenomena caused by size differences of the molecules and the residual part represents the energetic interactions. In UNIFAC model the combinatorial part of UNIQUAC is used, and for the residual part, a model based on the group contribution has been developed. The combinatorial part for a component system containing  $nc$  different molecules, is given by

$$\ln \gamma_i^C = 1 + \phi_i + \ln \phi_i - \frac{z}{2} \left( 1 - \frac{\phi_i}{\theta_i} + \ln \frac{\phi_i}{\theta_i} \right) \quad (3.14)$$

$$\phi_i = \frac{r_i}{\sum_j^{nc} x_j r_j} \quad (3.15)$$

$$r_i = \sum_k v_k^i R_k \quad (3.16)$$

$$\theta_i = \frac{q_i}{\sum_j^{nc} x_j q_j} \quad (3.17)$$

$$q_i = \sum_k v_k^i Q_k \quad (3.18)$$

$Q_k$  and  $R_k$  are the scaled van der Waals surface area and volume parameters respectively for each group and  $z$  is the coordination number that equals 10. The residual part, dealing with the  $ng$  kinds of groups in the mixture, can be obtained by the following relations:

---

<sup>4</sup>Refer [44] for a detailed description of UNIFAC.

$$\ln \gamma_i^R = \sum_k^{ng} \nu_k^{(i)} (\ln \Gamma_k - \ln \Gamma_k^{(i)}) \quad (3.19)$$

$$\ln \Gamma_k = Q_k (1 - \ln(\sum_m^{ng} \Theta_m \Psi_{mk})) - \sum_m^{ng} \frac{\Theta_m \Psi_{km}}{\sum_n^{ng} \Theta_n \Psi_{nm}} \quad (3.20)$$

$$(3.21)$$

the group-group interaction parameter is given by

$$\Psi_{nm} = \exp(-a_{nm}/T) \quad (3.22)$$

$$a_{nm} \neq a_{mn}$$

and the group area fraction  $\Theta_m$  and group mole fraction  $X_m$  are given by the following equations

$$\Theta_m = \frac{Q_m X_m}{\sum_n^{ng} X_n Q_n} \quad (3.23)$$

$$X_m = \frac{\sum_j^{nc} \nu_m^j}{\sum_j^{nc} \sum_n^{ng} \nu_n^j x_j} \quad (3.24)$$

The UNIFAC-Dortmund model differs from UNIFAC in that the combinatorial part is slightly modified, and different van der Waals quantities and new temperature dependent interaction parameters are introduced. The combinatorial part of UNIFAC-Dortmund is similar to Equation 3.14 and is given by:

$$\ln \gamma_i^C = 1 + \phi'_i + \ln \phi'_i - \frac{z}{2} (1 - \frac{\phi_i}{\theta_i} + \ln \frac{\phi_i}{\theta_i}) \quad (3.25)$$

$$\phi'_i = \frac{r_i^{3/4}}{\sum_j^{nc} x_j r_j^{3/4}} \quad (3.26)$$

The new temperature dependent parameters are given by:

$$\Psi_{nm} = \exp((-a_{nm} + b_{nm}T + c_{nm}T^2)/T) \quad (3.27)$$

UNIFAC groups, subgroups and parameters for a multicomponent system containing glycerol, methanol, methyl oleate, 1-monoolein and 1,3-diolein are given in Appendix A.2.

**Table 3.1:** Division of molecules into groups according to UNIFAC-LLE/VLE.

	$CH_3$	$CH_2$	$CH$	$CH_3COO$	$OH$	$C_2H_2$	$CH_2COO$
Methyl oleate ( $C_{19}H_{36}O_2$ )	1	14	0	1	0	1	0
Glycerol ( $C_3H_8O_3$ )	0	2	1	0	3	0	0
Methanol <sup>a</sup> ( $CH_3OH$ )	1	0	0	0	1	0	0
Monoolein ( $C_{21}H_{40}O_4$ )	1	15	1	0	2	1	1
Diolein ( $C_{39}H_{72}O_5$ )	28	1	0	0	1	2	2

<sup>a</sup> grouped as  $CH_3OH$  in UNIFAC-VLE

Initially, the UNIFAC method was used to predict the equilibrium concentrations for the present transesterification system. Although the UNIFAC-LLE uses parameters derived from data in the temperature range 10-40°C [46], but some investigators have used UNIFAC for glycerolysis reaction system at 150°C [47, 48]. In this work, both parameter sets, derived from LLE and VLE data were used with the UNIFAC model. The model predictions for the ternary glycerol-methanol-methyl oleate at 60°C were in good agreement with the experimental results, however, large deviations from experimental data were observed in the presence of high fractions of monoglyceride.

Since the UNIFAC model was not able to predict the equilibrium compositions correctly, a modified version of UNIFAC, UNIFAC-Dortmund method was tested. UNIFAC-Dortmund was introduced by Weidlich and Gmehling [49] in 1987. This method has several advantages over UNIFAC. Some advantages relevant to the present system are; (a): it uses a single set of parameters for LLE and VLE prediction that are valid in the temperature range of about 15-150°C, (b): it accounts for the secondary and tertiary -OH groups, and (c): it can be used for dilute solute concentrations. Table 3.1 shows the major components present in the FAME glycerolysis reaction mixture and their group division according to UNIFAC. While dividing the components into groups, for modeling purpose, it was assumed that the methyl ester is 100% methyl oleate, monoolein is 100% 1-monoglyceride and diolein is 100% 1,3-diglyceride. No triolein was taken into account as it was observed only in small quantities in the reaction mixture in earlier experiments [1]. The grouping is slightly modified for UNIFAC-Dortmund [50] and is shown in Table 3.2. The model equations were solved using a MATLAB (version 6) program.

**Table 3.2:** Division of molecules into groups according to UNIFAC-Dortmund.

	CH <sub>3</sub>	CH <sub>2</sub>	CH	CH <sub>3</sub> COO	OH	C <sub>2</sub> H <sub>2</sub>	CH <sub>2</sub> COO	OH-s	CH <sub>3</sub> OH
Methyl oleate	1	14	0	1	0	1	0	0	0
Glycerol	0	2	1	0	2	0	0	1	0
Methanol	0	0	0	0	0	0	0	0	1
Monoolein	1	15	1	0	1	1	1	1	0
Diolein	28	1	0	0	0	2	2	1	0

### 3.2.3 Phase equilibrium computation

In a liquid-liquid system, if the number of moles of component  $i$  in the feed are given by  $F_i$ , and at equilibrium the phases are split into  $L'$  and  $L''$  moles with component mole fractions  $x'_i$  and  $x''_i$  respectively, the phase compositions can be calculated by the following equations:

$$x'_i L' + x''_i L'' - F_i = 0 \quad (3.28)$$

$$x'_i \gamma'_i - x''_i \gamma''_i = 0 \quad (3.29)$$

$$\sum_i x'_i - 1 = 0 \quad (3.30)$$

$$\sum_i x''_i - 1 = 0 \quad (3.31)$$

The above equations represent  $2n + 2$  equations for  $2n + 2$  variables for a two phase system with  $n$  components. If a vapor phase is also present in equilibrium with the two liquid phases, then the system has  $3n + 3$  variables. In this case Equation 3.28 is replaced by:

$$y_i V + x'_i L' + x''_i L'' - F_i = 0 \quad (3.32)$$

where  $V$  is the moles in vapor phase and  $y_i$  is the component mole fraction in vapor. The summation equation for vapor phase is given by:

$$\sum_i y_i - 1 = 0 \quad (3.33)$$

At low pressures, ideal gas behavior can be assumed, hence  $\phi_i^v = 1$  in Equation 3.11, and  $f_i^o = p_i^o$ , the saturation pressure of pure component  $i$  at system temperature. With these simplifications, using the activity coefficient method, the condition at equilibrium can be expressed as:

$$x'_i \gamma'_i p_i^o = x''_i \gamma''_i p_i^o = y_i P \quad (3.34)$$

Equations 3.33 and 3.34 represent the additional  $n + 1$  conditions required to calculate the  $3n + 3$  variables in a VLLE system. This system of non-linear equations can be solved by Newton method [51]. The calculation of LLE generally requires precise initial guess values. The activity coefficients are sensitive to small changes in mole fractions, which can make the solver diverge easily or converge to a false solution representing the original feed composition. This makes LLE calculations more difficult than calculating VLE. MATLAB programs were used to solve the LLE equations. The solution did not converge for the VLLE calculations (with methanol at higher temperatures). For simulation of systems involving vapor phase, a built-in procedure in ASPEN Custom Modeler was used (Chapter 4).

### 3.3 Experimental

As mentioned earlier, Kimmel found in his work that the glycerol concentration in the ester phase increases with conversion during FAME glycerolysis reaction. LLE calculations with component system glycerol-monoolein-methyl oleate showed that an increasing concentration of monoolein leads to higher equilibrium concentrations of glycerol in the ester phase. Computation of LLE with glycerol-diolein-methyl oleate ternary also showed a little increase in glycerol concentration in the ester phase with increasing diolein concentration<sup>5</sup>. The experimentally measured values of glycerol concentrations during the reaction were much higher than those predicted by computation. It was assumed that in the reaction system, the ester phase is always nearly saturated with glycerol, or in other words, the two phases were assumed to be in a quasi physical equilibrium. For a better understanding of the system, an appropriate activity coefficient model was needed. The aim of the LLE experimental work was two-fold, firstly, to see if monoglyceride was really responsible for the observed effect and also to see if methanol plays a role in increasing the mutual solubility of the two phases, and secondly, for the validation of the model to be used further for process simulations (UNIFAC, UNIFAC-Dortmund). Experiments with pure diolein were not performed due to its very high cost.

---

<sup>5</sup>Monoolein and diolein are the mono- and diglycerides produced by the glycerolysis of methyl oleate

### 3.3.1 Materials and analytical equipment

The chemical used for the liquid-liquid phase equilibrium experiments were: glycerol (>99%, Sigma), methanol (>99.9%, Roth) and  $\alpha$ -monoolein (>99%, Fluka). For experiments with glycerol-monoolein-methyl oleate, pure methyl oleate (99%, Aldrich) was used whereas technical grade methyl oleate (>75%, Lancaster) was used for the experiments with glycerol-methyl oleate binary and glycerol-methyl oleate-methanol ternary systems. The analysis of the supplied technical grade methyl oleate showed that the actual methyl oleate (C18:1) content was  $85 \pm 1\%$  and the overall content of C18 (C18:0-C18:3) was  $97 \pm 1\%$ . The samples were analyzed by gas chromatography. 1,4-dioxane (>99.8%, Roth) was used as solvent for sample preparation. N,O-bis-(Trimethylsilyl)-trifluoroacetamide (BSTFA) (98%, ABCR) was used as silylating agent. Hexadecane (>98%, Fluka) was used as an internal standard. The pure chemicals mentioned above were used for the calibration. The analysis was done using a Hewlett-Packard 5890 Series-II GC with capillary column and flame ionization detector. The GC column (DB5-HT, J & W) had a length of 30 m and an inner diameter of 0.32 mm. A deactivated fused silica tubing (3 m x 0.53 mm) coated with cyanophenylmethyl (VARIAN) was used as precolumn. Nitrogen gas was used as carrier.

### 3.3.2 Experimental setup and procedure

The experiments with glycerol-methyl oleate binary and glycerol-methyl oleate-methanol ternary system were carried out in a 50 ml vessel in which stirring was provided by a magnetic stirrer. A vessel of smaller volume (5 ml) was used for the glycerol-methyl oleate-monoolein system, as pure monoolein and methyl ester are rather expensive. The initial liquid volume taken in the vessel was  $\sim 2$  ml in the latter case. The commonly available stirrers could not provide good mixing in this small volume with two fast separating liquid phases. So a teflon impeller was fabricated to achieve better liquid-liquid contacting. For the binary system, the two liquids were stirred at a high speed at the desired temperature for 6 hours. Samples taken at 20 minutes, 120 minutes and 360 minutes of stirring at the specified temperature did not show any significant difference in composition. Later, all samples were collected at 150 minutes of stirring. For the two ternary systems, similar experimental procedure was employed. The two immiscible components (glycerol and methyl ester) were added into the reactor in a specific molar ratio (glycerol: methyl oleate= 4:1), and the third component (methanol or monoolein) was added in steps to get phase compositions for different tie lines. The jacketed glass vessels were heated to the desired temperature



by a thermostatically controlled temperature bath. The temperature was measured using a PT-100 probe. Once the desired temperature was reached, it remained constant throughout the experiment, except at the time of sampling (max.  $-1.0^{\circ}\text{C}$ ). The phases were stirred at a high speed under well dispersed conditions for 150 minutes and then allowed to separate till both the phases were clear. This took a few minutes to a few hours. Samples were taken from both the phases with a clean  $10\ \mu\text{l}$  GC syringe (Ito corporation, Japan). Before taking the actual sample, the syringe was rinsed 4 times with the liquid. Maximum possible care was taken not to disturb the phases during sample withdrawal and to get the samples as clean as possible. In the experiments with methanol, after stopping the stirring, the methanol condensed on the vessel lid was not allowed to fall back into the liquid.

### 3.3.3 Analysis

The samples were analyzed by gas chromatography. The details of analysis are given in Section 5.1.

## 3.4 Results and discussion

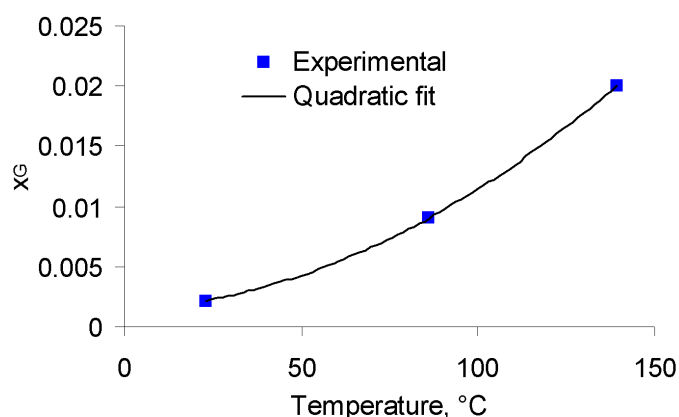
### 3.4.1 Glycerol-methyl oleate (binary): Effect of temperature

This two component system represents the initial components in the FAME glycerolysis reaction. One of the factors affecting the initial reaction rate is the solubility of glycerol in the ester phase at the reaction temperature. Figure 3.1 shows the solubility of glycerol in the ester phase at three different temperatures. No ester was detected in the glycerol phase in the LLE experiments.

### 3.4.2 Ternary LLE: Comparison of experimental and predicted data

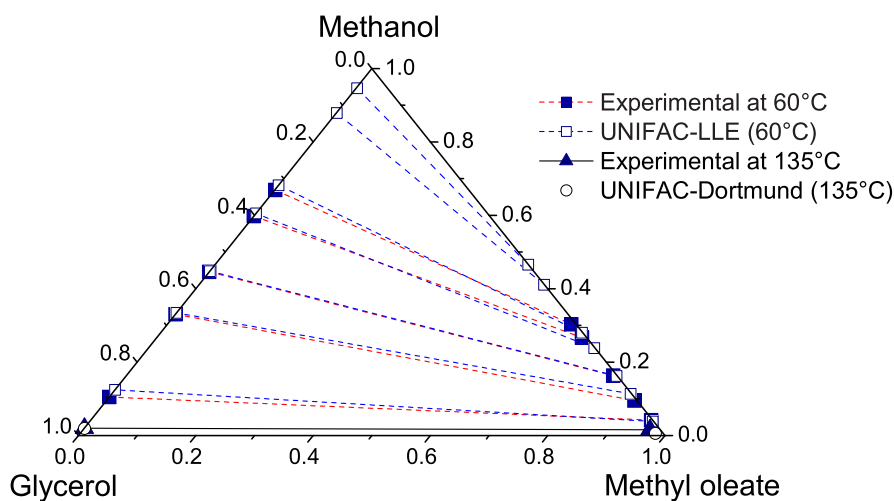
*Ternary 1: Glycerol-methanol-methyl oleate*

Figure 3.2 shows the comparison of the experimental LLE data with the predictions using UNIFAC-LLE. Similar results were obtained by using VLE parameters and by UNIFAC-Dortmund. Figure 3.2 also shows a single tie line obtained experimentally at  $135^{\circ}\text{C}$  and calculated with UNIFAC-Dortmund. More experimental tie line data at  $135^{\circ}\text{C}$  could not be collected as methanol is present only in small amount in the liquid



**Figure 3.1:** Equilibrium mole fraction of glycerol in methyl oleate ( $x_G$ ) at different temperatures.

phase at this temperature at atmospheric pressure. These data show that temperature has a little effect on the glycerol-methyl ester solubility in the range studied. The models predict well the immiscibility between glycerol and ester. Also, the prediction for methanol concentration in both the phases is good. For the data presented at 135°C, only the liquid phases were considered.



**Figure 3.2:** Ternary diagram for glycerol-methanol-methyl oleate at 60°C (with one tie line at 135°C). Comparison of experimental data with calculations using UNIFAC-LLE.

#### *Ternary 2: Glycerol-monoolein-methyl oleate*

Figure 3.3 shows the experimental data and the calculated equilibrium mole fractions for the two phases at equilibrium at 135°C. The predictions for glycerol phase are in good agreement with the experimental values. The predictions for the ester phase are only qualitatively correct, in the sense that they show increasing glycerol solubility in

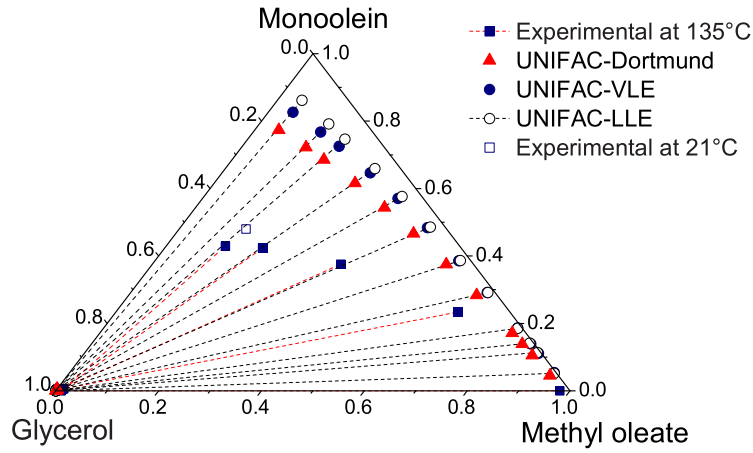


**Figure 3.3:** Ternary diagram for glycerol-monoolein-methyl oleate at 135°C. Comparison of experimental data with calculations using UNIFAC models.

the ester phase on adding monoglyceride.

None of the models could give acceptable results. The best trend was shown by UNIFAC-Dortmund. The consideration of the secondary OH group in glycerol and monoolein as OH-p or OH-s did not make any significant difference.

### 3.4.3 Reliability of experimental data

Tobias and Othmer [52] introduced a correlation (tie-line correlation) that is often used to check the consistency of experimental ternary LLE data. According to this correlation

$$\log \frac{1-a_1}{a_1} = n \cdot \log \frac{1-b_2}{b_2} + S \quad (3.35)$$

where  $a_1$  is the weight fraction of solvent in the solvent rich phase and  $b_2$  is the weight fraction of diluent in the diluent rich phase. A straight line with a slope  $n$  is obtained when  $\log \frac{1-a_1}{a_1}$  is plotted against  $\log \frac{1-b_2}{b_2}$ . For immiscible solvent-diluent, the slope  $n$  equals unity. This is also found true when mole fractions are used instead of weight fractions in the tie line correlation. The Othmer-Tobias plots for the glycerol-methanol-methyl oleate and glycerol-methyl oleate-monoolein ternaries are shown in Figure 3.4.

**Table 3.3:** Composition of points on the tie lines in the ternary diagram for glycerol-methanol-methyl oleate at 60°C (values with superscript *a* represent the data at 135°C).

Ester phase			Glycerol phase		
$x'_{MeOH}$	$x'_G$	$x'_{ME}$	$x''_{MeOH}$	$x''_G$	$x''_{ME}$
0.043	0.002	0.955	0.105	0.895	0.000
0.098	0.008	0.894	0.331	0.669	0.000
0.163	0.007	0.830	0.446	0.554	0.000
0.267	0.008	0.725	0.598	0.402	0.000
0.303	0.008	0.689	0.669	0.330	0.001
0.016 <sup>a</sup>	0.018 <sup>a</sup>	0.966 <sup>a</sup>	0.020 <sup>a</sup>	0.980 <sup>a</sup>	0.000 <sup>a</sup>

**Table 3.4:** Composition of points on the tie lines in the ternary diagram for glycerol-monoolein-methyl oleate at 135°C.

Ester phase			Glycerol phase		
$x'_{MG}$	$x'_G$	$x'_{ME}$	$x''_{MG}$	$x''_G$	$x''_{ME}$
0.234	0.100	0.666	0.004	0.990	0.007
0.375	0.258	0.367	0.005	0.987	0.008
0.423	0.386	0.190	0.006	0.983	0.011
0.429	0.456	0.115	0.006	0.981	0.013

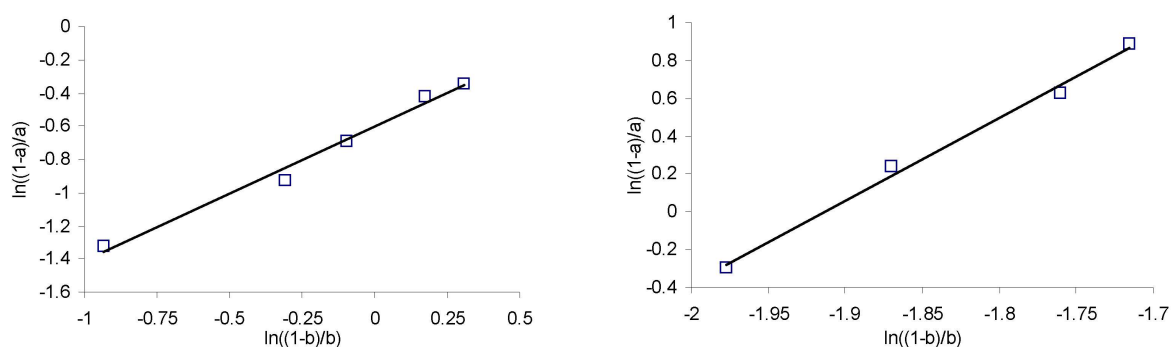


**Figure 3.4:** Othmer-Tobias plots for the experimental ternary LLE data for glycerol-methanol-methyl oleate at 60°C (left) and glycerol-methyl oleate-monoolein at 135°C (right). *a*=mole fraction of methyl oleate in the ester phase, *b*=mole fraction of glycerol in the glycerol phase.

### 3.5 Summary

During the FAME glycerolysis reaction with high dispersed phase fractions and under well agitated conditions, the two liquid phases can be safely assumed to be nearly in physical equilibrium. The reaction under these conditions is controlled by phase equilibrium. The experiments on LLE with glycerol-methyl ester binary showed a low solubility of glycerol in ester at reaction temperatures. From reaction investigations, it was known that the glycerol concentration in the ester phase increases considerably with conversion. Computation of LLE with different ternaries demonstrated that the products mono- and diglycerides lead to higher equilibrium solubility of glycerol in the ester phase. Experiments with glycerol-monoglyceride-methyl ester confirmed that monoglyceride lead to the observed trend. Though qualitatively correct, the LLE computations showed large deviations from the experimental data. However, the LLE experimental data was close to that obtained from reaction runs [53]. As a result, the predictive thermodynamic models used for LLE computations were not considered further for process simulations. Other thermodynamic models e.g. NRTL could not be used owing to missing parameters and lack of sufficient binary data for the estimation of missing parameters. Consequently in further work, an empirical correlation was used to determine the glycerol solubility in the ester phase during the reaction.

## Chapter 4

# Investigations in Reactor with Single Bubble Cap Tray

One of the initial objectives of this work was to investigate the feasibility of using a tray column as a continuous reactor for the base catalyzed glycerolysis of fatty acid methyl esters. No previous information was available on this reaction in a tray column, therefore as a first step, experiments were carried out in a lab scale reactor with a single bubble cap tray. An experimental assembly was set up to study the liquid-liquid mixing and reaction on a distillation tray (Figure 4.1). Though sieve trays are generally used for distillation because of their lesser costs, bubble cap trays are preferred for liquid-liquid reactions as they provide higher liquid holdup even at low vapor flow rates [51, 54]. The potential advantages of using a distillation column included achieving faster reaction and higher equilibrium conversion by removing the by-product methanol efficiently from the liquid reaction mixture.

In the last few decades, the use of distillation columns for carrying out equilibrium limited liquid phase reactions gained popularity due to their cost saving advantages over conventional processes where reaction and separation required different stages [54, 55]. Most of the available literature on reactive distillation columns does not take into account the cases involving the existence of the reactants as two liquid phases. A necessary condition in such cases is the dispersion of one phase into the other to provide sufficient contact area for mass transfer (if the reaction is not too slow) or reaction (if the reaction is taking place at the interface). As the two reactants separate quite fast on stopping the agitation during FAME glycerolysis, one possible problem in a tray column could be the separation of the two phases leading to slower reaction rate and accumulation of the heavier reactant on the trays. So the objective of the studies on FAME glycerolysis in tray column included the investigation of: (a) dispersion forma-

tion (liquid phase mixing) and drop size distribution in the liquid-liquid system and (b) the reaction rate on a bubble cap tray. The liquid mixing on the trays is induced by the vapors passing through the liquid. In the present case, the liquid phase mixing on a single tray was achieved by flowing nitrogen gas through the bubble cap.

## 4.1 Liquid mixing and drop size analysis on a bubble cap tray

### 4.1.1 Materials

Glycerol (>99%, Sigma) and methyl oleate (>75%, Lancaster) were used as the reactants. The catalyst used was sodium methylate (30% in methanol, Fluka). Some physical properties of glycerol and methyl oleate are given in Table 4.1.

### 4.1.2 Experimental setup

The experimental setup is shown in Figure 4.1. The apparatus consisted of a double wall glass cylinder fitted with a single bubble cap tray at the bottom and a photographic assembly. The diameter of the tray was 97 mm. The cylinder height was 200 mm. The bubble cap (Figure 4.2) had 15 circular holes with each hole having a diameter of 3 mm. The weir height was 31 mm. The bubble cap tray design was taken from a pilot scale distillation column [56] that is used to study reactive distillation of some esterification and transesterification reaction processes at the Process Technology Department (*Dynamik und Betrieb technischer Anlagen*) in the Technical University Berlin. The photographic assembly consisted of a non interlaced CCD camera (CV-M10 BX, JAI) fitted with an air-cooled endoscope and integrated with a high speed flash and a data acquisition system (Figure 4.3) [57]. The endoscope length was 32 cm. The flash with a half intensity width of 5  $\mu$ s was synchronized with the camera and frame grabber by a Visual Basic program [1]. The flash was triggered manually through a computer and the image was recorded in the computer and could be seen on screen at the same time. The frame grabber took 0.04 second to grab one frame. In this manner, still photographs in real time were obtained that were later analyzed manually with the help of a software that measured drop diameter in terms of pixels. The software to determine the drop sizes was developed at the Process Engineering Institute (*Institut für Verfahrenstechnik*) in the Technical University Berlin. The sizes thus obtained were

multiplied by a calibration factor to get the real drop sizes. The digital pictures were calibrated against a standard scale (Figure 4.4). The reactor feed consisted of glycerol and methyl oleate in a volume ratio of 2:3. This corresponds to a molar ratio of approximately 3:1 and to a dispersed phase fraction of 0.4 when the glycerol phase is completely dispersed into the ester phase. A glycerol-ester molar ratio of 2:1 was generally employed in the earlier experiments on reaction in a stirred tank. It was known that a higher excess of glycerol does not influence the reaction rate. But higher glycerol volume had to be used with the bubble cap tray to get a minimum height of the glycerol layer above the slots. The total liquid holdup on the tray was about  $150\text{ cm}^3$  and it was limited by the weir height. The reactor was heated by an oil bath with thermostatically controlled temperature (Haake F3/S). The temperature was measured by a PT-100 temperature sensor. The liquid mixture was agitated by nitrogen gas bubbles rising through the liquid. The nitrogen flow was measured and controlled using a rotameter. The temperature inside the reactor was maintained at  $135 \pm 1^\circ\text{C}$  throughout the experiments. The droplets in the liquid dispersion were photographed directly. The photographs were taken at the mid-depth of the liquid and at two different radial locations separated by an angle of 90 degrees. The catalyst was added after capturing sufficient number of frames so as to get a minimum of 250 drop pictures without reaction. The amount of the catalyst added was 1 wt% of the total feed. The time of addition of catalyst was taken as the start time for the reaction. No drops could be seen directly after the addition of catalyst, probably due to boiling of methanol that was used as a solvent for the catalyst and is also a product of the reaction. Capturing the drop photographs was continued until the methyl ester reacted nearly completely. The drop pictures were taken for different gas flow rates. Bubble or froth regime was observed during all the experimental runs. Unexpectedly, the presence of nitrogen bubbles did not hinder the drop-photography. Only in some frames a big bubble would "black out" the picture. In many frames some small bubbles were seen, which were easy to differentiate from drops. One such bubble can be seen at the top right corner in Figure 4.7. No foaming was observed except a little at the time of addition of the catalyst. The equipment was rinsed thoroughly with hot water followed by rinsing with methanol and then air dried before each new experimental run.

### 4.1.3 Results and discussion

#### *Minimum mixing time:*

The drop photographs taken after starting the gas flow showed no considerable variation in the size distribution after 1-3 minutes of agitation. Though slight variations



in the Sauter mean diameter ( $<5\%$ ) and the drop size distributions were found even after 1 hour of agitation, the variations are not taken into consideration since these were less than the error in reproducing the results ( $\pm 8\%$ ). The minimum mixing times were found to be slightly more (2-5 minutes) for a reacted mixture, where the continuous phase (ester phase) was also more viscous than pure components (Table 4.1). The viscosities were measured by a rotation viscometer (Contraves Rheomat 115).

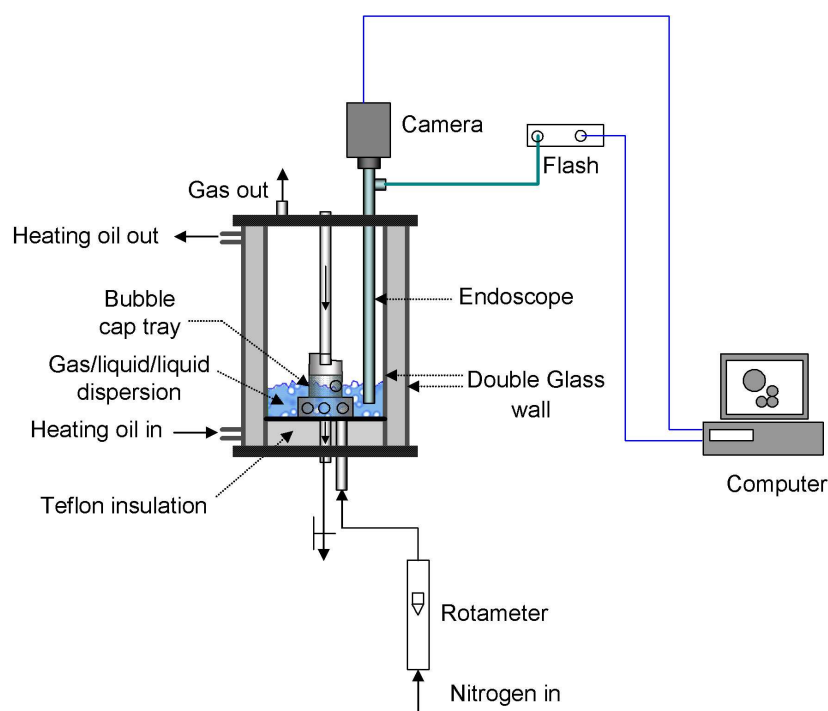


**Figure 4.1:** Experimental setup: Reactor with single bubble cap tray.

***Dispersion on the bubble cap tray: minimum gas velocity required for complete dispersion:***

At very low gas flow rates (incipience of bubbling), the dispersion formation could be roughly observed visually for the non-reacting liquid phases. The gas bubbles enter the glycerol phase, rise up, break the interface and enter the ester phase. The bubbles carry some glycerol into the ester layer, which falls back through the ester layer as the bubble escapes the liquid. In this way a dispersion of glycerol in ester layer is formed, though a very small amount of glycerol is dispersed at such low gas flow rates. At higher gas flow rates, more amount of glycerol is dispersed but a direct visual observation is not possible. Still the type of dispersion can be known by observing the settling behavior after stopping the agitation [58]. This is illustrated in Figure 4.5. Henceforth in this chapter, the term gas velocity,  $V$  (m/s) will refer to the velocity of gas through the bubble cap holes. At low gas velocities (approx.  $<1$  m/s), only a fraction of glycerol phase is dispersed and three distinct layers could be observed, namely, a glycerol

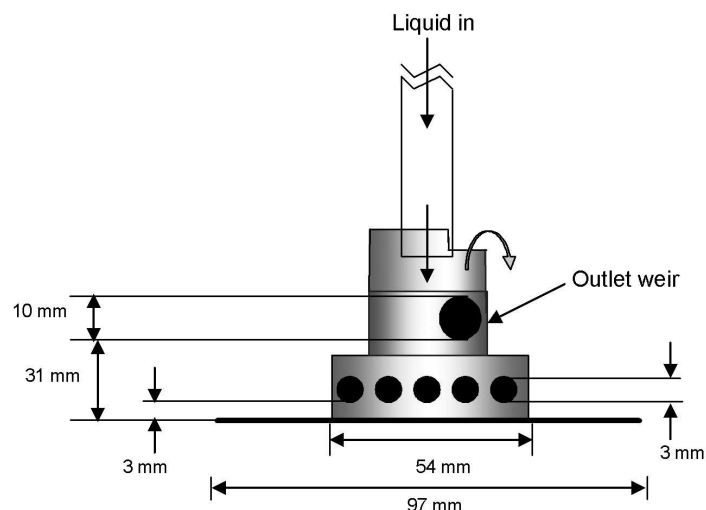


**Figure 4.2:** Bubble cap tray details.

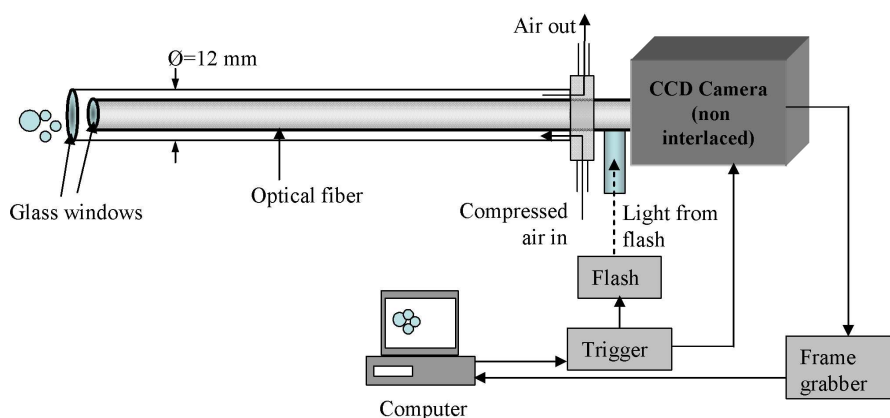


**Figure 4.3:** Photographic assembly used to take photographs of drops directly in the reaction mixture.

layer at the bottom, a glycerol in methyl ester (G/ME) dispersion in the middle and an ester layer at the top. On further increasing the gas velocity (approx. 1.5 m/s), the upper layer disappears and the middle layer grows up to the top and the bottom glycerol layer becomes thinner. At further higher gas velocities (approx. 3 m/s), the glycerol layer disperses completely into the ester phase. Phase inversion was observed in some cases during the addition of catalyst, but those cases were not considered. On stopping the gas flow, the two phases separated completely within a minute, which is quite fast for a two phase system. The phases took more time to separate (2-3 minutes) after the reaction. In all the experiments, the glycerol phase was found to be the dispersed phase. The minimum gas velocity required to completely disperse one liquid phase into another,  $V_{min}$  (m/s), was found to be dependent on the initial height of the heavy phase (height of the lower liquid layer before starting the gas flow), which is in

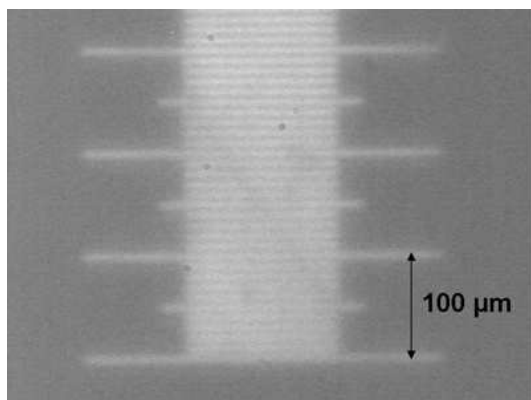


**Figure 4.4:** Calibration scale for the CCD camera.

turn a factor depending on the geometry of the bubble cap. A completely dispersed phase is defined here as a state when no separate layer or stagnant pockets of liquid could be seen anywhere on the tray. The completely dispersed phase mentioned here may be different from a homogeneously dispersed phase. It was found that  $V_{min}$  was lower during and after the reaction compared to that without reaction, indicating that it may also be dependent on other factors like interfacial tension, viscosity and density of the liquids. Figure 4.6 shows  $V_{min}$  for different initial heights of glycerol layer without reaction and after the completion of the reaction. Slightly different values were found with increasing and decreasing the gas flow rates and with repeated experimental runs. The values shown in Figure 4.6 represent the averaged values with the error bars showing the scatter for different observations. The difference in the values found between liquid phases before and after the reaction can be attributed to the difference in the interfacial tension between the two phases before and after the reaction (Table 4.1). The surface- and interfacial-tension were measured by pendant drop method [59] using contact angle meter (Dataphysics OCA 15).

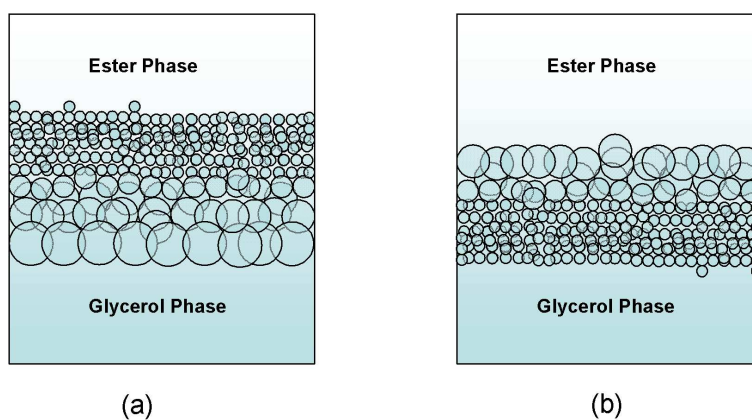


**Figure 4.5:** Settling behavior of (a) G/ME and (b) ME/G dispersion.

**Table 4.1:** Fluid properties.

Liquid	Density at 20°C (g/ml)	Viscosity at 20°C (cP)	<i>Predicted<sup>a</sup></i> <i>viscosity at</i> 135°C (cP)	Surface tension at 20°C (mN/m)
glycerol	1.26	956.7	5.2	61
methyl oleate	0.87	3.6	0.5	28
<i>Reaction mixture</i>				
glycerol layer	1.25 <sup>b</sup>	142.3 <sup>b</sup>	2.9	33 ± 1 <sup>c</sup>
methyl oleate layer	0.90 <sup>b</sup>	16.0 <sup>b</sup>	1.5	28

Liquid/Liquid	Interfacial tension (mN/m) at 20°C
Glycerol/Methyl oleate	14.0 ± 0.5
(Glycerol+monolein) <sup>d</sup> /Methyl oleate	4.5 ± 0.5
(Glycerol+catalyst) <sup>d</sup> /Methyl oleate	1.5 ± 0.5
Glycerol phase/Ester phase from reaction	1.5 ± 1 <sup>c</sup>

<sup>a</sup> Calculated by Lewis and Squires' liquid viscosity correlation [42] (See Appendix A.1), <sup>b</sup> Measured from samples cooled to 20°C taken at 70 minutes after adding the catalyst. <sup>c</sup> Measured from samples cooled to 20°C taken at 15, 30, and 45 minutes after adding the catalyst. <sup>d</sup> Mixture prepared at 135°C.

### ***Drop size distribution:***

Photographs of the drops without and during the reaction are shown in Figure 4.7. Figure 4.8(a) shows the drop size distributions before and during the reaction for a particular run. No significant difference was found in the drop size distributions at different radial positions. It was observed that the drop sizes reduce dramatically within 2-3 minutes after the addition of the catalyst. This happens primarily due to the sudden decrease in the interfacial tension probably because of the formation of small amounts of soaps by the reaction. Measurements of interfacial tension of samples taken at different times show that there is a sharp decrease in the interfacial tension after the addition of catalyst (Table 4.1). It is not very clear if this happens mainly because of monoglycerides [37] or due to small amounts of soaps produced by the catalyst [27]. Surface- and interfacial-tension measurements with pure components indicated that monoglyceride alone does not lead to such small values of interfacial tension as observed in the reaction samples. The interfacial tension between glycerol with added catalyst (30% in methanol) and methyl oleate were near to those observed in the reaction, indicating that the catalyst is more efficient in reducing the drop sizes than monoglycerides. The drop size distributions were fitted by both normal and lognormal distributions (Figure 4.8(b)). Most of the distributions were slightly better fitted by a lognormal distribu-

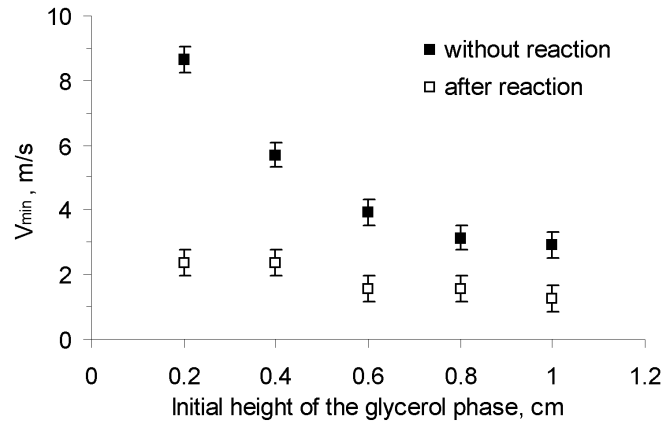


Figure 4.6: Minimum gas velocity required to obtain a complete dispersion on the bubble cap tray.

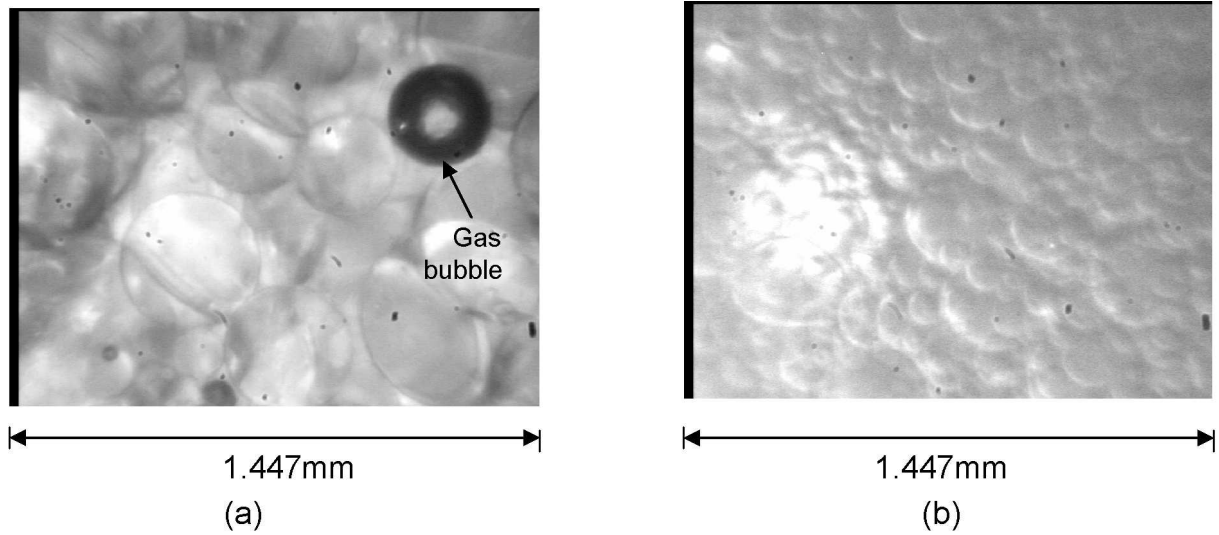


Figure 4.7: Drop pictures: (a): before the reaction, (b): 30 min after the start of the reaction.

tion for drop sizes with and without reaction. In the present study, 250-500 drops were analyzed to find the drop size distributions and to calculate the Sauter mean diameters.

#### *Effect of gas velocity:*

Figure 4.9 shows the drop size distributions obtained with different gas flow rates. The effect of gas velocity on Sauter mean diameter is shown in Figure 4.10. For the glycerol-methyl oleate dispersion without reaction, the dependency of the Sauter mean diameter,  $d_{32}(\mu m)$ , on the gas velocity,  $V (m/s)$ , was found to be related by:

$$d_{32} \propto V^{-0.17} \quad (4.1)$$

For the reacting liquids, no effect of gas flow on Sauter mean diameter could be observed. No significant effect of gas flow rate on the type of distribution was observed.

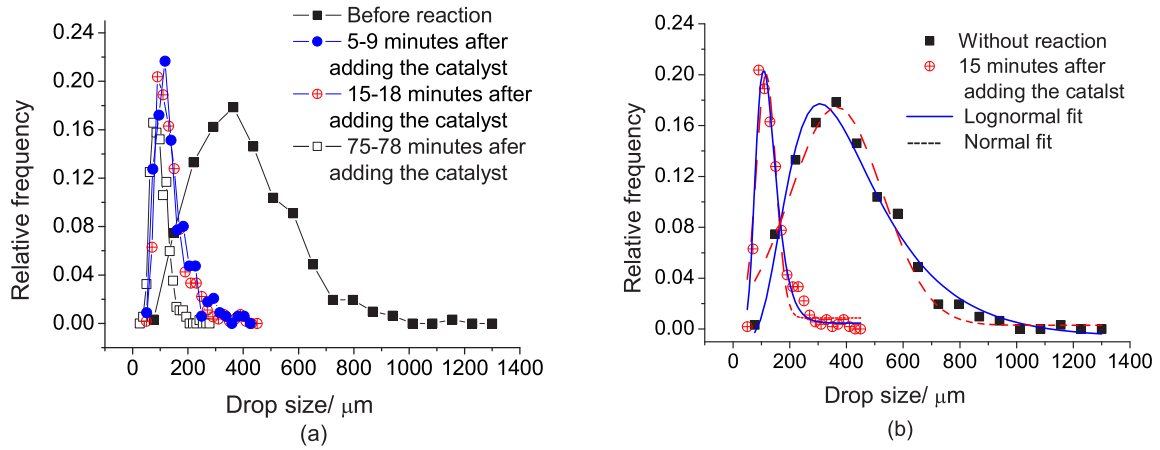


**Figure 4.8:** Drop size distributions before and during a reaction run,  $V=4.7$  m/s. Y axis: Relative frequency=(number of drops in a given diameter interval)/(total number of drops analysed). (a) Experimental data, (b) normal and lognormal fitting to experimental data. For the distribution without reaction, mean=365.4 and standard deviation=162.1. For the distribution 15 min. after adding the catalyst, mean=116.1 and standard deviation=34.5.

### Power supplied by gas flow

The power supplied to the vessel content by the gas flow is responsible for the mixing and interfacial area generation in the three phase system. Bernoulli's equation written for gas between location  $o$  (just above the bubble cap slots) and location  $s$  (liquid surface) [60] gives (neglecting the frictional losses, and assuming the gas to be ideal):

$$W = \frac{V_o^2 - V_s^2}{2} + \frac{p_o}{\rho_{Go}} \ln \frac{p_o}{p_s} + (Z_o - Z_s)g \quad (4.2)$$

where  $W$  is the work done per unit mass of gas on the vessel content,  $V$  and  $\rho_G$  are the gas velocity and density,  $Z$  is the height,  $p$  is the pressure and  $g$  is the acceleration due to gravity. The power delivered by the gas can be calculated as:

$$P = W\dot{m} \quad (4.3)$$

where  $\dot{m}$  is the gas mass flow rate. Based on Equations 4.2 and 4.3, a plot of estimated power delivered against gas velocity is shown in Figure 4.11(a). For a comparison with a standard stirred tank<sup>1</sup>, a plot of power delivered against stirrer speed is shown in Figure 4.11(b). The power delivered to a unit volume of liquid of density  $\rho$  in a stirred tank by an impeller with a diameter  $D$  and rotating at a speed of  $n$  rpm can be estimated as [61]:

$$(P/V) = \frac{N_p n^3 D^5 \rho}{V} \quad (4.4)$$

<sup>1</sup>See Appendix A.4

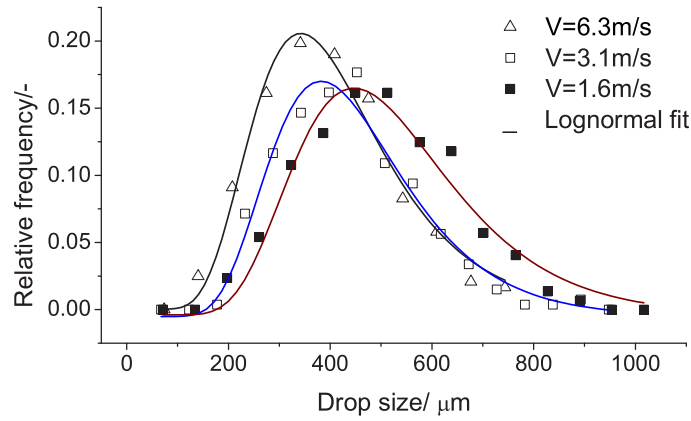


**Figure 4.9:** Effect of gas velocity on drop size distribution.

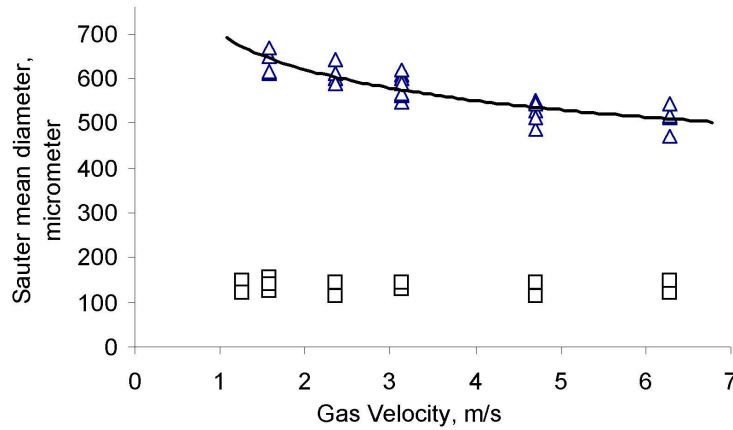


**Figure 4.10:** Effect of gas velocity on Sauter mean diameter.  $\triangle$  without reaction,  $\square$  30-35 minutes after the addition of the catalyst, - fitted curve.

where  $V$  is the liquid volume and  $N_p$  is the power number that can be taken as 5 for turbulent flow with standard impeller design [61].

Figure 4.11(a) shows a linear dependency of power delivered per unit volume on the gas velocity. Figure 4.12(a) shows that more power can be delivered to the liquid with the same gas velocity if the liquid volume is kept same and the liquid height above the slots is increased. This can be implemented by using a tray with modified design, e.g. with a lower level of slots or with a smaller base area to hold liquid. The extra power comes at the expense of the increased hydrodynamic pressure. Figure 4.12(b) shows the effect when the liquid volume is also allowed to increase with the liquid level above the slots. This does not lead to any advantage and there is a small decrease in power input to the tray content.

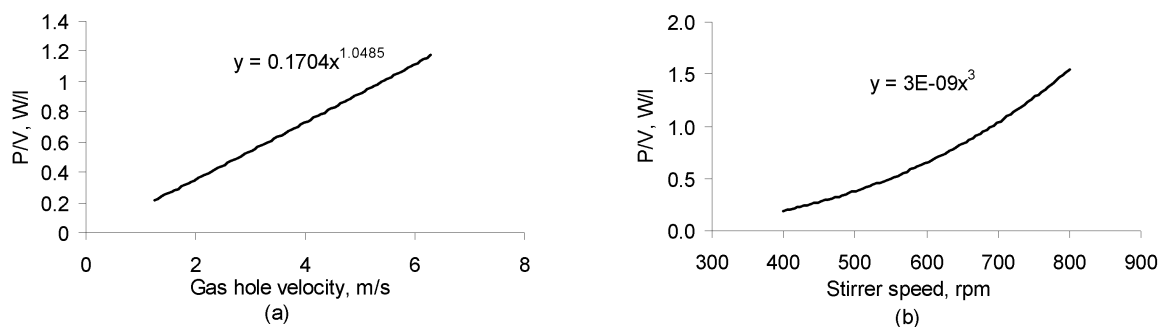


**Figure 4.11:** (a) Estimated power delivered by gas flow to vessel content vs gas velocity. Gas density =  $1.14 \text{ kg/m}^3$ . (b) Estimated power delivered to vessel content in a stirred tank vs stirrer speed. The liquid is assumed to have a density of  $1000 \text{ kg/m}^3$ . The equations represent the trend.

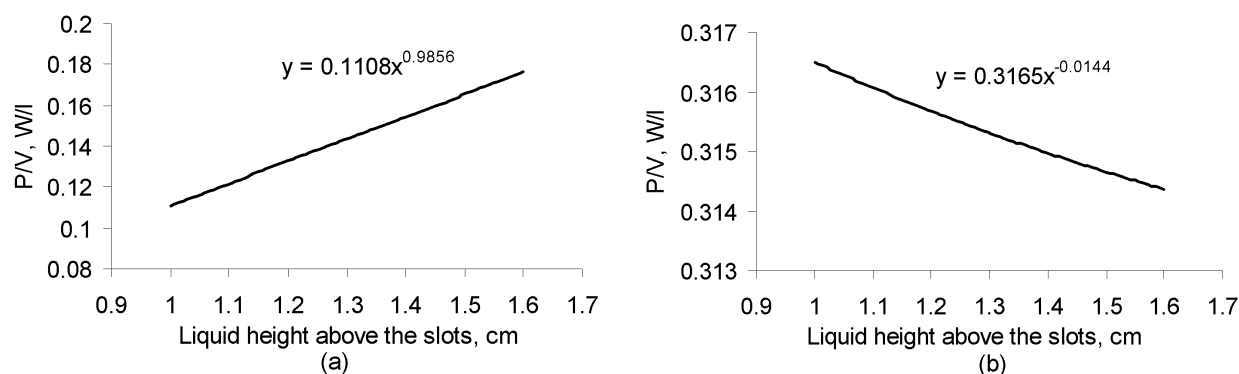


**Figure 4.12:** Estimated power delivered by gas flow at a constant gas velocity ( $=1.6 \text{ m/s}$ ) to vessel content vs the height of liquid surface above the slots. (a) The liquid volume is taken to be constant and the height of liquid surface is assumed to change by changing the tray geometry. (b) The tray geometry is taken to be fixed, the liquid volume changes according to the height of the liquid surface. The liquid is assumed to have a density of  $1000 \text{ kg/m}^3$  and the gas density =  $1.14 \text{ kg/m}^3$ . The equations represent the trend.

## 4.2 Reaction on the bubble cap tray

The liquid dispersion formation on the bubble cap tray was found to be satisfactory also with relatively low gas flow rates. As the next step in this series, the reaction rate was studied in this reactor geometry. Reactions were carried out in liquid-batch mode, whereas the by-product methanol was continuously removed by nitrogen flow. The chemicals used for reaction study were the same as used for liquid mixing studies (Section 4.1.1). The chemical analysis of reaction samples was done by gas chromatography. Details of the apparatus used for analysis are described in Section 3.3.1.



### 4.2.1 Experimental setup and procedure

The experimental setup and general procedure used were the same as described in Section 4.1. The reactions were carried out at  $143 \pm 2^\circ\text{C}$ . Reaction runs were carried out at different strip gas flow rates to study its effect on reaction rate. Samples from the reaction mixture were collected at different reaction times. A stainless steel needle with a metal valve (Luer lock) and a glass syringe were used to withdraw samples from the reaction mixture. One additional sample was taken before the addition of the catalyst in all experimental runs. For each sample, 2-3 ml liquid was withdrawn from the reaction mixture using a syringe. The liquid was allowed to separate into two layers for less than a minute in the syringe, then about 1 ml was taken from the upper phase (ester phase) for further analysis and the rest was injected back into the reactor. The ester phase sample contained finely dispersed glycerol which was not separated, as the objective was to measure only the methyl ester and glyceride concentration in the sample. The time of collecting the ester phase was recorded as the time of sampling. This sample was then immediately chilled in an ice bath to stop the reaction. Analysis of the same sample after 60 minutes in ice and after 12 hours at room temperature showed no difference in conversion. So it can be safely assumed that the reaction stops at room temperature.

#### *Analysis*

The samples were silylated with BSTFA before being analyzed by gas chromatography. The details of analysis are given in Section 5.1. As mentioned in Section 5.1, the glycerol phase contained no components other than methanol in significant amounts, so the complete conversion and product concentration profile could be obtained by analyzing the samples containing ester phase only. During the investigation of reaction kinetics on the bubble cap tray, the effect of glycerol concentration in the ester phase was not known. The concentration of glycerol dissolved in the ester phase was believed to stay nearly constant. Therefore, the sampling procedure and the GC analytical method were focused only on the measurement of the limiting reactant methyl ester and the products mono- and diglycerides. A different GC method than mentioned in Section 5.1 was used here. The inlet temperature of the GC column was kept constant at  $38^\circ\text{C}$ . The total time of analyzing one sample was 93.2 minutes. The temperature program ramped in 4 steps, first, the initial column temperature was kept constant at  $35^\circ\text{C}$  for 20 minutes, second, the temperature was raised by  $5^\circ\text{C}/\text{min}$  to  $90^\circ\text{C}$  and held at  $90^\circ\text{C}$  for 12 minutes, third, the temperature was raised to  $370^\circ\text{C}$  with a rate of  $7^\circ\text{C}/\text{min}$  and held for 2 minutes, and finally the column was cooled to  $40^\circ\text{C}$  at a rate of  $40^\circ\text{C}/\text{min}$ . The GC results were analyzed for ester conversion and monoglyceride selectivity. Some

common definitions that are used often in the text are defined below.

**Conversion (X):** Conversion of fatty acid methyl ester is defined as:

$$X = \frac{N_0^R - N_t^R}{N_0^R} \quad (4.5)$$

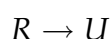
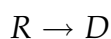
where  $N_0^R$  is the number of moles of the limiting reactant in the feed and  $N_t^R$  is the number of moles of the limiting reactant in the reactor at time  $t$ . In the present work, Equation 5.6, which can be derived from the above equation, is used for calculating conversion. For flow reactors, the condition at the exit is considered instead of that at a final time in Equation 5.6. In this work the conversion was always based on methyl oleate.

**Selectivity (S) and yield (Y) of a desired product:** Throughout the text, the term selectivity and yield are used to mean overall selectivity and overall yield. The definitions of these terms are taken the same as the definitions of the German translations *Selektivität* and *Ausbeute* as defined in [62].

$$S = \frac{N_t^D}{(N_0^R - N_t^R)} \cdot \frac{|\nu_R|}{|\nu_D|} \quad (4.6)$$

$$Y = S \cdot X = \frac{N_t^D}{N_0^R} \cdot \frac{|\nu_R|}{|\nu_D|} \quad (4.7)$$

Here  $N_t^D$  represents the moles of the desired product produced in the reactor after a reaction time  $t$  and  $\nu$  is the respective stoichiometric coefficient. It is to be noted that some (American) textbooks ([63, 64]) have different definitions of these terms. For example for the parallel reactions:



the selectivity and yield of the desired product  $D$  are defined as:

$$S = \frac{N_t^D}{N_t^U} \quad (4.8)$$

$$Y = \frac{N_t^D}{N_0^R - N_t^R} \quad (4.9)$$

where the superscript  $U$  refers to the undesired product. Here it could be seen that the term yield as defined in these textbooks is similar to the term *Selektivität* in German literature. The term selectivity is defined differently. In most of the published articles, these terms are not defined specifically, hence a direct comparison of selectivity with the published literature based on numerical value can not be done.

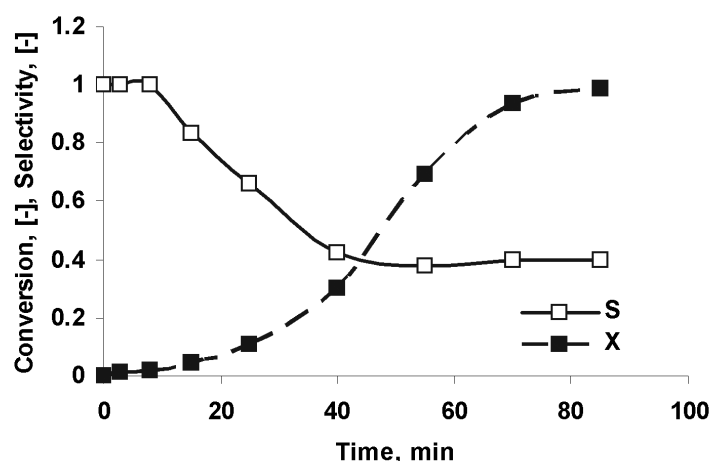


**Figure 4.13:** Ester conversion (X) and monoglyceride selectivity (S) on the bubble cap tray.  $T=143^{\circ}\text{C}$ , gas velocity=1.6 m/s.

## 4.2.2 Results and discussion

Faster reactions and higher conversions were obtained on the bubble cap tray in comparison to a stirred batch reactor<sup>2</sup>. Figure 4.13 shows the ester conversion and monoglyceride selectivity obtained from a typical reaction run. Higher selectivity of monoglycerides is desirable as monoglycerides are better emulsifiers than diglycerides. Figure 4.14 shows a comparison with reaction in a stirred tank at a pressure of 300 mbar. Compared to the stirred tank reactor, the selectivity of monoglycerides was not altered much on the bubble cap tray.

### *Effect of gas velocity on reaction rate*

Figure 4.15 shows the effect of gas velocity on the reaction rate. No obvious effect could be observed in the range of gas velocities investigated. The conversion profiles were not very good reproducible. Figure 4.15 also shows two runs carried out under the same conditions. The reproducibility of conversion profile was generally within  $\pm 10\%$  (absolute). In the experiments in stirred tank reactor at atmospheric pressure, the reproducibility of the conversion profile was found to be within  $\pm 2\%$  (absolute). The relatively poor reproducibility with methanol stripping by inert gas may be due to chaotic gas flow patterns and the unknown effects of gas flow on the physical properties of the complex two liquid-phase reaction system. The variation in gas flow was expected to affect the methanol concentration in the reaction mixture and the dispersion of the liquid phases. On this basis, higher gas velocity was expected to give faster reactions. No methanol was detected in any of the experiments in the ester phase. So

<sup>2</sup>Refer Chapter 5 for investigations in batch reactor

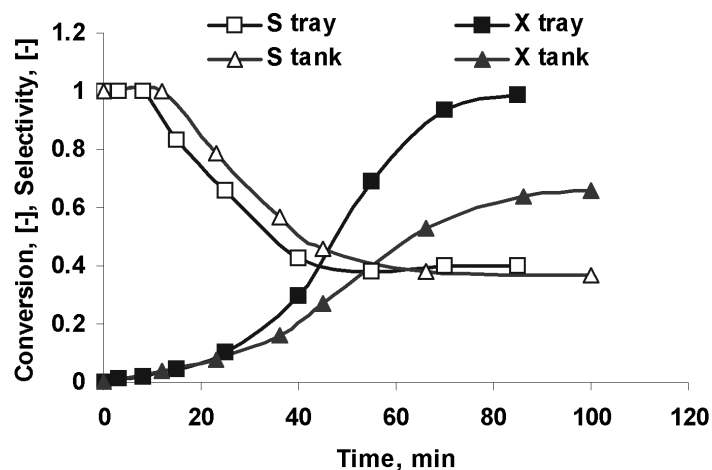


**Figure 4.14:** Comparison of ester conversion (X) and monoglyceride selectivity (S) on the bubble cap tray and in the stirred tank reactor. Reaction conditions in the stirred tank:  $T=140^{\circ}\text{C}$ ,  $P=300$  mbar, Stirrer speed=500 rpm. For the bubble cap tray:  $T=143^{\circ}\text{C}$ ,  $P=1$  bar, gas velocity=1.6 m/s. (Data at 300 mbar from [1]).

only the dispersion was expected to be affected by the gas flow. But as shown in figure 4.10, gas flow rate had a small effect on the drop sizes. The shape of conversion curve was the same in all cases, the reaction was slow in the beginning and then accelerated after some amount of conversion (0.1-0.2) and finally slowed down before reaching nearly 100% after 60-90 minutes.

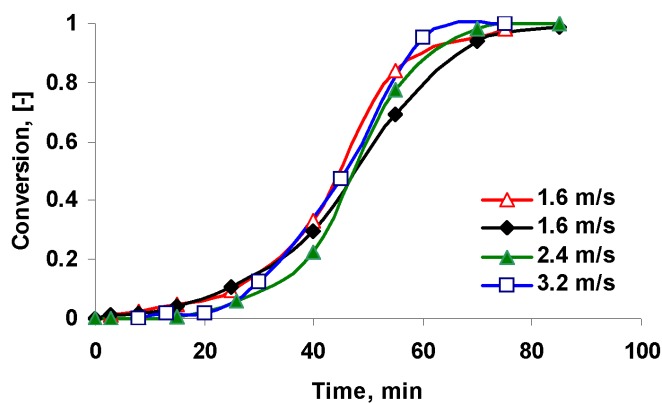


**Figure 4.15:** Effect of the gas velocity on ester conversion rate. The two curves at 1.6 m/s correspond to two different experiments carried out under the same operating conditions.  $T=143^{\circ}\text{C}$  for all experimental runs.

### 4.3 Modeling and simulation

Distillation is the most widely used separation process and a vast amount of literature has been published on the construction and operation of distillation columns. After the success of reactive distillation for methyl acetate production by Eastman Chemical Company, the concept of using a single column as reactor-separator has gained much interest in research and development. Many mathematical models for simulating distillation columns are also present in the literature, mostly for two phase distillation.

In this work the intended use of a tray column was different from the usual reactive distillation. Here it was considered as a cascade of mixed reactors, with the liquid reactants (feed) flowing in a co-current manner from the top to the bottom. No reboiler or reflux would be required. Other assumptions made in the process model were: (1) the complete column is maintained at reaction temperature, (2) an inert gas (Nitrogen) is supplied at the bottom, methanol vapors and nitrogen gas provide the mixing of the two liquid phases on the trays and (3) the reacted product is collected at the bottom of the column. In this assembly, an efficient removal of methanol from the liquid mixture was expected, giving rise to faster reaction and no mechanical agitation would be required. The column was modeled as a cascade of CSTRs (Figure 4.16).

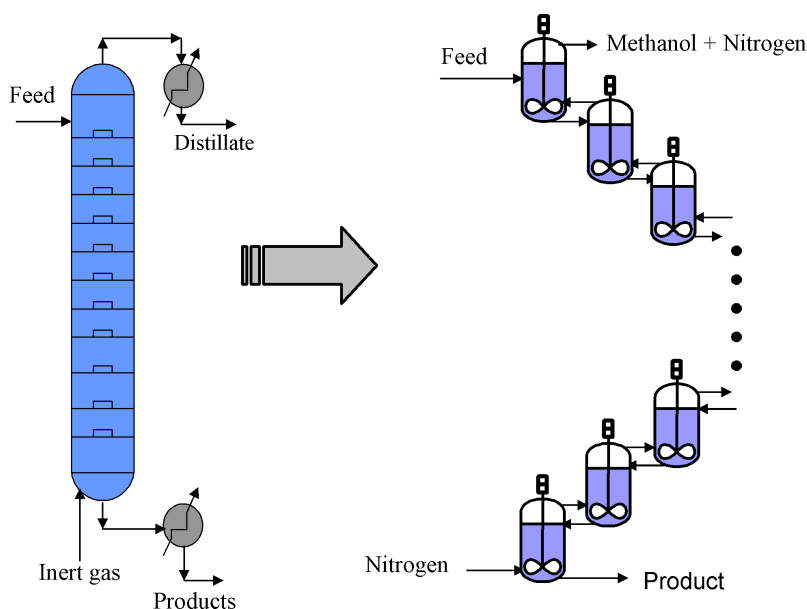
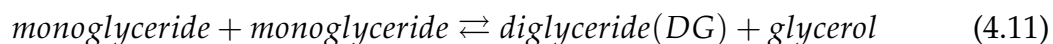
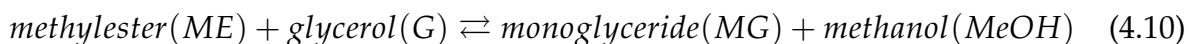


**Figure 4.16:** Tray column modeled as a cascade of mixed reactors. In one variation (*model 1*) the concentration of methanol and glycerol in the ester phase were modeled using empirical relations. In the second variation (*model 2*) incoming feed on each tray was assumed to be in phase-equilibrium, which was modeled using an activity coefficient model.

### 4.3.1 Reaction modeling

The reaction kinetics was modeled using the semi-empirical model suggested by Kimmel [1]. The reaction was modeled as a homogeneous reaction taking place in the ester phase. The reaction steps were modeled as:



From the above chemical equations, the mass balance for a batch reactor can be written as:

$$\frac{dC_{ME}}{dt} = -k_{1f}C_G C_{ME} + k_{1r}C_{MG}C_{MeOH} \quad (4.12)$$

$$\frac{dC_{MG}}{dt} = k_{1f}C_G C_{ME} - k_{1r}C_{MG}C_{MeOH} - 2k_{2f}C_{MG}^2 + 2k_{2r}C_{DG}C_G \quad (4.13)$$

$$\frac{dC_{DG}}{dt} = k_{2f}C_{MG}^2 - k_{2r}C_{DG}C_G \quad (4.14)$$

where  $k$ 's are the reaction rate constants (Table 4.3). In these equations, all concentrations refer to the ester phase only. From experiments, the methanol concentration in the ester phase was found to be nearly constant,

$$C_{MeOH} = \text{constant} \quad (4.15)$$

The glycerol concentration in the ester phase was found to be increasing with conversion and it was correlated as:

$$C_G = A \cdot X + B \quad (4.16)$$

Based on experiments of the glycerolysis of methyl esters of oleic and palmitic acid, Kimmel provided numerical values for the parameters used in this model. The numerical values of some parameters from Kimmel's work that were used for simulations here, are reproduced in Table 4.3. During the experiments on bubble cap tray, no methanol was detected in the ester phase. In Equation 4.16, parameters  $A$ ,  $B$  were chosen to fit the experimental data obtained from the bubble cap tray reactor. The values of  $A$  and  $B$  were found to be 0.4-0.8 and 0.06 mol/kg, respectively, for stirred tank<sup>3</sup> at different pressures and with stripping by nitrogen at 135°C. For bubble cap tray, the values used were 0.8 and 0.005 mol/kg for  $A$  and  $B$ , respectively. The smaller value of  $B$  reflects inefficient initial liquid mixing on the bubble cap tray.

---

<sup>3</sup>See Section 5.2

**Table 4.3:** Kinetic parameters for the reactions represented in Equations 4.10 and 4.11. Source: [1].

Reaction	k at 130°C kg/(mol.min)	$E_A$ kJ/mol
1f (reaction 1 forward ( $ME + G \rightarrow MG + MeOH$ ))	0.0828	49
1r (reaction 1 reverse ( $MG + MeOH \rightarrow ME + G$ ))	0.7017	69
2f (reaction 2 forward ( $MG + MG \rightarrow DG + G$ ))	0.0732	57
2r (reaction 2 reverse ( $DG + G \rightarrow MG + MG$ ))	0.1027	107

The kinetic model was considered suitable for simulations of a cascade of bubble cap trays. Two variations were used to model the column. In both variations each tray was considered as a well mixed continuous reactor, where the reaction is taking place in the ester phase. The glycerol phase acts as a reservoir for the reactant glycerol. Under steady state operation, the composition of the components in the ester phase is governed by the following equation:

$$-r_i = \frac{C_i^{in} - C_i^{out}}{\tau} \quad (4.17)$$

where  $\tau$  is the residence time on the tray, which is assumed to be constant for each tray and  $r_i$  is given by the right hand side term of Equations 4.12-4.14. In one variation (model 1), the empirical relations (Equations 4.15 and 4.16) were used to calculate the methanol and glycerol concentrations in the ester phase and the product glycerides are assumed to be present only in the ester phase all the time. In the second variation (model 2), the incoming feed to each tray is assumed to attain a physical equilibrium first, and thereafter the reaction is modeled to take place in the ester phase. UNIFAC-Dortmund was used to calculate the activity coefficients in model 2. This model is illustrated in Figure 4.17. A built-in procedure in ASPEN Custom Modeler was used for calculating the three-phase equilibrium. Two additional generation equations were used in this model for methanol and glycerol:

$$r_{MeOH} = k_{1f}C_G C_{ME} - k_{1r}C_{MG}C_{MeOH} \quad (4.18)$$

$$r_G = -k_{1f}C_G C_{ME} + k_{1r}C_{MG}C_{MeOH} + k_{2f}C_{MG}^2 - k_{2r}C_{DG}C_G \quad (4.19)$$

and accordingly, two equations are added in Equation 4.17

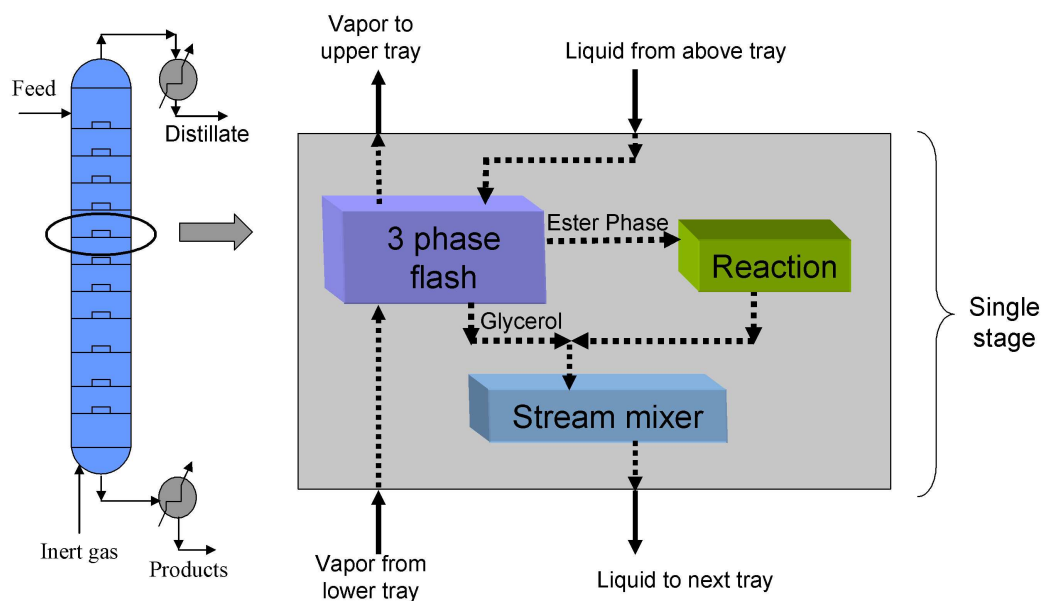


Figure 4.17: Model 2 of the the tray column as implemented in Aspen Custom Modeler.

### 4.3.2 Results and discussion

A comparison of model calculations with experimental data from a reaction run on the bubble cap tray is shown in Figure 4.18. The agreement between experimental and calculated data was found acceptable for further simulations using this model.

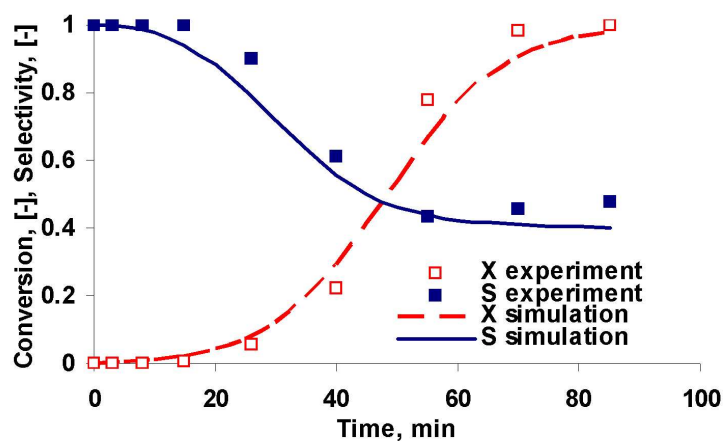
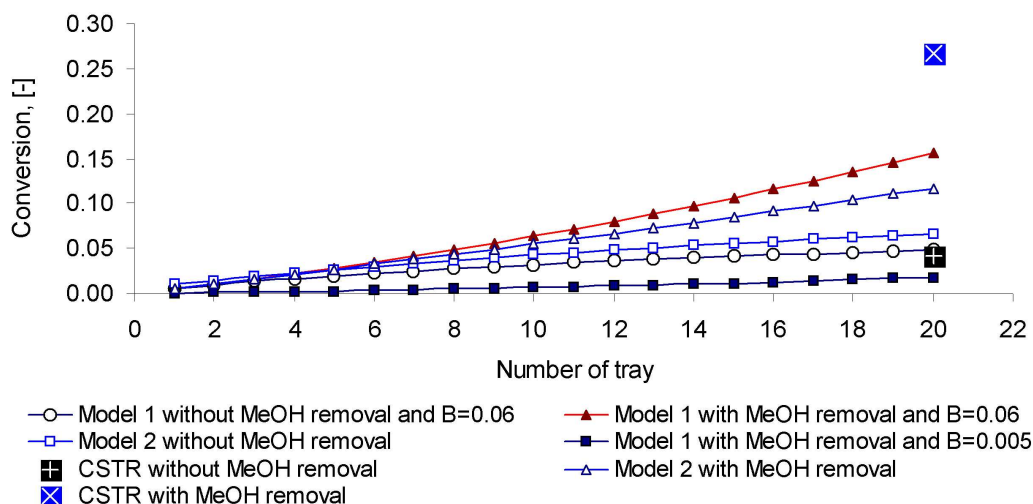


Figure 4.18: Comparison of simulation and experimental data. X=conversion, S=monoglyceride selectivity. Experimental conditions: T=143°C, gas velocity=3.4 m/s.

A column with 20 trays was simulated using model 1 and model 2. All simulations were performed using ASPEN Custom Modeler. For each model, simulations were carried out with and without considering methanol in the liquid phase. Nearly complete removal of methanol in the liquid phase can be realized by stripping methanol



by an inert gas. No mass transfer limitation effects were considered in model 2. In model 1, the (initial) mass transfer effect is lumped into the parameter  $B$  in Equation 4.16. The initial mass transfer effects can be minimized by modifying the tray design for better liquid dispersion. For comparison with this possibility, simulations were also carried out with value of parameter  $B$  obtained from experiments in stirred tank. The simulation results are represented in Figure 4.19.



**Figure 4.19:** Comparison of ester conversion obtained by simulation of reaction in a tower with 20 trays with different conditions at 135°C. A value of  $B=0.005$  in Equation 4.16 was obtained by fitting the model to experimental data from the bubble cap tray.  $B=0.06$  is obtained from stirred tank. A lower value of  $B$  indicates the presence of an initial mass transfer regime that results from inefficient initial mixing conditions on the tray. In Model 1,  $C_{MeOH}=0.2$  mol/kg for cases without Methanol removal and  $C_{MeOH}=0$  mol/kg for cases with methanol removal. The two data points for CSTR represent the conversion in a CSTR with a volume equal to the total liquid holdup on 20 trays.

The liquid phase residence time on each tray was taken as 1 minute in all the simulations. All cases show low conversion of ester compared to a single CSTR with a residence time of 20 minutes assuming complete methanol removal. The results show that the ester conversion is very low with methanol in equilibrium with the liquid phases. Therefore, use of an inert gas for additional methanol stripping is advantageous. The predictions of model 2 and model 1 were similar for low conversions when  $B=0.06$  mol/kg (Equation 4.16) was used in model 1. This represents the saturation concentration of glycerol in methyl oleate at the reaction temperature and its use in model 1 implies the absence of initial mass transfer limitations. As it was shown in Section 3.2, UNIFAC-Dortmund predicts less than actual concentration of glycerol in the ester phase with increasing monoglyceride concentration. This explains the lower conversions predicted by using UNIFAC-Dortmund. From the simulations results, the

yield of monoglycerides was found to be lesser in a tray column in the best case (11%) than in a single CSTR (14%) having the same volume as that of 20 trays. In comparison to this, simulations using the parameters obtained from experiments on the bubble cap tray showed much lower monoglycerides yield (1.7%) for a column with 20 trays. Based on these results a single CSTR with methanol stripping by an inert gas was considered to be a better option than a cascade of bubble cap trays. The tray column was not considered for further investigations.

## 4.4 Summary

The mixing of two liquid phases on the bubble cap tray was found to be sufficient for a liquid-liquid reaction, although it was not better than in a stirred tank. The Sauter mean diameters were 1.5-3 times bigger than in a stirred tank<sup>4</sup>. The drop size distribution was similar to that generally obtained in stirred tanks. Complete dispersion could be obtained also at relatively low gas flow rates giving a bubbly flow. An estimate for the power delivered by gas flow to the tray content was made using Bernoulli's equation. The estimated power delivered on a bubble cap tray was of similar magnitude as that estimated for a stirred tank. The height of the heavier liquid surface as well as the height of total liquid was found to be important for better dispersion formation. On this basis, bubble caps with slots at a lower level are expected to produce better agitation in the liquid phase.

The studies with reaction showed that in comparison to a stirred tank, faster reaction and higher conversion can be attained on a tray. But simulations showed that a cascade of trays brought no advantage over a single stage with a bigger volume. Moreover due to the inferior initial mixing on the bubble cap tray, the reaction in a cascade of trays would be even slower. Based on the experimental results and simulations, it was concluded that a single CSTR with methanol being stripped in a similar manner as done in a tray column would lead to faster conversions than in a tray column. As a result, the tray column was not considered for further investigations and later work was focussed on a CSTR with methanol removal.

---

<sup>4</sup>Refer [40] for information on drop size analysis in a stirred tank

## Chapter 5

# Investigations on FAME Glycerolysis in Stirred Tank Reactor

The samples from reaction on the bubble cap tray were analyzed for methyl ester and mono-, diglycerides only as the initial objective was to study the ester conversion and monoglyceride selectivity on the tray. The GC analysis of the ester phase showed high mass deficit (max. 40%) which was thought to be arising mainly because of the unaccounted finely dispersed glycerol in the ester phase. Later, it was discovered that the dissolved glycerol concentration in the ester phase increased significantly during reaction which also affected the reaction rate. Hence, for kinetic modeling, it was necessary to quantify the change in glycerol concentration in the ester phase during the reaction. Also, Kimmel [1] reported very low amounts of triglycerides ( $<1$  wt%) in his experiments and the formation of triglycerides was not taken into account in his kinetic model. In the experiments with bubble cap tray, higher amounts of triglycerides were estimated ( $\sim 10$  wt%). To account for the observed triglycerides formation at higher conversions, it was necessary to add a third step in the kinetic model. Moreover, precise experimental data were needed to determine the corresponding rate constants. The reliability of an experimental result is limited by the precision of measurement, therefore improvements were made in the sampling and analytical methods. The gas chromatography (GC) method was optimized to measure the fractions of all components in the reaction mixture. The sampling method was also improved to measure the glycerol concentration in the ester phase. The FAME glycerolysis reaction was carried out in a stirred tank reactor with and without methanol stripping by an inert gas. It was observed that at higher stirring speeds ( $>450$  rpm), the reaction rate was independent of the stirring speed. Therefore, all the experiments were carried out at a higher speed (550 rpm) to avoid mass transfer limitation effects.

## 5.1 Experimental

### 5.1.1 Materials

The reactants and catalyst used were the same as mentioned in Section 4.1.1. The details of the chemicals used for calibration and the analytical equipment are given in Sections 1.2 and 3.3.1.

### 5.1.2 Experimental set-up and procedure

A double wall glass reactor (Wertheim LF-100) was used to carry out the reaction. The volume of the reactants in the reactor was 300 ml. The reactor was equipped with four baffles and a six-blade turbine stirrer for stirring the liquids. Heating was provided by a thermostatically controlled oil bath (Haake F6/B5). The reactants were fed into the reactor in the desired molar ratio and then stirred and heated to 135°C. In the experiments with forced methanol removal, nitrogen gas was bubbled through the liquid (at 5 liter per minute) by a distributor at the reactor bottom. This distributor was essentially a silicone tube (3 mm inner diameter) rounded into a circle with holes around the periphery (2 mm x 4). The catalyst (1 wt%  $\text{NaOCH}_3$  based on total amount of reactants) was added after attaining the desired temperature. The time of catalyst addition was taken as the start of the reaction. The reactor temperature was kept constant at  $135 \pm 1.0^\circ\text{C}$  after adding the catalyst. The stirrer was placed in the upper phase and the dispersion obtained was glycerol in methyl ester (G/ME) type. A 2:1 molar feed ratio of glycerol:ester was used in all experiments with G/ME type of dispersion. The stirrer was set at 550 rpm. In some experimental runs, phase inversion was observed during catalyst addition. Initially, in order to maintain the consistency of experimental conditions, only the experiments with G/ME dispersion were considered. Later, to confirm the effect of emulsion type, an experiment was carried out with ME/G dispersion. In this case, the stirrer was placed in the lower phase and a glycerol:ester feed ratio of 3:1 was used. The dispersion type was judged on the basis of apparent viscosity difference and the difference in settling time. ME/G dispersions were more viscous and needed more time to separate into two phases than G/ME dispersions. The dispersion type was also confirmed by visually observing the settling behavior after stopping the stirrer [58]. The settling behavior for both types of dispersions is illustrated in Figure 4.5. During all the experiments, a part of the methanol produced left the reactor continuously, so in a strict sense the experiments were semi-batch. But the term batch reactor is being used here referring to the liquid phase in the reactor.

### *Sampling procedure:*

The sampling in a reacting two phase system can be difficult and different procedures could lead to different results. Moreover, incomplete information on sampling and analysis procedure may lead to ambiguities in interpreting the results. Therefore, the sampling and analysis procedure was also investigated to obtain reliable data. Some investigators wash the samples from transesterification reaction mixture with water in order to remove the alcohols before analysis. This procedure was not followed in this study as the aim was also to measure the glycerol and methanol concentration in the reaction samples. Samples were taken at different times from the reaction mixture. About 2-3 ml liquid from the reaction mixture was withdrawn by a preheated glass syringe after rinsing the syringe four times with the reactor content. The liquid in the syringe was allowed to separate into two layers for less than a minute (ester phase was still somewhat turbid). GC analysis of samples from the lower layer (glycerol) showed only small amounts of ester and product glycerides (Table 5.1). So for investigating the kinetics, only the upper layer was studied in more detail. Initially, three series of samples were taken with slightly differing methods. Method A: the 2 ml sample was kept at 135°C in an oven until the upper phase was transparent which took about 5-30 minutes and the upper phase was then analyzed. Method B: one drop (about 10 mg) of the ester phase was added into a small vial, cooled in an ice bath and silylated. Method C: the upper and lower layers were allowed to separate for 2 minutes, the upper layer was collected in a vial and immediately cooled in an ice bath and then silylated after 1-3 hours. The samples in method C were centrifuged at 4000 rpm for 10 minutes to get a clear transparent phase before silylation. Samples without centrifugation often showed a relatively higher (up to 20%) glycerol concentration. The procedure for sample preparation and analysis was same for all sampling methods.

For sample preparation, 20  $\mu\text{l}$  of the sample was added into 1 ml of a solution containing 0.383 wt% hexadecane, 1 wt% acetic acid and the rest 1,4-dioxane. Hexadecane served as an internal standard for the GC analysis and the acid was added to neutralize the catalyst. The catalyst was neutralized to avoid damage to the GC column by the catalyst. 200-250  $\mu\text{l}$  BSTFA was added to this mixture and the samples were kept at 80°C for 3 hours for silylation. After silylation, the samples were injected into the GC column. The injection volume was 5.0  $\mu\text{l}$  (splitless). The inlet temperature of the GC column was kept constant at 40°C. The total time of analyzing one sample was 61.5 minutes. The temperature program was ramped in four steps, first, the initial column temperature was kept constant at 38°C for 15 minutes, second, the temperature was raised by 1°C/min to 46°C, third, the temperature was raised to 370°C with a rate of 16°C/min and held at 370°C for 10 minutes, and finally the column was cooled to

40°C at a rate of 40°C/min. The chromatogram thus obtained was analyzed for the composition of the sample. The preparation of samples is schematically shown in Figure 5.1. Figure 5.2 demonstrates the temperature program used for the GC column for the analysis of the present multicomponent system.

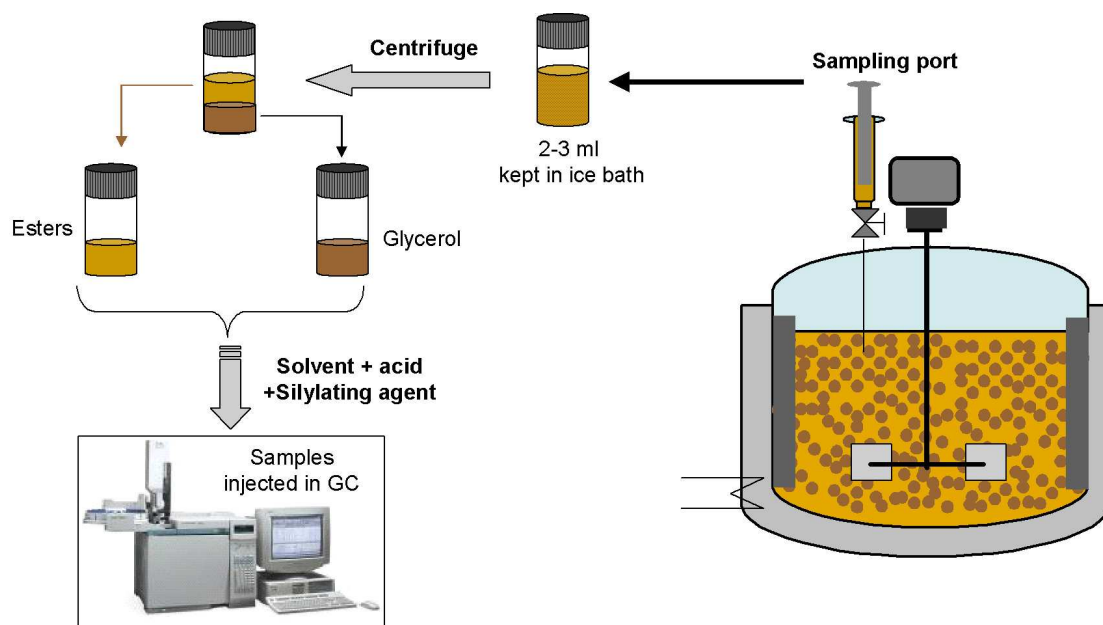


**Figure 5.1:** Steps in preparation of samples for GC analysis.

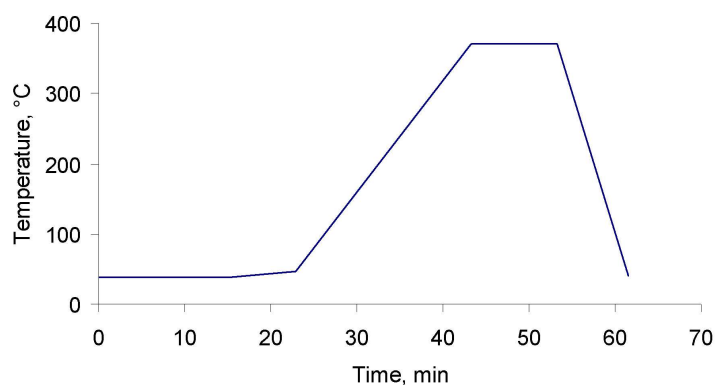


**Figure 5.2:** The GC-column temperature program used for the separation of components in glycerolysis reaction mixture.

### 5.1.3 Data analysis

The mass of a component  $i$ ,  $m_i$  in the injected sample is proportional to the area of the GC peak,  $A_i$ :

$$m_i \propto f_i A_i \quad (5.1)$$

where  $f_i$  is the response factor of component  $i$  obtained by calibration based on the internal standard [65,66]. The mole fraction,  $x_i$  of a component  $i$  in the injected sample was calculated as:

$$x_i = \frac{m_i / M_i}{\sum_{\text{all components}} (m_i / M_i)} \quad (5.2)$$

where  $M_i$  is the molecular weight of component  $i$ . The concentration (mol/kg) was obtained as:

$$C_i = \frac{x_i \times 1000}{\sum x_i M_i} \quad (5.3)$$

Prior to this work, the mass fractions were calculated based on the internal standard as:

$$w_i = \frac{f_i \cdot m_{std} \cdot A_i}{A_{std} \cdot m_{sample}} \quad (5.4)$$

here  $m_{std}$  and  $m_{sample}$  are the known weights of the internal standard and the reaction mixture in the solution to be injected into GC and  $A$  is the corresponding area under the chromatogram. The concentrations were calculated based on these  $w_i$  as:

$$C_i = \frac{w_i}{M_i} \cdot 1000 \quad (5.5)$$

This method had the disadvantage that the errors in gravimetry were included in the calculated concentration. Generally, this method is preferred when some of the total components have to be measured. The method based on Equations 5.2-5.3, that was followed in this study is more precise but it has the disadvantage that all the component peaks have to be integrated. The mass deficit for a GC injection was generally 0.5-5%. For determining the conversion, the ester phase was analyzed on a methanol and glycerol free basis. Since there was a considerable increase in the glycerol concentration in the ester phase, conversion based on the concentration of methyl oleate in the ester phase would lead to false (overestimated) values. The ester conversion,  $X$ , at a time  $t$  was calculated as:

$$X = 1 - \frac{x'_{ME_t}}{x'_{ME_t} + x'_{MG_t} + 2 \times x'_{DG_t} + 3 \times x'_{TG_t}} \quad (5.6)$$

where  $x'_{i_t}$  are the mole fractions calculated on a glycerol and methanol free basis.

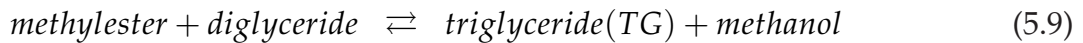
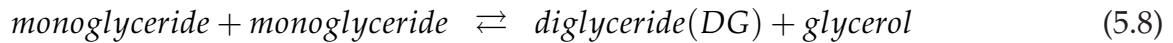
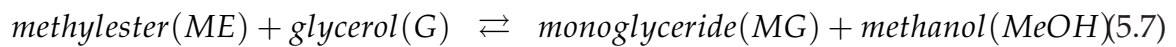


**Table 5.1:** Composition of the two phases from a reaction mixture at ester conversion=31%. Reaction conditions: T=135°C, P=1 bar, without methanol stripping. All compositions are in mol%.

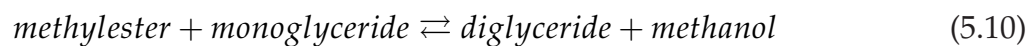
	Ester phase	Glycerol phase
Methanol	7.05	6.93
Glycerol	14.75	92.63
Methyl ester	59.01	0.30
Monoglycerides	12.07	0.14
Diglycerides	6.55	0.00
Triglycerides	0.57	0.00

## 5.2 Modeling and simulation

The kinetic model suggested by Kimmel [1] was used for the present glycerolysis reaction and a third reaction step was added to account for triglyceride formation. The formation of triglycerides was modeled as a series reaction step as it was observed to appear after mono- and diglycerides in all reaction runs. The complete reaction steps were modeled as:



In the literature [25], the reaction step for the production of diglyceride is suggested as:



The use of Equation 5.8 gave better selectivity profiles than Equation 5.10 [1]. Moreover Equation 5.10 indicates that the monoglyceride concentration-time curve is very likely to show a maximum, if methanol is completely removed. However, a maximum in monoglyceride concentration profile was not observed in any of the experiments.

The mass balance for a batch reactor leads to the following equations:

$$\frac{dC_{ME}}{dt} = -k_{1f}C_GC_{ME} + k_{1r}C_{MG}C_{MeOH} - k_{3f}C_{DG}C_{ME} + k_{3r}C_{TG}C_{MeOH} \quad (5.11)$$

$$\frac{dC_{MG}}{dt} = k_{1f}C_GC_{ME} - k_{1r}C_{MG}C_{MeOH} - 2k_{2f}C_{MG}^2 + 2k_{2r}C_{DG}C_G \quad (5.12)$$

$$\frac{dC_{DG}}{dt} = k_{2f}C_{MG}^2 - k_{2r}C_{DG}C_G - k_{3f}C_{DG}C_{ME} + k_{3r}C_{TG}C_{MeOH} \quad (5.13)$$

$$\frac{dC_{TG}}{dt} = k_{3f}C_{DG}C_{ME} - k_{3r}C_{TG}C_{MeOH} \quad (5.14)$$



where  $k_1$ ,  $k_2$ ,  $k_3$  represent the reaction rate constants in reactions 5.7-5.9 respectively, and the subscripts  $f$  and  $r$  represent forward and reverse reactions respectively. The methanol and glycerol concentrations in the ester phase were modeled as:

$$C_{MeOH} = Constant \quad (5.15)$$

$$C_G = A \cdot X + B \quad (5.16)$$

Equation 5.16 shows a linear dependence of glycerol concentration on ester conversion. From the experimental data it was found that this is not always exactly true, but this simple relation gave acceptable results for different experimental conditions. Therefore, this equation was used further for simulations. Here  $B$  was taken as 0.06 mol/kg, which is the experimentally measured solubility of glycerol in methyl oleate at the reaction temperature (135°C). Based on experimental results,  $C_{MeOH}$  was taken as 0.20 mol/kg and 0.01 mol/kg for reactions without and with methanol stripping respectively.

The six kinetic constants in the Equations 5.11-5.14 were obtained by fitting the Equations 5.11-5.16 simultaneously to the experimental data. The data were taken from experiments with and without methanol stripping at a constant temperature. Each reaction dataset contained 10-15 concentration-time data points for each of the components methyl ester, monoglycerides, diglycerides and triglycerides. The values of rate constants are given in Table 5.2. The concentration terms used in the model and measured experimentally are based on the mass of the ester phase. The mass of ester phase increases during the reaction due to formation of glycerides that are found in the ester phase only and due to dissolved glycerol. This increase could be up to 20% based on the initial ester weight. For kinetic modeling, the mass is assumed to be constant. The comparison of simulation and experimental results shown later demonstrates that this did not lead to any significant deviations.

**Table 5.2:** Estimated kinetic parameters for reactions represented in Equations 5.7-5.9

Parameter	Value
$k_{1f}$	$0.074 \text{ kg.mol}^{-1}.\text{min}^{-1}$
$k_{1r}$	$0.645 \text{ kg.mol}^{-1}.\text{min}^{-1}$
$k_{2f}$	$0.348 \text{ kg.mol}^{-1}.\text{min}^{-1}$
$k_{2r}$	$0.717 \text{ kg.mol}^{-1}.\text{min}^{-1}$
$k_{3f}$	$0.004 \text{ kg.mol}^{-1}.\text{min}^{-1}$
$k_{3r}$	$0.227 \text{ kg.mol}^{-1}.\text{min}^{-1}$
$A$	$0.8 \text{ mol/kg}$ (without methanol stripping) $0.4\text{-}0.8 \text{ mol/kg}$ (with methanol stripping and under vacuum)
$B$	$0.06 \text{ mol/kg}$
$C_{MeOH}$	$0.20 \text{ mol/kg}$ (without methanol stripping) $0.01 \text{ mol/kg}$ (with methanol stripping) ( $<0.20 \text{ mol/kg}$ under vacuum)

### 5.3 Results and discussion

Figure 5.3(a) shows the conversions in a batch reaction run obtained by different sampling methods. Conversions obtained from method *B* (samples taken directly from ester phase at reaction temperature without letting the phases separate completely) and *C* (samples cooled to room temperature and centrifuged) were the same. The conversion obtained from method *A* (samples taken from ester phase at reaction temperature after letting the dispersed glycerol separate) were slightly higher in comparison to methods *B* and *C*.

Figure 5.3(b) shows the glycerol concentrations in the ester phase as determined by different sampling methods. As expected, the method *B* shows the highest concentrations as the samples were turbid. The finely dispersed glycerol leads to overestimated concentration values. The concentrations shown by method *C* are lower than actual in the reactor, as the samples were cooled and prepared at room temperature. Method *A* lies in the middle and represents the actual situation better. Unexpectedly, the samples taken at  $135^{\circ}\text{C}$  (method *A*) and at room temperature (method *C*) did not show much difference in glycerol concentration. Figure 5.3(c) shows the mono- and diglycerides concentrations in the samples obtained by different sampling methods. No major effect of sampling method was seen in the product distribution. It was observed that the data obtained by method *C* were consistent, better reproducible than other methods and the samples were easier to prepare. Therefore, this procedure was used for

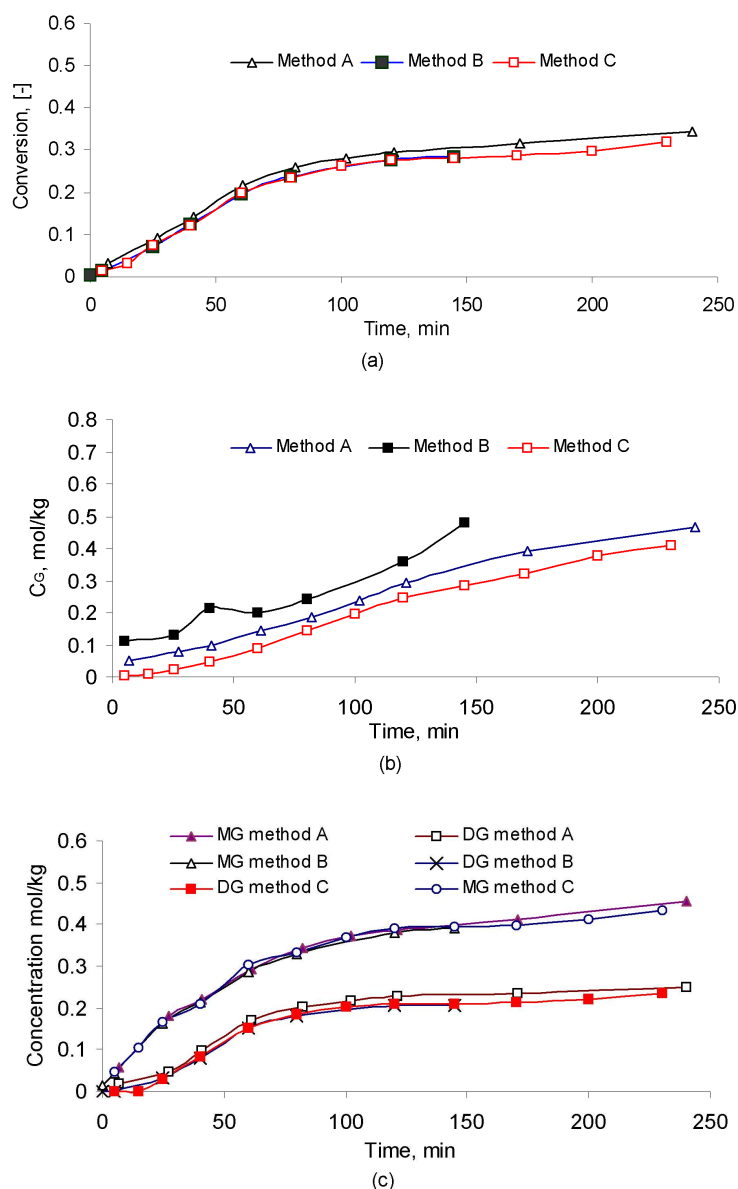


**Figure 5.3:** Effect of sampling method on (a) measured ester conversion, (b) glycerol concentration in the ester phase and (c) Mono- and diglyceride concentrations. Different sampling methods are represented by method A, method B and method C. Method A: samples were taken from ester phase from the reaction mixture and kept at the reaction temperature until the finely dispersed glycerol settled and a clear ester phase was obtained. Method B: samples were taken directly from ester phase at reaction temperature without letting the phases separate completely. Method C: samples taken from the reaction mixture were cooled to room temperature and centrifuged to obtain a clear ester phase.

collecting data that were later used for the calculation of the kinetic parameters. All experimental data represented in subsequent figures, where sampling was involved, were collected as described for method C.

### 5.3.1 Batch reactor without methanol stripping

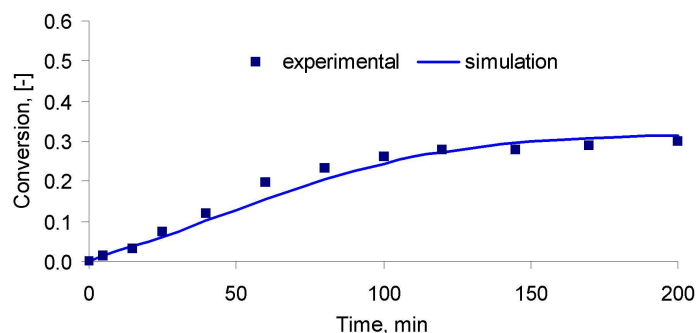


Figure 5.4: Variation of ester conversion with time in a stirred tank reactor without methanol stripping.

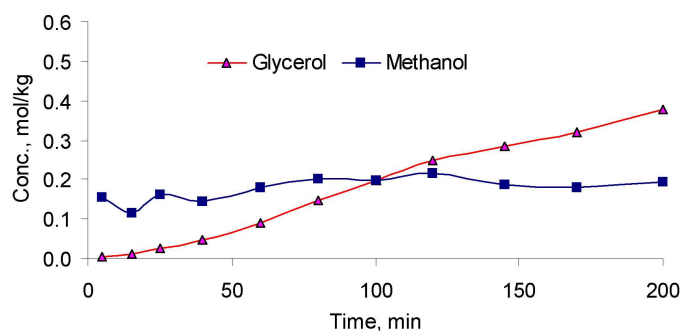
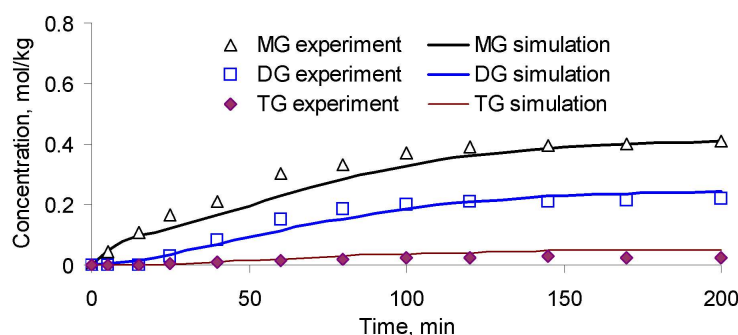
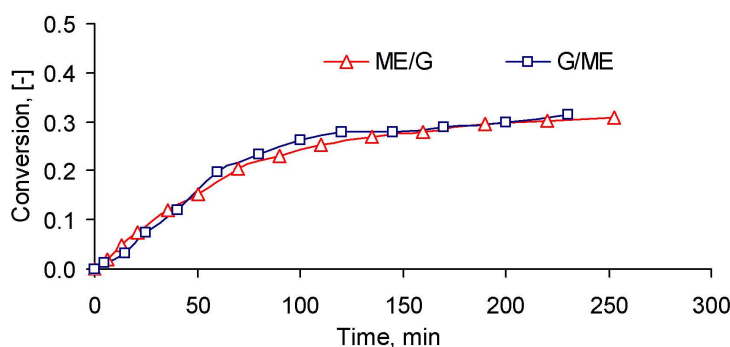


Figure 5.5: Variation of glycerol and methanol concentrations in the ester layer with time during the reaction in the stirred tank reactor without methanol stripping.

Figure 5.4 shows the ester conversion with time for a reaction run without inert gas flow. The reaction is quite slow and approaches a low equilibrium conversion at atmospheric pressure. The methanol and glycerol concentrations in the samples taken at room temperature are shown in Figure 5.5. Since methanol is very volatile and it is continuously produced, its amount in the liquid phase at reaction temperature is determined by the operating pressure and to a lesser extent by the liquid composition. At constant pressure, the concentration of methanol in the ester phase was found to be nearly constant. Figure 5.6 shows the concentration profiles of the produced glycerides. Figures 5.4 and 5.6 also show a good agreement between experimental and simulation results. The reaction was also carried out with ester in glycerol dispersion (ME/G) to study the effect of emulsion type. No significant difference was found in reaction rates in G/ME and ME/G dispersions as can be seen in Figure 5.7. As discussed in Section 3.1.2, the ME/G dispersion has a higher interfacial area than G/ME dispersion ( $\sim 2.9\times$ ). Figure 5.7 favors the hypothesis that mass transfer is not a limiting factor under well dispersed conditions.



**Figure 5.6:** Experimental and simulated time profiles of product glycerides in the stirred tank reactor without methanol stripping.



**Figure 5.7:** Effect of dispersion type on the variation of ester conversion with time in a stirred tank reactor without methanol stripping. ME/G represents the conversion profile obtained from an experiment with esters dispersed in glycerol. G/ME represents the conversion profile from reaction where glycerol was dispersed in esters.

### 5.3.2 Batch reactor with methanol stripping by inert gas

The results obtained from reaction on bubble cap tray (Section 4.2) showed that the reaction could be accelerated and forced to complete conversion by removing methanol from the reaction mixture. Comparison with reactions carried out under vacuum (300, 450 and 600 mbar) and at 1 bar with nitrogen purge [1] showed that methanol stripping by an inert gas was more efficient than applying vacuum. Figure 5.8 shows a comparison of conversion-time curves obtained from reaction runs with methanol removal by inert gas stripping and by applying vacuum. Figure 5.9 shows product concentration profiles with methanol stripping. A comparison of simulated profiles with experimentally obtained data is also shown in the figures. The experiments with methanol stripping showed lower glycerol concentrations in the ester phase than in experiments without methanol stripping for the corresponding conversion values. This lead to a lower value of parameter  $A$  in Equation 5.16 for this case (Table 5.2). Figure 5.10 shows

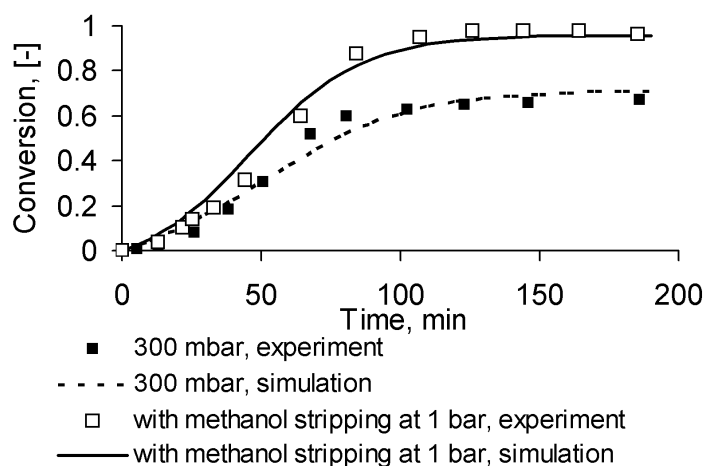


**Figure 5.8:** Ester conversion in a stirred tank reactor with methanol removal by stripping at 135°C and 1 bar and by vacuum at 140°C (The data at 300 mbar are taken from [1]).

the variation of glycerol concentration in the ester phase against conversion. The reproducibility of the conversion profile in reactions with methanol stripping was not very good and the slower initial regime was longer in some cases<sup>1</sup>. However, the end conversion approached unity in each reaction run. The glycerol concentration in ester phase was found to be lower in reactions with longer initial slow regime and the monoglyceride selectivity was also found to vary accordingly. It was discovered (Section 3.4) that the amount of monoglyceride controls the glycerol concentration in the ester phase, but factors causing smaller variation in the glycerol concentration are not known.

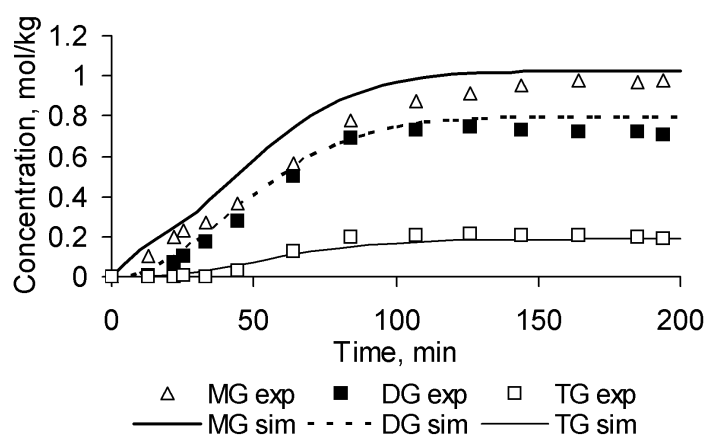


**Figure 5.9:** Experimental and simulated profiles of product glycerides in the stirred tank reactor with methanol stripping (exp=experimental, sim=simulation).

<sup>1</sup>See also Section 4.2

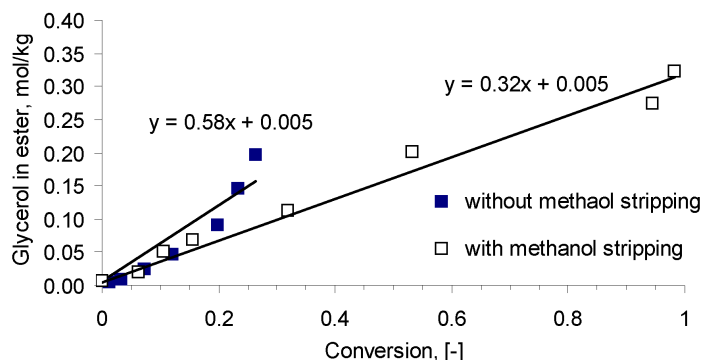


**Figure 5.10:** Dissolved glycerol concentration in the ester phase as determined by GC analysis of samples taken from the reactor at different reaction times. The data represents two experimental runs at 135°C and 1 bar. One experiment was carried out with methanol stripping and the other without. The straight lines represent linear fit.

## 5.4 Summary

Experiments were carried out to study the kinetics of base catalyzed FAME glycerolysis. The semi-empirical kinetic model suggested by Kimmel was extended to account for the formation of triglycerides. The predictions for the methyl ester conversion and product concentration profiles using this model under well mixed conditions were acceptable. Mass transfer effects were not found to be rate limiting under well agitated conditions. Experiments with methanol stripping by nitrogen gas flow showed faster reaction and nearly complete ester conversion. From experiments and simulations, it was found that both methanol and glycerol concentration control the reaction rate and the equilibrium conversion. The methanol concentration could be reduced by applying vacuum or by stripping the reaction mixture by an inert gas. Stripping by an inert gas was found to be more efficient. With the kinetic model used, the ester conversion could be predicted within 12% deviation. The individual component concentrations showed relatively higher deviations (up to 20%). Compared to reactions without methanol stripping, the experiments with methanol stripping showed inferior reproducibility. Differences in glycerol concentration at similar conversions were found in experiments with and without methanol removal. Also, reactions with higher glycerol concentrations showed higher monoglyceride selectivity. At present the factors that lead to differences in the glycerol concentration in the ester phase are not known.

## Chapter 6

# Investigations in Continuous Flow Reactors

After the establishment of a kinetic model for the glycerolysis of fatty acid methyl esters, the final objective was to select a continuous process for this reaction. For this purpose, the reaction was simulated in some common reactor configurations. These included, (a) a single continuous flow stirred tank reactor (CSTR), (b) a single plug flow reactor (PFR), (c) cascade of two CSTRs, (d) cascade of a CSTR and a PFR and (e) a CSTR with a recycle stream containing monoglycerides. Ideal flow pattern was assumed in all the cases. Based on simulation results, a single CSTR was selected for experimental verification.

### 6.1 Simulation of some continuous processes

The reaction steps are shown in Section 5.2. The component mass balance for an ideal CSTR can be written as:

$$\frac{dC_i}{dt} = r_i + \frac{V_0}{V}(C_i^{feed} - C_i) \quad (6.1)$$

Under steady state this reduces to:

$$\tau = \frac{V}{V_0} = \frac{C_i^{feed} - C_i}{-r_i} \quad (6.2)$$

where  $C_i$  represents the concentration of component  $i$  in the ester phase in the reactor,  $V$  is the total liquid volume in reactor,  $V_0$  is the volumetric feed flow rate,  $\tau$  is the nominal



residence time and  $r_i$  represents the production rate by reaction for component  $i$ . The reaction rate terms for the components involved in the present reaction are given by:

$$r_{ME} = -k_{1f}C_G C_{ME} + k_{1r}C_{MG} C_{MeOH} - k_{3f}C_{DG} C_{ME} + k_{3r}C_{TG} C_{MeOH} \quad (6.3)$$

$$r_{MG} = k_{1f}C_G C_{ME} - k_{1r}C_{MG} C_{MeOH} - 2k_{2f}C_{MG}^2 + 2k_{2r}C_{DG} C_G \quad (6.4)$$

$$r_{DG} = k_{2f}C_{MG}^2 - k_{2r}C_{DG} C_G - k_{3f}C_{DG} C_{ME} + k_{3r}C_{TG} C_{MeOH} \quad (6.5)$$

$$r_{TG} = k_{3f}C_{DG} C_{ME} - k_{3r}C_{TG} C_{MeOH} \quad (6.6)$$

Here also the methanol and glycerol concentrations were defined empirically by Equations 5.15 and 5.16. Figure 6.1 shows the conversion and monoglyceride selectivity obtained by simulations for a CSTR as a function of nominal residence time.

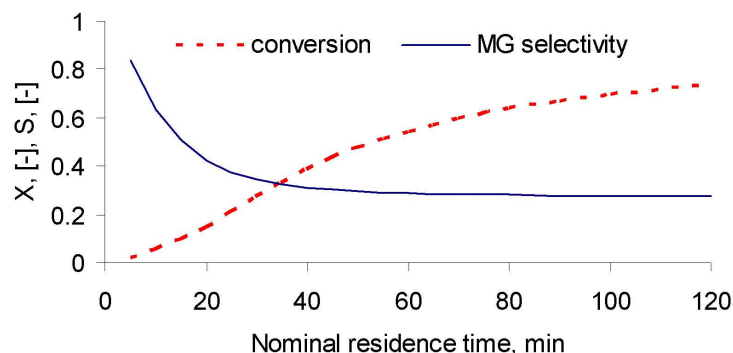


**Figure 6.1:** Simulation of ester conversion ( $X$ ) and monoglyceride selectivity ( $S$ ) in a continuous flow stirred tank reactor with methanol removal at 135°C as a function of residence time.

For an ideal plug flow reactor (PFR), the component mass balance can be written as:

$$\tau = \frac{V}{V_0} = \int_{C_i^{exit}}^{C_i^{feed}} \frac{dC_i}{-r_i} \quad (6.7)$$

which is identical to a batch reactor with reaction time  $\tau$ . In this equation the reaction rate terms,  $r_i$ , are given by Equations 6.3-6.6. From Figure 6.2 it can be seen that the residence time required even for intermediate conversion is very long for a continuous process in a PFR. In comparison to a CSTR, a PFR gives no significant improvement in monoglyceride selectivity as shown in Figure 6.3. There could be additional problems with a tubular reactor. Here it is assumed that the reaction is homogeneous (in the ester phase), which requires that mass transfer is not rate limiting, an assumption which is valid only when the phases are well mixed. In the absence of stirring, the phases tend to separate and the reaction would slow down due to mass transfer limitations. Hence a normal pipe won't suffice for this reaction. Static mixers producing high shear and a

good plug flow behavior could solve this problem but even then the length of the pipe required would be too long for such a reaction. A German patent [67] mentions using a 6 m long static mixer for base catalyzed fat glycerolysis with a nominal residence time of 0.5-5 minutes.

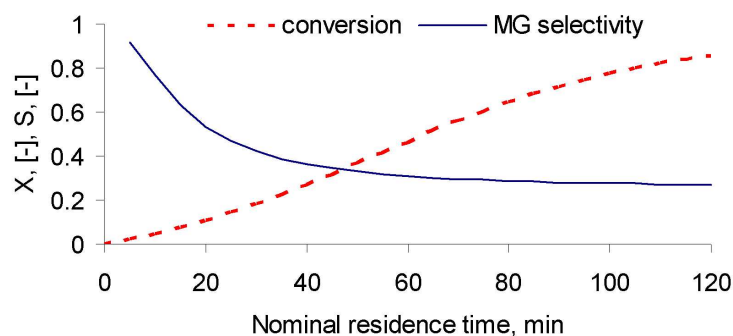


**Figure 6.2:** Simulation of ester conversion and monoglyceride selectivity in an ideal plug flow reactor with methanol removal at  $T=135^{\circ}\text{C}$ ,  $P=1$  bar.

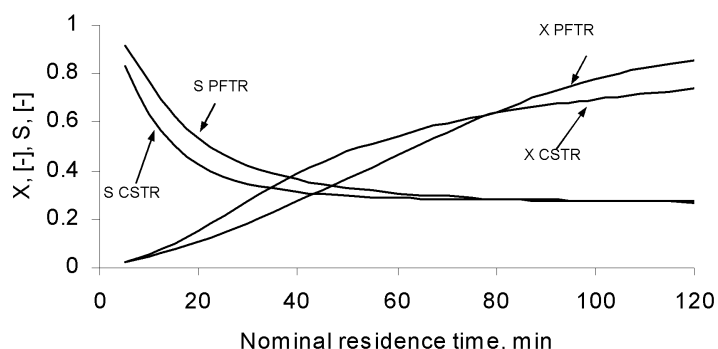


**Figure 6.3:** Comparison of simulated ester conversion (X) and monoglyceride selectivity (S) in an ideal CSTR and PFR at  $T=135^{\circ}\text{C}$ ,  $P=1$  bar.

Figure 6.3 also indicates that a cascade of CSTRs would not bring any significant improvement in conversion or selectivity, as that would approach plug flow profiles. A comparison of monoglyceride yield in a single CSTR and in a cascade of two CSTRs is shown in Figure 6.4. Here, yield is defined as the product of ester conversion and monoglyceride selectivity. A comparison of conversion profiles in Figure 6.3 also suggests that faster conversions could be obtained in a reactor combination of a CSTR followed by a PFR. Figure 6.5 shows the simulated conversion profile obtained by such a combination that would be more time efficient for higher conversions. But the residence times required in the tubular reactor are still too high and the acceleration in conversion not so good. Therefore, although theoretically more efficient than a single CSTR, this is probably not a practical option.

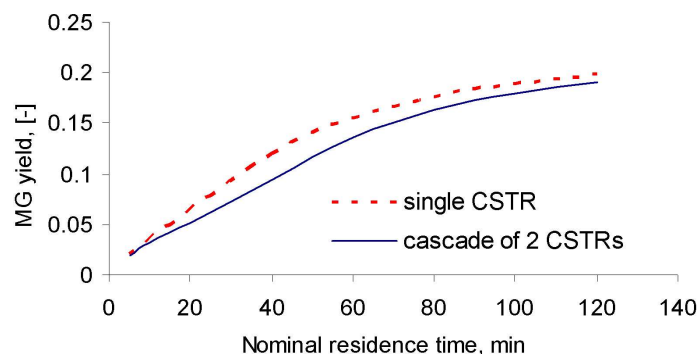


**Figure 6.4:** Comparison of simulated monoglyceride yield in a single CSTR and in a cascade of 2 CSTRs at  $T=135^{\circ}\text{C}$ ,  $P=1$  bar.

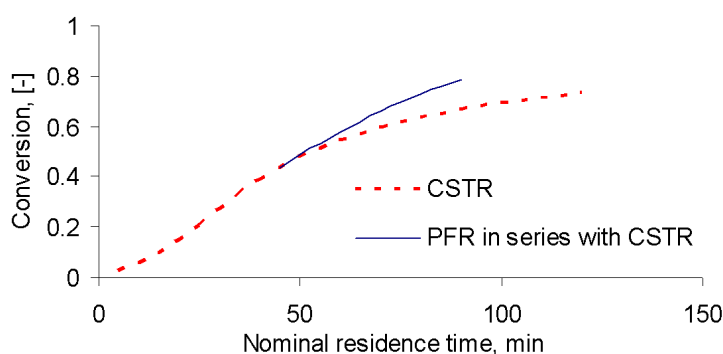


**Figure 6.5:** Simulation of ester conversion in a cascade of CSTR and PFR at  $T=135^{\circ}\text{C}$ ,  $P=1$  bar.

The conversion-time curve in a batch reactor shows autocatalytic behavior, so recycling a part of the product stream containing monoglycerides was expected to give higher reactor efficiency. A US patent [68] on fat glycerolysis mentions returning a part of the product stream containing monoglyceride back into the reactor. The US patent [27] on FAME glycerolysis also mentions recycling monoglyceride to the inlet of reactor to increase the reaction velocities. For the reaction investigated here, simulations showed that no advantages were obtained in monoglyceride yield by considering such recycle stream.

In all these simulations, it was assumed that methanol is efficiently removed from the liquid reaction mixture. Hence, for  $C_{\text{MeOH}}$  (Equation 5.15), a constant value of 0.01 mol/kg was used based on the experiments carried out in batch mode<sup>1</sup>. Methanol can be removed from the reaction mixture by applying vacuum or by passing an inert gas through the liquid. A constant value of 0.4 for parameter  $A$  (Equation 5.16) was used in all simulations. Values of other parameters used are given in Table 5.2. The

<sup>1</sup>See Section 5.2

assumption of a linear dependence of glycerol in ester phase in modeling of continuous process was found to be valid from experimental data. Figure 6.6 shows the variation in the glycerol concentration in the ester phase against conversion obtained from an experiment that was run in continuous and batch modes (details of the experiment are given in the following section).

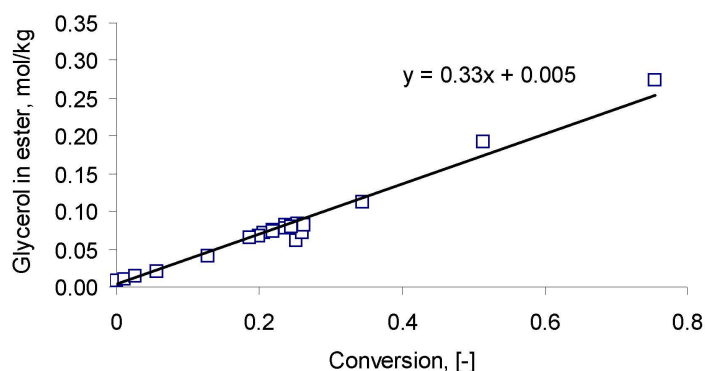


**Figure 6.6:** Experimentally determined concentration of glycerol in ester phase in an experimental run in successive batch-continuous-batch modes at 135°C and 1 bar with methanol stripping by nitrogen gas. Conversion in initial batch mode=0.0-0.26 (reaction time=0-45 minutes). Conversion in continuous mode= 0.26-0.19 (45-300 minutes). Nominal residence time in continuous mode=30 minutes. Conversion in second batch mode=0.19-0.75 (300-355 minutes). □: experimental data, -: linear fit.

Based on the above simulation results, a single CSTR without a recycle stream was chosen for experimental verification. An experimental unit with a CSTR was installed and experiments were performed to verify the simulation results.

## 6.2 Experimental

### 6.2.1 Materials

The materials used were same as mentioned in Section 5.1.

### 6.2.2 Experimental setup and procedure

The experimental setup is shown in Figure 6.7. The main parts of the set-up were: feed reservoirs, diaphragm pumps (CGM prominent, A2001 with teflon diaphragm) and a glass reactor (Wertheim-LF100). The catalyst sodium methylate dissolved in methanol was mixed with glycerol in an amount to yield 1 wt% of total reactant. Two

feed reservoirs, one containing methyl ester and one containing glycerol+catalyst were preheated to 75°C. This was done to reduce the viscosity of glycerol to ease pumping. Preheating the feed also facilitated the temperature control in the reactor during continuous operation. The pumps were calibrated with respective fluids at reaction conditions and were preset to give the desired flow rate during the reaction. The reaction was carried out at 135°C. The temperature was measured by a PT-100 probe. Heating was provided by a thermostatically controlled oil bath (Haake, F6/B5). The oil temperature was controlled to  $\pm 0.1^\circ\text{C}$ . The reaction was run initially in batch mode for about 1.5-2 times the desired nominal residence time to reach an intermediate conversion. The initial liquid volume in the reactor was 300 ml (200 ml methyl ester + 100 ml glycerol). The feed and the product outlet pumps were switched on simultaneously to start the continuous mode. The temperature dropped by about 3-5°C on starting the pumps. The temperature was soon restored to the set point and it was maintained within  $\pm 1.5^\circ\text{C}$  thereafter. The reaction mixture was pumped out at a constant rate. The product stream was cooled by heat exchange with cold water as the temperature limit of fluid for the pumps was 50°C. The outlet fluid was collected in a calibrated cylinder and the volume of both phases was monitored every 20 minutes to assure that both phases had a constant residence time in the reactor. Reactions without methanol stripping were not considered for continuous operation because the reaction is very slow and gives low equilibrium conversion without methanol removal. All the experiments in continuous mode were carried out with methanol stripping by nitrogen. The nominal residence time was chosen by simulations to get a desired value of conversion. The reaction in continuous mode was run for a minimum of 5 residence times. This was roughly the time needed to reach steady state if the continuous mode were started at zero conversion. During the continuous mode, some decline in the residence time (up to 5 minutes) is expected, as the liquid volume inside the reactor reduced somewhat with time due to sample withdrawal and methanol removal. At the end of the continuous mode, the pumps were switched off simultaneously, and the reaction was allowed to proceed further for some time in batch mode, which would be in effect similar to connecting an ideal plug flow reactor to the CSTR in series. During the reaction runs, samples were taken directly from the liquid phase in reactor at different times. The method of sampling and data analysis is explained in Section [5.1](#).

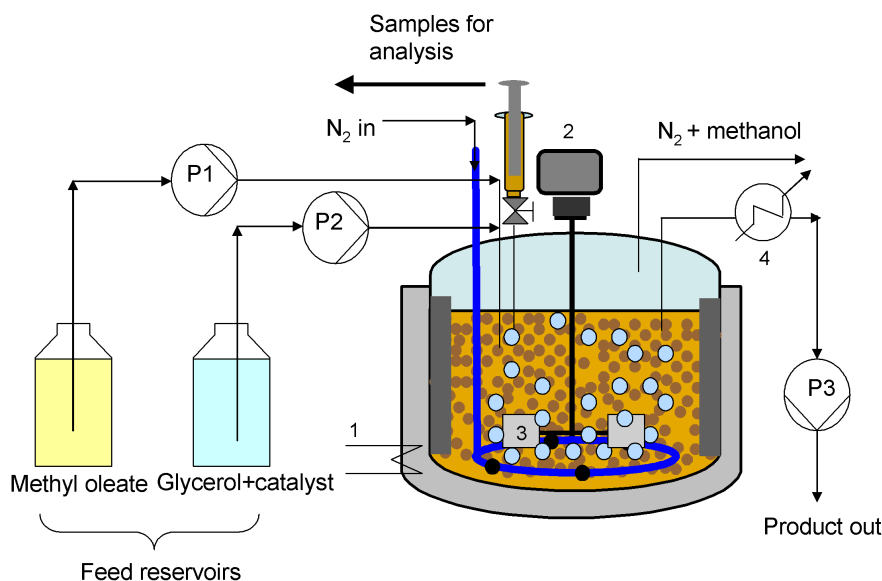


**Figure 6.7:** Experimental setup. (P1, P2, P3: pumps, 1: oil heating, 2: motor, 3: 6 blade turbine stirrer, 4: heat exchanger).

## 6.3 Results and discussion

Figures 6.8(a) and 6.8(b) show the comparison between ester conversion and mono-glyceride selectivity profiles obtained from experiment and simulation. The comparison is shown for a complete experimental run including the batch modes before and after the continuous operation. The reaction presented in Figure 6.8 was run for 75 minutes in batch mode, then from 75 to 275 minutes in continuous mode, and after that it was run further for 35 minutes again in batch mode. The nominal residence time based on the initial liquid volume in the reactor and the feed pumping rate was 40 minutes. The predicted conversion and selectivity data were mostly within 12% of measured values. For continuous operation, lower steady state conversions were obtained by experiments than predicted by simulation.

Figures 6.9(a) and 6.9(b) represent the conversion and selectivity data for a similar experiment where the nominal residence time for the continuous operation was 30 minutes. The duration of the initial batch run was 45 minutes. The continuous mode was run for 300 minutes, i.e. for 8.5 reactor volume replacements and then, finally, the reactor was operated in batch mode for another 55 minutes. Here also the simulations are in agreement with the experimental data, although the experimentally obtained conversions are again slightly lower than the calculated data. In this case, the run was switched over from batch to continuous mode at a conversion value near the steady state conversion, hence a very small transition was observed in this run. The exper-

experimental data show lower values of conversion after 200 minutes, which could result due to the reduction in the liquid volume inside the reactor because of sample withdrawal and methanol removal. Since the liquid streams were pumped into and out of the reactor at a constant rate, this leads to lowering of average residence time. In the FAME glycerolysis reaction, the monoglyceride selectivity follows the opposite trend than the conversion (Figure 6.1). Hence, deviations in opposite direction are seen in the selectivity data in Figure 6.9(b).

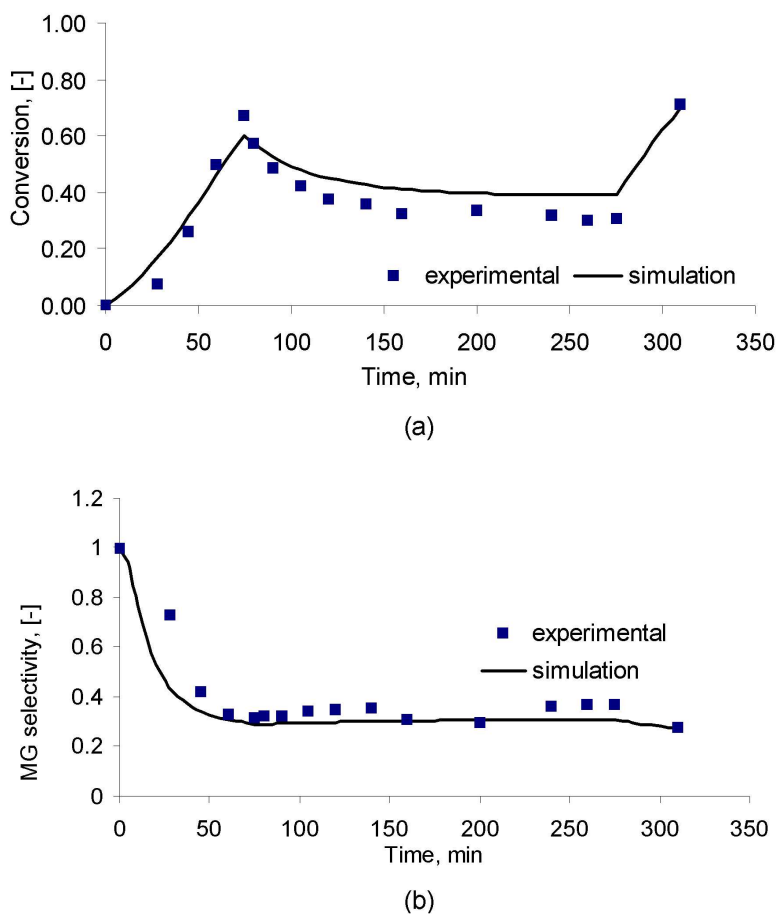


**Figure 6.8:** Simulation and experimentally determined variation in (a) ester conversion and (b) monoglyceride selectivity in an experimental run. 0-75 minutes: batch mode, 75-275 minutes: continuous mode, 275-310 minutes: batch mode. Nominal residence time in continuous mode was 40 minutes.  $T=135^{\circ}\text{C}$ ,  $P=1$  bar, catalyst=1 wt%, strip gas flow rate=5 lpm.

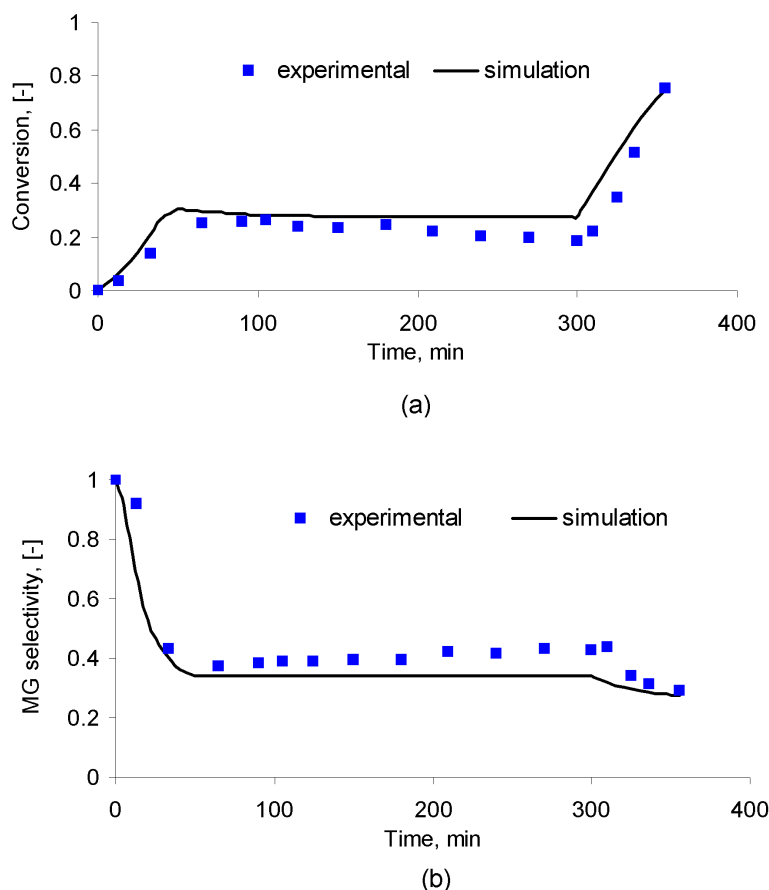


**Figure 6.9:** Simulation and experimentally determined variation in (a) ester conversion and (b) mono-glyceride selectivity in an experimental run. 0-45 minutes: batch mode, 45-300 minutes: continuous mode, 300-355 minutes: batch mode. Nominal residence time in continuous mode was 30 minutes.  $T=135^{\circ}\text{C}$ ,  $P=1$  bar, catalyst=1 wt%, strip gas flow rate=5 lpm.

## 6.4 Summary

The base catalyzed glycerolysis of methyl ester was simulated in flow reactors. Simulations for selected continuous processes were performed using the semi-empirical kinetic model presented in Chapter 5. Based on simulation results, a single CSTR was considered to be preferable to other alternatives that were simulated and it was chosen for experimental verification. The experiments were carried out at a constant temperature of  $135^{\circ}\text{C}$  with different nominal residence times. The yields of monoglycerides achieved were not higher than other processes used to produce them<sup>2</sup>. Faster reaction rates and higher monoglycerides yields are expected at higher temperatures due to the effect of temperature on reaction rate and on glycerol and methanol concentrations in the ester phase as well. Although simulations show this trend, it is not possible to

<sup>2</sup>See Chapter 2



predict the reaction behavior with a known accuracy at present. For the simulation of the reaction at higher temperatures, data on glycerol solubility under actual reaction conditions are needed. The experiments under investigation in the stirred tank reactor in transition and steady state modes showed good agreement with the simulated data. In these experiments, the ester conversion and monoglyceride selectivity in batch reactor and continuous mode could be generally predicted within 12% deviation with the present model. This model can be further used for preliminary design and selection of processes for FAME glycerolysis. In addition, a process has been developed to manufacture mono-diglycerides in continuous mode.

# Appendix A

## A.1 Component data calculations

**Diffusivity coefficient in liquids,  $D_{AB}$ :**

The diffusion coefficient of glycerol in methyl oleate was estimated using the *Wilke-Chang correlation* [60]:

$$D_{AB}^o = \frac{117.3 \times 10^{-18} (\varphi M_B)^{0.5} T}{\mu \nu_A^{0.6}} \quad (\text{A.1})$$

where  $D_{AB}^o (m^2/s)$  is the diffusivity of  $A$  in very dilute solution in solvent  $B$ ,  $M_B (kg/kmol)$  is the molecular weight of the solvent,  $T (K)$  is the temperature,  $\mu (kg/m.s)$  is the solution viscosity,  $\nu_A (m^3/kmol)$  is the solute molal volume at normal boiling point and  $\varphi$  is the association factor for the solvent. For the diffusivity of glycerol in methyl oleate at  $135^\circ\text{C}$ :

$$M_B = 296.5$$

$$\mu = 0.7 \text{ cP (from Lewis and Squires correlation [42])}$$

$$\varphi = 1 \text{ (for unassociated solvents [60])}$$

$\nu_A = 86.85 \text{ cm}^3/\text{mol}$  (Source: ASPEN Plus database) With this correlation the diffusivity of glycerol in methyl oleate was calculated to be  $5.1 \times 10^{-9} m^2/s$ .

**Liquid phase mass transfer coefficient,  $k_{lA}$ :**

This was estimated for the continuous phase using the correlation of *Calderbank and Moo-Young*, which can be used for an agitated system with small drops or bubbles [61,69]. According to this correlation

$$k_{lA} = 0.13 \left( \frac{(P/V)\mu}{\rho^2} \right)^{1/4} \left( \frac{\mu}{\rho D_{AB}} \right)^{-2/3} \quad (\text{A.2})$$

$\mu$  and  $\rho$  are the viscosity and density of the continuous phase and  $(P/V)$  is the power delivered per unit volume of vessel content. For the glycerol-ester system at  $135^\circ\text{C}$

(P/V) can be calculated as shown in Equation 4.4. With an rpm of  $600 \text{ min}^{-1}$  the value of  $k_{IA}$  was calculated to be  $1 \times 10^{-4} \text{ ms}^{-1}$ .

### Liquid viscosity

When the liquid viscosity is known at some temperature, the unknown viscosity at a desired temperature can be calculated by *Lewis and Squires viscosity-temperature correlation* [42] as:

$$\eta_T^{-0.2661} = \eta_k^{-0.2661} + \frac{T - T_k}{233} \quad (\text{A.3})$$

where  $\eta_T(\text{cP})$  is the liquid viscosity at  $T(^{\circ}\text{C}$  or  $\text{K})$  and  $\eta_k(\text{cP})$  is the known value of liquid viscosity at  $T_k$ .

## A.2 Group distribution and parameters for UNIFAC and UNIFAC-Dortmund

**Table A.1:** Group assignment for the UNIFAC method [42].

group number	main group	subgroup
1	$\text{CH}_2$	$\text{CH}_3$ $\text{CH}_2$ $\text{CH}$
2	$\text{C}=\text{C}$	$\text{C}_2\text{H}_2$
5	$\text{OH}$	$\text{OH}$
6	$\text{CH}_3\text{OH}$	$\text{CH}_3\text{OH}$
11	$\text{CCOO}$	$\text{CH}_3\text{COO}$ $\text{CH}_2\text{COO}$

**Table A.2:** Interaction parameter according to UNIFAC-LLE [46].

	$\text{CH}_3$	$\text{CH}_2$	$\text{CH}$	$\text{CH}_3\text{COO}$	$\text{OH}$	$\text{C}_2\text{H}_2$	$\text{CH}_2\text{COO}$
$\text{CH}_3$	0	0	0	972.4	644.6	74.54	972.4
$\text{CH}_2$	0	0	0	972.4	644.6	74.54	972.4
$\text{CH}$	0	0	0	972.4	644.6	74.54	972.4
$\text{CH}_3\text{COO}$	-320.1	-320.1	-320.1	0	180.6	485.6	0
$\text{OH}$	328.2	328.2	328.2	195.6	0	470.7	195.6
$\text{C}_2\text{H}_2$	292.3	292.3	292.3	-577.5	724.4	0	-577.5
$\text{CH}_2\text{COO}$	-320.1	-320.1	-320.1	0	180.6	485.6	0

**Table A.3:** Binary interaction parameters used for UNIFAC-VLE [42].

	$CH_3$	$CH_2$	$CH$	$CH_3COO$	$OH$	$C_2H_2$	$CH_2COO$	$CH_3OH$
$CH_3$	0	0	0	232.1	986.5	86.02	232.1	697.2
$CH_2$	0	0	0	232.1	986.5	86.02	232.1	697.2
$CH$	0	0	0	232.1	986.5	86.02	232.1	697.2
$CH_3COO$	114.8	114.8	114.8	0	245.4	132.1	0	249.6
$OH$	156.4	156.4	156.4	101.1	0	457	101.1	-137.1
$C_2H_2$	-35.36	-35.36	-35.36	37.85	524.1	0	37.85	787.6
$CH_2COO$	114.8	114.8	114.8	0	245.4	132.1	0	249.6
$CH_3OH$	16.51	16.51	16.51	-10.72	249.1	-12.52	-10.72	0

**Table A.4:**  $R_k$  and  $Q_k$  Parameters for the UNIFAC method [42].

	$CH_3$	$CH_2$	$CH$	$CH_3COO$	$OH$	$C_2H_2$	$CH_2COO$	$CH_3OH$
$R_k$	0.9011	0.6744	0.4469	1.9031	1	1.1167	1.6764	1.4311
$Q_k$	0.848	0.54	0.228	1.728	1.2	0.867	1.42	1.432

**Table A.5:** Binary interaction parameters,  $a_{nm}$  and  $a_{mn}$  used for UNIFAC-Dortmund method [50].

	$CH_3$	$CH_2$	$CH$	$CH_3COO$	$OH$	$C_2H_2$	$CH_2COO$	$OH-s$	$CH_3OH$
$CH_3$	0	0	0	98.7	2777	189.7	98.7	2777	2409.4
$CH_2$	0	0	0	98.7	2777	189.7	98.7	2777	2409.4
$CH$	0	0	0	98.7	2777	189.7	98.7	2777	2409.4
$CH_3COO$	632.2	632.2	632.2	0	310.4	-582.8	0	310.4	294.76
$OH$	1606	1606	1606	973.8	0	1566	973.8	0	346.31
$C_2H_2$	-94.4	-94.4	-94.4	980.7	2649	0	980.7	2649	-628.07
$CH_2COO$	632.2	632.2	632.2	0	310.4	-582.8	0	310.4	294.76
$OH-s$	1606	1606	1606	973.8	0	1566	973.8	0	346.31
$CH_3OH$	82.593	82.593	82.593	299.23	-1218.2	-96.297	299.23	-1218.2	0

**Table A.6:** Binary interaction parameters,  $b_{nm}$  and  $b_{mn}$  used for UNIFAC-Dortmund method [50].

	$CH_3$	$CH_2$	$CH$	$CH_3COO$	$OH$	$C_2H_2$	$CH_2COO$	$OH-s$	$CH_3OH$
$CH_3$	0	0	0	1.9294	-4.674	-0.2723	1.9294	-4.674	-3.0099
$CH_2$	0	0	0	1.9294	-4.674	-0.2723	1.9294	-4.674	-3.0099
$CH$	0	0	0	1.9294	-4.674	-0.2723	1.9294	-4.674	-3.0099
$CH_3COO$	-3.3912	-3.3912	-3.3912	0	1.538	1.6732	0	1.538	0.3745
$OH$	-4.746	-4.746	-4.746	-5.633	0	-5.809	-5.633	0	-2.4583
$C_2H_2$	0.0617	0.0617	0.0617	-2.4224	-6.508	0	-2.4224	-6.508	10
$CH_2COO$	-3.3912	-3.3912	-3.3912	0	1.538	1.6732	0	1.538	0.3745
$OH-s$	4.746	-4.746	-4.746	-5.633	0	-5.809	-5.633	0	-2.4583
$CH_3OH$	-0.4857	-0.4857	-0.4857	-1.2702	9.7928	0.6304	-1.2702	9.7928	0

**Table A.7:** Binary interaction parameters,  $c_{nm}$  and  $c_{mn}$  used for UNIFAC-Dortmund method [50].

	$CH_3$	$CH_2$	$CH$	$CH_3COO$	$OH$	$C_2H_2$	$CH_2COO$	$OH-s$	$CH_3OH$
$CH_3$	0	0	0	-0.0031	0.0016	0	-0.0031	0.0016	0
$CH_2$	0	0	0	-0.0031	0.0016	0	-0.0031	0.0016	0
$CH$	0	0	0	-0.0031	0.0016	0	-0.0031	0.0016	0
$CH_3COO$	0.0039	0.0039	0.0039	0	-0.0049	0	0	-0.0049	0
$OH$	0.0009	0.0009	0.0009	0.0077	0	0.0052	0.0077	0	0.002929
$C_2H_2$	0	0	0	0	0.0048	0	0	0.0048	-0.01497
$CH_2COO$	0.0039	0.0039	0.0039	0	-0.0049	0	0	-0.0049	0
$OH-s$	0.0009	0.0009	0.0009	0.0077	0	0.0052	0.0077	0	0.002929
$CH_3OH$	0	0	0	0	-0.01616	-0.0018	0	-0.01616	0

**Table A.8:**  $R_k$  and  $Q_k$  Parameters for UNIFAC-Dortmund method [50].

	$CH_3$	$CH_2$	$CH$	$CH_3COO$	$OH$	$C_2H_2$	$CH_2COO$	$OH-s$	$CH_3OH$
$R_k$	0.6325	0.6325	0.6325	1.27	1.2302	1.2832	1.27	1.063	0.8585
$Q_k$	1.0608	0.7081	0.3554	1.6286	0.8927	1.2489	1.4228	0.8663	0.9938

### A.3 GC calibration

Figure A.1 shows a chromatogram obtained with pure chemicals that were used for calibration. A typical chromatogram obtained from a reaction run with methanol removal is shown in Figure A.2. The temperature program employed for the GC column is described in Section 5.1. Figures A.3-A.8 show the calibration plots for all the reactants and products. The straight lines show the fitted linear trend with intercept made zero. Calibration data for each component is plotted in two ways. In one plot, the ratio of the component and the standard (hexadecane) areas under GC peak ( $A_i/A_{std}$ ) is plotted against the ratio of known weights of the components and the standard in the injected sample ( $W_i/W_{std}$ ). The reverse ratios are plotted in the second plot. Ideally, the slopes of the two calibration plots obtained this way should be inverse of each other.

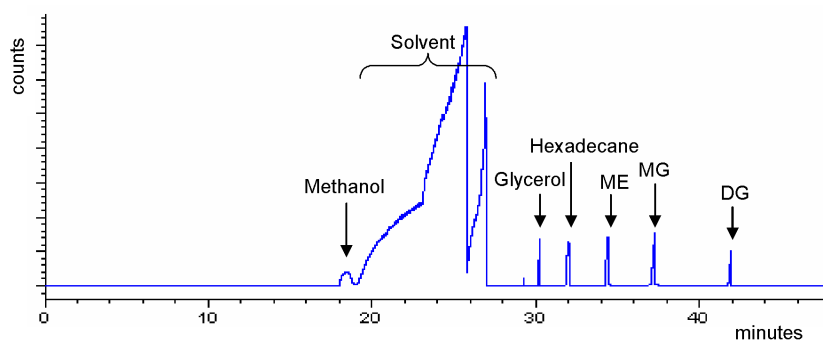


**Figure A.1:** A typical chromatogram showing different component peaks ME: methyl oleate, MG: monoolein, DG: diolein. Triolein peak appears at 45 minutes (not shown in the figure).

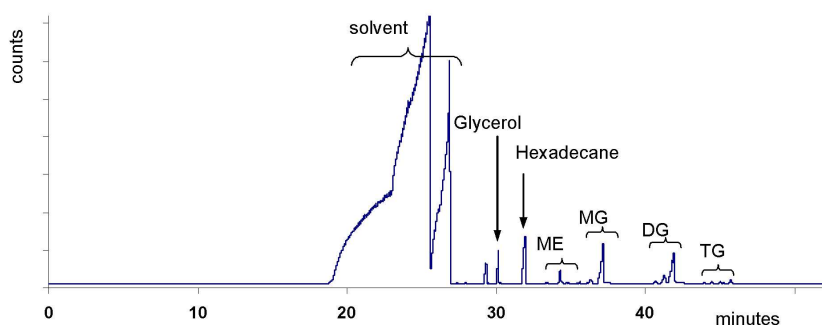


**Figure A.2:** A typical chromatogram showing different component peaks in a sample taken during reaction with methanol stripping. ME: methyl oleate, MG: monoglycerides, DG: diglycerides. TG: triglycerides.

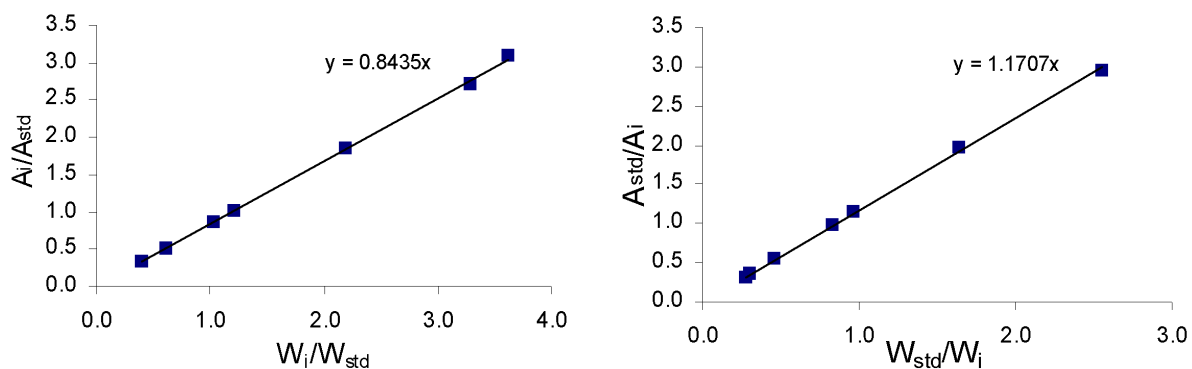


Figure A.3: Calibration plots for methyl oleate (methyl ester).

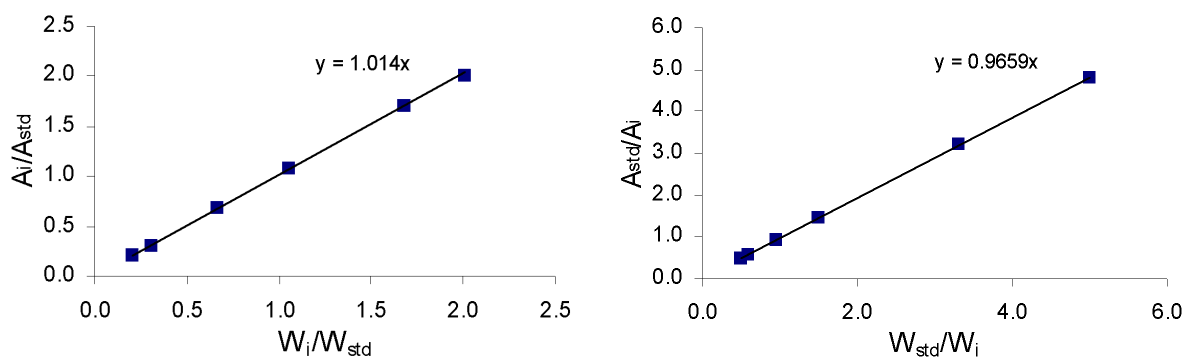


Figure A.4: Calibration plots for monoolein (monoglyceride).

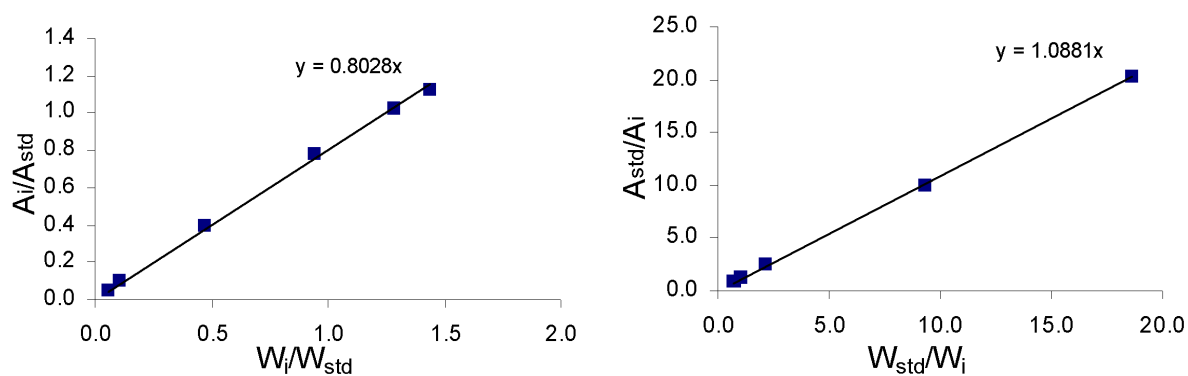


Figure A.5: Calibration plots for diolein (diglyceride).

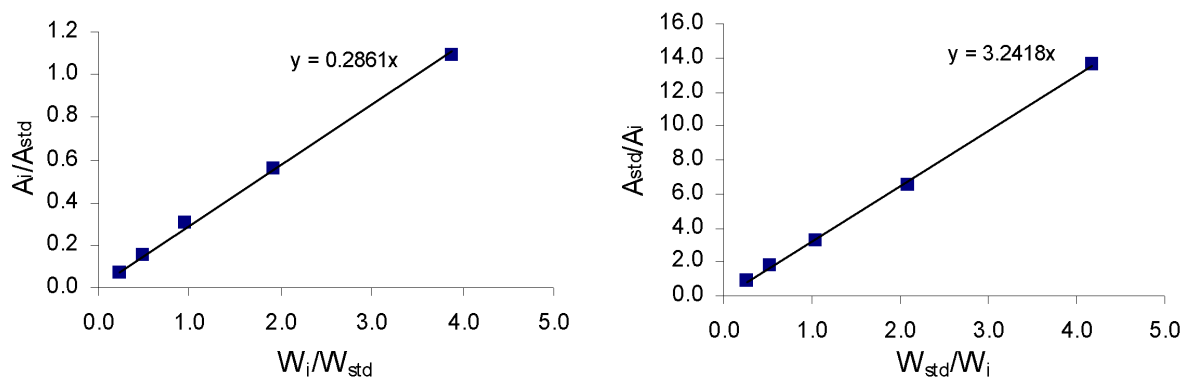


Figure A.6: Calibration plots for triolein (triglyceride).

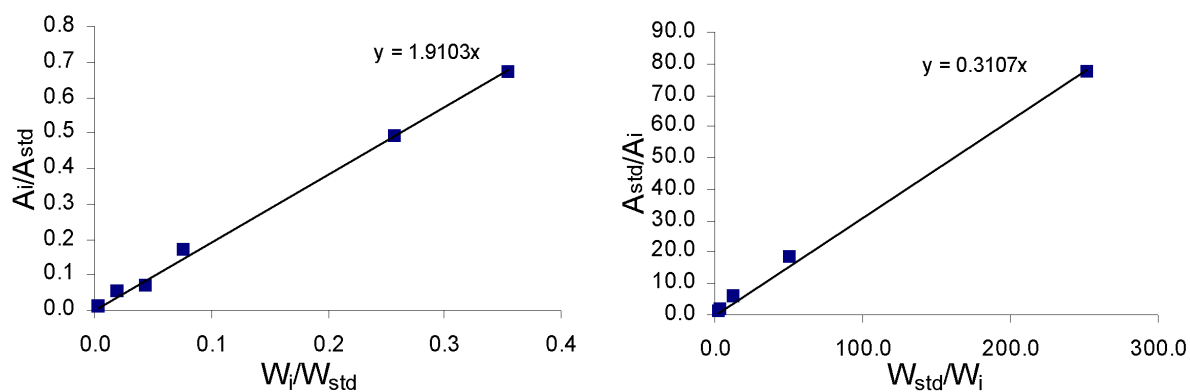


Figure A.7: Calibration plots for methanol.

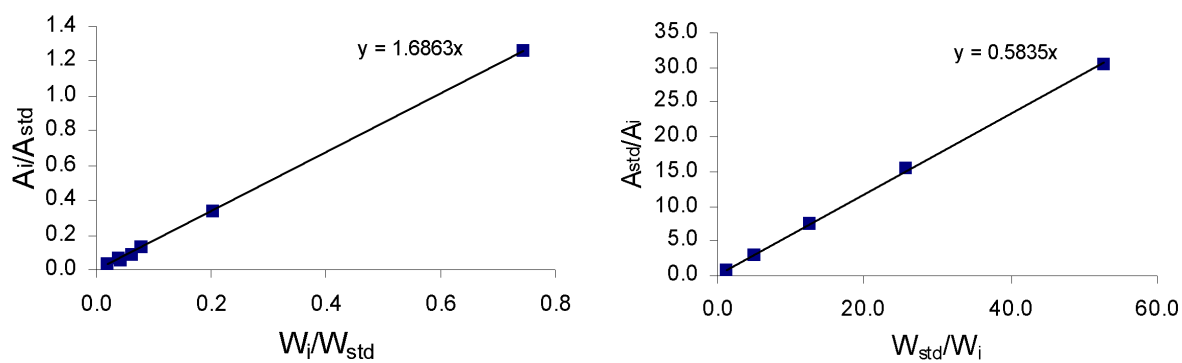
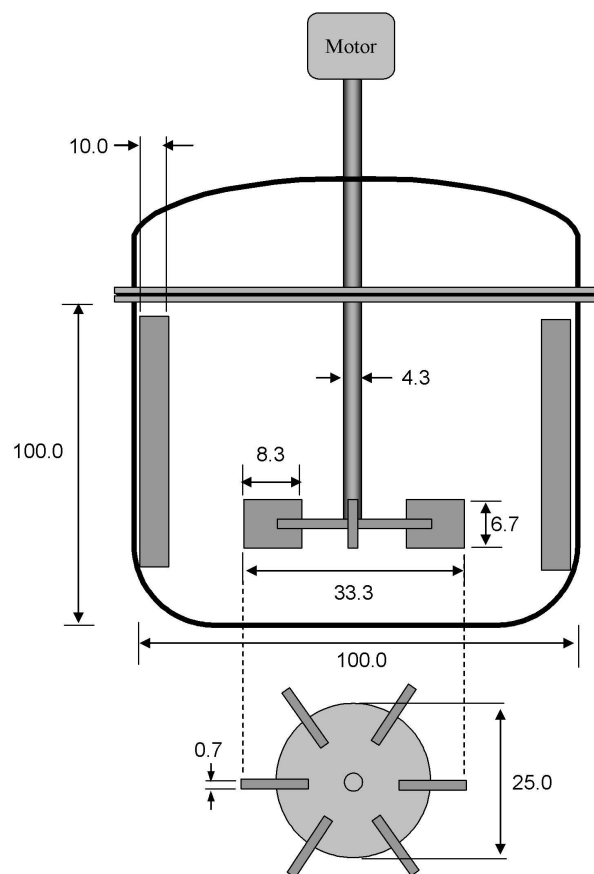


Figure A.8: Calibration plots for glycerol.



## A.4 Stirred tank design

The dimensions of the stirred tank used as standard reactor are given in Figure A.9.



**Figure A.9:** Dimensions of the glass reactor (Wertheim LF-100) and impeller. All dimensions are in millimeters.

# Bibliography

- [1] T. Kimmel. *Kinetic Investigation of the Base-Catalyzed Glycerolysis of Fatty Acid Methyl Esters*. PhD thesis, Institut für Chemie, T. U. Berlin, Germany, 2004.
- [2] T. Kimmel. Beiträge zur Umesterung von Fettsäuremethylestern mit Glycerin durch Reaktivrektifikation. Master's thesis, Institut für Chemie und Institut für Prozeß- und Anlagentechnik, T. U. Berlin, Germany, 1998.
- [3] R. D. O'Brien. *Fats and Oils: Formulating and Processing for Applications, Second Edition*. CRC press LLC, USA, 2004.
- [4] R. J. Whitehurst. *Emulsifiers in Food Technology*. Blackwell Publishing, U.K., 2004.
- [5] G. Schuster. *Emulgatoren für Lebensmittel*. Springer Verlag, Berlin, 1985.
- [6] B. R. Harris, 1933. US Patent 1,917,249.
- [7] H. Birnbaum. The monoglycerides: Manufacture, concentration, derivatives and application. *Bakers Digest*, December:6, 1981.
- [8] N. Krog. Functions of emulsifiers in food systems. *J. Am. Oil Chem. Soc.*, 54(2):124, 1977.
- [9] H. Birnbaum. Emulsifiers. *Bakers Digest*, October:46, 1955.
- [10] C. Henry. Monoglycerides: The universal emulsifier. *Cereal foods world*, 40(10):734, 1995.
- [11] J. B. Lauridsen. Food emulsifiers: Surface activity, edibility, manufacture, composition and application. *J. Am. Oil Chem. Soc.*, 53:400, 1976.
- [12] E. Boyle. Monoglycerides in food systems: Current and future uses. *Food Tech.*, 51(8):52, 1997.
- [13] A. Meffert. Technical uses of fatty acid esters. *J. Am. Oil Chem. Soc.*, 61(2):255, 1984.

- [14] N. O. V. Sonntag. Glycerolysis of fats and methyl esters: Status, review and critique. *J. Am. Oil Chem. Soc.*, 59(10):795, 1982.
- [15] A. Grün, 1924. US Patent 1,505,560.
- [16] N. B. K. Thengumpillil, Penumarthi V., and A. L. Ayyangari, 2002. US Patent 6,500,974.
- [17] F. Temelli, J. W. King, and G. R. List. Conversion of oils to monoglycerids by glycerolysis in supercritical carbon dioxide media. *J. Am. Oil Chem. Soc.*, 73(6):699, 1996.
- [18] W. G. Alsop and I. J. Krems, 1963. US Patent 3,083,216.
- [19] W. Stein, 1964. US Patent 3,160,646.
- [20] R. Schroder and K. Oba, 1992. US Patent 5,153,126.
- [21] A. Zaks and A. T. Gross, 1994. US Patent 5,316,927.
- [22] W. Kaewthong, S. Sirisansaneeyakul, P. Prasertsan, and A. H-Kittikun. Continuous production of monoacylglycerols by glycerolysis of palm olein with immobilized lipase. *Proc. Biochem.*, 40:1525, 2005.
- [23] T. Yang, M. Rebsdorf, U. Engelrud, and X. Xu. Enzymatic production of monoacylglycerols containing polyunsaturated fatty acids through an efficient glycerolysis system. *J. Agric. Food. Chem.*, 53:1475, 2005.
- [24] H. Nouredдини and D. Zhu. Kinetics of transesterification of soybean oil. *J. Am. Oil Chem. Soc.*, 74(11):1457, 1997.
- [25] H. Nouredдини and V. Medikonduru. Glycerolysis of fats and methyl esters. *J. Am. Oil Chem. Soc.*, 74(4):419, 1997.
- [26] H. Nouredдини, D. W. Harkey, and M. R. Gutsman. A continuous process for the glycerolysis of soybean oil. *J. Am. Oil Chem. Soc.*, 81(2):203, 2004.
- [27] L. Jeromin, G. Wozny, and P. Li, 2000. US Patent 6,127,561.
- [28] F. Ma, A. Milford, and A. Hanna. Biodiesel production: A review. *Biores. Tech.*, 70:1, 1999.
- [29] H. Nouredдини, D. Harkey, and V. Medikonduru. A continuous process for the conversion of vegetable oils into methyl esters of fatty acids. *J. Am. Oil Chem. Soc.*, 75(12):1775, 1998.

- [30] D. Darnoko and M. Cheryan. Continuous production of palm methyl esters. *J. Am. Oil Chem. Soc.*, 77(12):2000, 2000.
- [31] T. Dittmar, T. Dimmig, B. Ondruschka, B. Heyn, J. Haupt, and M. Lauterbach. Herstellung von Fettsäuremethalestern aus Rapsöl und Altfetten im kontinuierlichen Betrieb. *Chem. Ing. Tech.*, 75(5):601, 2003.
- [32] Y. Zhang, M. E. Dube, D. D. McLean, and M. Kates. Biodiesel production from waste cooking oil: 1. Process design and technological assessment. *Biores. Tech.*, 89:1, 2003.
- [33] B. Freedman, R. O. Butterfield, and E. H. Pryde. Transesterification kinetics of soybean oil. *J. Am. Oil Chem. Soc.*, 63(10):1375, 1986.
- [34] B. Freedman, E. H. Pryde, and T. L. Mounts. Variables affecting the yields of fatty esters from transesterified vegetable oils. *J. Am. Oil Chem. Soc.*, 61:1638, 1984.
- [35] D. Darnoko and M. Cheryan. Kinetics of palm oil transesterification in a batch reactor. *J. Am. Oil Chem. Soc.*, 77(12):1263, 2000.
- [36] T. Dittmar, T. Dimmig, B. Ondruschka, B. Heyn, J. Haupt, and M. Lauterbach. Herstellung von Fettsäuremethalestern aus Rapsöl und Altfetten im diskontinuierlichen Betrieb. *Chem. Ing. Tech.*, 75(5):595, 2003.
- [37] W. D. Bossaert, D. E. De Vos, W. M. Van Rhijn, J. Bullen, P. J. Grobet, and P. A. Jacobs. Mesoporous sulfonic acids as selective heterogeneous catalysts for the synthesis of monoglycerides. *J. Cat.*, 182:156, 1999.
- [38] T. Cerce, S. Peter, and W. Weidner. Biodiesel-transesterification of biological oils with liquid catalysts: Thermodynamic properties of oil-methanol-amine mixtures. *Ind. Eng. Chem. Res.*, 44:9535, 2005.
- [39] L. K. Doraiswami and M. M. Sharma. *Heterogeneous Reactions: Analysis, Examples, and Reactor Design, Volume 2: Fluid-fluid-solid Reactions*. Wiley, New York, 1984.
- [40] T. Kimmel, M. Joshi, and R. Schomäcker. Tropfengrößenbestimmung mittels Mikrophotographie in Reaktiven Flüssig/Flüssig Systemen bei hohem Anteil an disperser Phase. *Chem. Ing. Tech.*, 74(9):1281, 2002.
- [41] Aspen Technology, Inc. USA. *Aspen Plus: Reference Manual-Volume 2*, aspen plus release 9<sup>th</sup> edition.
- [42] R. C. Reid, J. M. Prausnitz, and B. E. Poling. *The Properties of Gases and Liquids, Fourth Edition*. McGraw-Hill Inc, New York, 1987.

- [43] A. Fredenslund, R. L. Jones, and J. M. Prausnitz. Group-contribution estimation of activity coefficients in nonideal liquid mixtures. *AIChE J.*, 21(6):1086, 1975.
- [44] A. Fredenslund, J. Gmehling, and P. Rasmussen. *Vapor-Liquid Equilibria using UNIFAC- A Group Contribution Method*. Elsevier, Amsterdam, 1977.
- [45] D. S. Abrams and J. M. Prausnitz. Statistical thermodynamics of liquid mixtures: A new expression for the excess gibbs energy of partly or completely miscible systems. *AIChE J.*, 21(1):116, 1975.
- [46] T. Magnussen, P. Rasmussen, and A. Fredenslund. Parameter table for prediction of liquid-liquid equilibria. *Ind. Eng. Chem. Res.*, 20:331, 1981.
- [47] G. Wollmann, B. Gutsche, E. Peukert, and L. Jeromin. Glycerinolyse-Modellierung und Auslegung einer Reaktion mit einer Mischungslücke der Reaktanten. *Fat Sci. Technol.*, 90:507, 1988.
- [48] J. Hofmockel. Analyse und Optimierung der Umesterung von Fettsäuremethylestern mit Glycerin. Master's thesis, Institut für Prozeß- und Anlagentechnik, T. U. Berlin, Germany, 1997.
- [49] U. Weidlich and J. Gmehling. A modified UNIFAC model. 1. Prediction of VLE,  $h^e$  and  $\gamma^\infty$ . *Ind. Eng. Chem. Res.*, 26:1372, 1987.
- [50] J. Gmehling, Li J., and M. Schiller. A modified UNIFAC model. 2. Present parameter matrix and results for different thermodynamic properties. *Ind. Eng. Chem. Res.*, 32:178, 1993.
- [51] H. Kister. *Distillation Design*. McGraw-Hill, USA, 1992.
- [52] D. F. Othmer and P. E. Tobias. Tie line correlation. *Ind. Eng. Chem. Res.*, 34(6):693, 1942.
- [53] F. Sobotka. Experimentelle und theoretische Untersuchung zu den flüssig-flüssig Phasengleichgewichten in System Glycerin, Fettsäuremethylester und Fettsäuremonoglycerid. Master's thesis, Institut für Chemie, T. U. Berlin, Germany, 2005.
- [54] R. Krishna. Reactive separation: More ways to skin a cat. *Chem. Eng. Sci.*, 57:1491, 2002.
- [55] M. F. Malone and M. F. Doherty. Reactive distillation. *Ind. Eng. Chem. Res.*, 39(11):3953, 2000.

- [56] F. Reepmeyer, J. U. Repke, and G. Wozny. Time optimal start-up strategies for reactive distillation columns. *Chem. Eng. Sci.*, 59:4339, 2004.
- [57] J. Ritter and M. Kraume. Inline-Messtechnik zur Tropfengrößenbestimmung in flüssigen Zweiphasensystemen bei hohen Dispersphasenanteilen. *Chem. Ing. Tech.*, 71(7):717, 1999.
- [58] W. A. Rodger, Jr. V. G. Trice, and J. H. Rushton. Effect of fluid motion on interfacial areas of dispersions. *Chem. Eng. Prog.*, 52(12):515, 1956.
- [59] A. W. Adamson. *Physical Chemistry of Surfaces, Fifth Edition*. John Wiley and Sons, Inc., New York, 1990.
- [60] R. E. Treybal. *Mass transfer operations, Third Edition*. McGraw-Hill Book Company, Singapore, 1981.
- [61] R. H. Perry and R. W. Green. *Perry's Chemical Engineers' Handbook, Seventh Edition*. McGraw Hill, USA, 1997.
- [62] M. Baerns, H. Hoffmann, and A. Renken. *Chemische Reaktionstechnik. Lehrbuch der technischen Chemie-1*. Thieme Verlag, Stuttgart, 1987.
- [63] H. S. Fogler. *Elements of Chemical Reaction Engineering, Third Edition*. Prentice Hall Inc., USA, 1999.
- [64] O. Levenspiel. *Chemical Reaction Engineering, Third Edition*. John Wiley and Sons Inc., USA, 1999.
- [65] D. J. Raal and A. L. Mühlbauer. *Phase Equilibria: Measurement and Computation*. Taylor and Francis, USA, 1997.
- [66] W. Gottwald. *GC für Anwender*. VCH Verlagsgesellschaft mbH, Weinheim, Germany, 1995.
- [67] G. Demmering and E. Gunter, 1981. German Patent 3,020,566.
- [68] H. Birnbaum, 1959. US Patent 2,875,221.
- [69] J. M. Zaldivar, E. Molga, M. A. Alos, H. Hernandez, and K. R. Westerterp. Aromatic nitrations by mixing acid. Slow liquid-liquid regime. *Chem. Eng. Proc.*, 34:543, 1995.

## Curriculum Vitae

Name: Devender Singh Negi  
Date/-place of Birth: 15 January 1978, Almora, India

10.2002 – 06.2006	Doctorate <i>Institut für Chemie, Technische Universität Berlin, Germany</i>
07.2000 – 12.2001	Master of Technology in Process Engineering and Design <i>Indian Institute of Technology Delhi, New Delhi, India</i>
10.1997 – 06.2000	Bachelor of Technology in Chemical Engineering <i>CSJM University, Kanpur, India</i>
06.1983 – 05.1995	School education Central School, Dehradun, India

## Parts of this work published/ submitted for publication:

Negi D.S., Rochlitz, A., Wozny, G., Schomäcker, R. Drop-Size Analysis in a Two- Phase Reactive Liquid-Liquid System on a Bubble-Cap Tray. *Ind. Eng. Chem. Res.*, 2005, 44(9), 3343-3347.

Negi, D. S., Sobotka, F., Kimmel, T., Wozny, G., Schomäcker, R. Liquid-Liquid Phase Equilibrium in Glycerol-Methanol-Methyl Oleate and Glycerol-Monoolein- Methyl Oleate Ternary Systems. *Ind. Eng. Chem. Res.*, 2006, 45(10), 3693-3696.

Negi, D. S., Sobotka, F., Kimmel, T., Wozny, G., Schomäcker, R. Glycerolysis of Fatty Acid Methyl Esters: 1. Investigations in Batch Reactor. *J. Am. Oil. Chem. Soc.*, *submitted*.

Negi, D. S., Kimmel, T., Wozny, G., Schomäcker, R. Glycerolysis of Fatty Acid Methyl Esters: 2. Simulation and Experiments in Continuous Reactors. *J. Am. Oil. Chem. Soc.*, *submitted*.